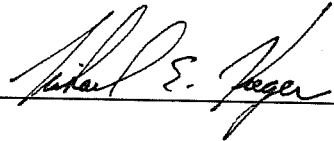


**PERFORMANCE OF POST-INSTALLED ANCHORS IN UNCRACKED  
CONCRETE UNDER SEISMIC, FATIGUE AND  
SHOCK LOADS**

**APPROVED:**

---



---

Copyright © 1993

by

Thomas H. Pechillo, Jr.

**PERFORMANCE OF POST-INSTALLED ANCHORS IN UNCRACKED  
CONCRETE UNDER SEISMIC, FATIGUE AND  
SHOCK LOADS**

**by**

**THOMAS HENRY PECHILLO, JR., B.S.C.E**

**THESIS**

**Presented to the Faculty of the Graduate School of  
The University of Texas at Austin  
in Partial Fulfillment  
of the Requirements  
for the Degree of**

**MASTER OF SCIENCE IN ENGINEERING**

**THE UNIVERSITY OF TEXAS AT AUSTIN**

**August 1993**

*To my mother and father,  
who have provided the love and support  
necessary for the writing of this thesis*



## ACKNOWLEDGEMENTS

The author would like to express his appreciation to Dr. Richard E. Klingner for his supervisory role in this thesis, as well as for his ability to ease my worries regarding the project and thesis.

The author is also grateful to Dr. Michael E. Kreger for taking the time out of his busy schedule to read and approve this thesis.

Sincere thanks go to Dr. Karl Frank, the director of the Ferguson Structural Engineering Laboratory, for his suggestions throughout the project, as well for sharing his seemingly infinite knowledge of servo-control systems.

This thesis would not have been possible without the loving support of my family, though the miles between Connecticut and Texas are many.

Tests would not have been conducted without the help of the Laboratory technical staff, namely, Blake Stasney, Wayne Fontenot, Pat Ball, Wayne Little, Ray Madonna and Ryan Green. In addition, the author wishes to thank the Laboratory administrative staff, namely, April Jenkins, Laurie Golding, Sharon Cunningham, and Joy Bradford.

A sincere thank-you goes to the "other anchor project" crew, who somehow always managed to recover their tools which the author "borrowed" for use on this project, and will continue this research. Thanks to ex-anchor guru David Dorr as well as the current graduate student crew: Wayne Clendennen, Yonggang Zhang, and Milton Rodriguez. Thanks to the "other project's" undergraduates, especially Ranjit Gupta and Chanaka Gunasekara. The author also wishes to thank this project's undergraduate assistant, Rajeev Chawla, especially for his help with the baseline shear tests.

Concrete would not have been placed without the patience of George Hall, who managed to continue to provide "accurate-strength" concrete.

Concrete thanks also go to Darin Riggleman, who was instrumental in providing last-minute placing assistance, as well as golf humor.

The author may not have weathered the storm without James Whitt, who showed that there was always someone else in the same boat.

The author's living conditions in Austin were made easier by Bruce English and Anahita Kapadia English, as well as by Jim Light and Tom the other guy Tom. Much-needed stress-relieving humor was provided by Calvin the dalmation, who continued to defy the laws of doggie-reason.

Emergency support services and BEvERages were provided by Robert Frosch, Jeff Borger, Rich Denio and Stacy Bartoletti. Good luck to you all.

Finally, the author would like to acknowledge the Structural Disasters softball team for somehow always putting the author's fielding misadventures into perspective by providing some of their own.

Tom Pechillo  
Austin, Texas  
May 1993

## TABLE OF CONTENTS

1. INTRODUCTION AND OBJECTIVES .....	1
1.1 Introduction .....	1
1.1.1 Connection Nomenclature .....	1
1.1.2 Significance of Post-Installed Anchors .....	1
1.1.3 Codes and Suitability Criteria .....	2
1.2 Objectives of Study .....	3
1.3 Objectives of Thesis .....	4
2. SCOPE .....	5
2.1 Anchor Types and Sizes Tested .....	5
2.2 Test Types .....	6
2.2.1 Baseline Tests .....	6
2.2.2 Seismic Tests .....	7
2.2.3 Fatigue Tests .....	7
2.2.4 Shock Tests .....	7
2.3 Other Test Variables .....	8
2.4 Test Nomenclature .....	9
3. BACKGROUND .....	10
3.1 Description of Anchor Types Tested .....	10
3.1.1 Expansion Anchors .....	10
3.1.2 Undercut Anchors .....	11
3.2 General Anchor Failure Modes under Monotonic Loading ..	12
3.2.1 Tension .....	12
3.2.2 Shear .....	17
3.3 Seismic Tests .....	19
3.3.1 Tensile Seismic Tests .....	19
3.3.2 Shear Seismic Tests .....	20
3.4 Fatigue Tests .....	21
3.4.1 Tensile Fatigue Tests .....	21
3.4.2 Shear Fatigue Tests .....	23
3.5 Shock Tests .....	24
4. DEVELOPMENT OF TEST PROGRAM .....	26
4.1 Concrete .....	26
4.1.1 Characteristics of Concrete Blocks .....	26

4.1.2	Mix Design .....	26
4.1.3	Concrete Casting .....	28
4.1.4	Test Cylinders .....	28
4.2	Baseline Tests .....	31
4.2.1	Loading for Baseline Tests .....	31
4.2.2	Test Setup for Baseline Tests .....	31
4.2.3	Instrumentation for Baseline Tests .....	36
4.2.4	Data Acquisition and Reduction for Baseline Tests .....	38
4.2.5	Test Procedures for Baseline Tests .....	39
4.3	Seismic Tests .....	43
4.3.1	Loading for Seismic Tests .....	43
4.3.2	Test Setup for Seismic Tests .....	46
4.3.3	Instrumentation for Seismic Tests .....	48
4.3.4	Data Acquisition and Reduction for Seismic Tests .	49
4.3.5	Test Procedures for Seismic Tests .....	49
4.4	Fatigue Tests .....	51
4.4.1	Loading for Fatigue Tests .....	51
4.4.2	Test Setup for Fatigue Tests .....	51
4.4.3	Instrumentation for Fatigue Tests .....	56
4.4.4	Data Acquisition and Reduction for Fatigue Tests .	57
4.4.5	Test Procedures for Fatigue Tests .....	57
4.5	Shock Tests .....	59
4.5.1	Loading for Shock Tests .....	59
4.5.2	Test Setup for Shock Tests .....	61
4.5.3	Instrumentation for Shock Tests .....	61
4.5.4	Data Acquisition and Reduction for Shock Tests ...	61
4.5.5	Test Procedures for Shock Tests .....	61
5.	TYPICAL RESULTS AND SIGNIFICANCE .....	63
5.1	Baseline Tests .....	63
5.1.1	Tensile Baseline Tests .....	63
5.1.2	Shear Baseline Tests .....	75
5.2	Seismic Tests .....	75
5.3	Fatigue Tests .....	75
5.3.1	Tensile Fatigue Tests .....	75
5.3.2	Shear Fatigue Tests .....	80
5.4	Shock Tests .....	80
5.5	Comparison of Baseline Tensile Test Results with Predicted Values .....	80

6. SUMMARY, CONCLUSIONS AND RECOMMENDATIONS . . . .	92
6.1 Summary . . . . .	92
6.2 Conclusions . . . . .	93
6.2.1 Anchor Installation and Concrete . . . . .	93
6.2.2 Baseline Tests . . . . .	94
6.2.3 Seismic Tests . . . . .	95
6.2.4 Fatigue Tests . . . . .	95
6.2.5 Shock Tests . . . . .	96
6.3 Recommendations . . . . .	96
6.3.1 Applications . . . . .	96
6.3.2 Suitability Criteria . . . . .	97
6.3.3 Further Research . . . . .	99
APPENDIX: Load-Displacement Results of All Tests . . . . .	101
REFERENCES . . . . .	131

## LIST OF TABLES

Table 2.1	Expansion and Undercut Anchors Used in Testing Program . . .	8
Table 4.1	Concrete Mix Design for Testing Program . . . . .	28
Table 5.1	Statistical Data for Tensile Baseline Test Failures . . . . .	74
Table 5.2	Predicted Ultimate Tensile Capacities for Anchors in Testing Program . . . . .	83
Table 5.3	Comparison of Predicted Failure Modes and Ultimate Capacities with Those Obtained Experimentally	
(a)	8 mm Expansion Anchor . . . . .	84
(b)	10 mm Expansion Anchor . . . . .	85
(c)	12 mm Expansion Anchor . . . . .	86
(d)	16 mm Expansion Anchor . . . . .	87
(e)	20 mm Expansion Anchor . . . . .	88
(f)	24 mm Expansion Anchor . . . . .	89
(g)	12 mm Undercut Anchor . . . . .	90
(h)	16 mm Undercut Anchor . . . . .	90
(i)	20 mm Undercut Anchor . . . . .	91

## LIST OF FIGURES

Figure 1.1 Typical steel-to-concrete connection .....	2
Figure 2.1 Typical torque-controlled expansion anchors: (a) standard; (b) flush .....	5
Figure 2.2 Typical undercut anchor .....	6
Figure 3.1 Undercut anchor installed in hole .....	11
Figure 3.2 (a) Tensile anchor fracture .....	13
Figure 3.2 (b) Tensile thread stripping failure .....	13
Figure 3.2 (c) Tensile concrete cone breakout .....	14
Figure 3.2 (d) Tensile anchor pullout .....	15
Figure 3.2 (e) Tensile anchor pull-through .....	16
Figure 3.3 (a) Shear anchor fracture .....	18
Figure 3.3 (b) Shear concrete breakout .....	18
Figure 3.3 (c) Shear anchor pullout .....	19
Figure 4.1 Typical concrete block .....	27
Figure 4.2 Pouring concrete from truck into bucket .....	29
Figure 4.3 Placing concrete from bucket into forms .....	29
Figure 4.4 Freshly cast concrete block .....	30
Figure 4.5 Casting concrete test cylinders .....	30
Figure 4.6 Typical baseline tensile loading shoe .....	32
Figure 4.7 Tensile ring testing fixture .....	34
Figure 4.8 Tensile ring testing fixture .....	34
Figure 4.9 Tensile beam testing fixture .....	35
Figure 4.10 Typical shear loading plate .....	37
Figure 4.11 Shear testing fixture .....	37
Figure 4.12 Schematic of data acquisition system for baseline tests .....	40
Figure 4.13 Undercutting tool for installation of undercut anchors .....	41
Figure 4.14 Tensile seismic waveform used in testing program .....	44
Figure 4.15 Shear seismic waveform used in testing program .....	45
Figure 4.16 Tensile loading shoe for dynamic tests .....	47
Figure 4.17 Tensile fatigue testing apparatus .....	53
Figure 4.18 Tensile fatigue testing fixture (testing in progress) .....	54
Figure 4.19 Alternate anchor locations for tensile fatigue failure .....	55
Figure 4.20 Shock waveform used in testing program .....	60
Figure 5.1 Tensile baseline expansion anchor fracture .....	64
Figure 5.2 Load-displacement curve for tensile baseline expansion anchor fracture (no slip) .....	64

Figure 5.3 Load-displacement curve for tensile baseline expansion anchor fracture (slip) .....	65
Figure 5.4 Load-displacement curve for tensile baseline undercut anchor fracture .....	66
Figure 5.5 Tensile baseline expansion anchor thread stripping .....	67
Figure 5.6 Load-displacement curve for tensile baseline expansion anchor thread stripping .....	67
Figure 5.7 Tensile baseline undercut anchor thread stripping .....	68
Figure 5.8 Load-displacement curve for tensile baseline undercut anchor thread stripping .....	68
Figure 5.9 Tensile baseline expansion anchor concrete cone breakout .	70
Figure 5.10 Load-displacement curve for tensile baseline expansion anchor concrete cone breakout .....	70
Figure 5.11 Tensile baseline expansion anchor pullout .....	72
Figure 5.12 Load-displacement curve for tensile baseline expansion anchor pullout .....	72
Figure 5.13 Tensile baseline expansion anchor pull-through .....	73
Figure 5.14 Load-displacement curve for tensile baseline expansion anchor pull-through .....	73
Figure 5.15 Tensile fatigue expansion anchor fracture .....	77
Figure 5.16 Load-displacement curve for tensile fatigue expansion anchor fracture .....	77
Figure 5.17 Tensile fatigue expansion anchor concrete cone breakout ..	78
Figure 5.18 Load-displacement curve for tensile fatigue expansion anchor concrete cone breakout .....	78
Figure 5.19 Tensile fatigue expansion anchor pullout .....	79
Figure 5.20 Load-displacement curve for tensile fatigue expansion anchor pullout .....	79



# 1. INTRODUCTION AND OBJECTIVES

## 1.1 Introduction

### 1.1.1 Connection Nomenclature

In structural engineering, some of the most frequently encountered connection details are those between structural steel and concrete. Such connections are typically accomplished through the use of anchors, which can either be cast-in-place or post-installed. By definition, cast-in-place anchors are set in their final position prior to concrete casting; post-installed anchors are installed in hardened concrete.

A typical application of anchors in a steel-to-concrete connection is shown in Figure 1.1. In general, the thickness of the baseplate is referred to as the "thickness fastened," and the entire steel assembly (baseplate and column in the case shown) is called the attachment. The anchors fasten the attachment to the concrete.

### 1.1.2 Significance of Post-Installed Anchors

Either cast-in-place or post-installed anchors may be used for steel-to-concrete connections in new construction. However, it is obvious that only post-installed anchors may be used for retrofit projects which call for connections to existing concrete. Since retrofit construction projects in the United States and abroad are currently increasing in number and scope, considerable interest has developed in products used in such projects. Thus, post-installed anchors are becoming an increasingly important aspect of

fastening technology. In this study, the performance of two types of post-installed concrete anchors subject to dynamic loads was investigated.

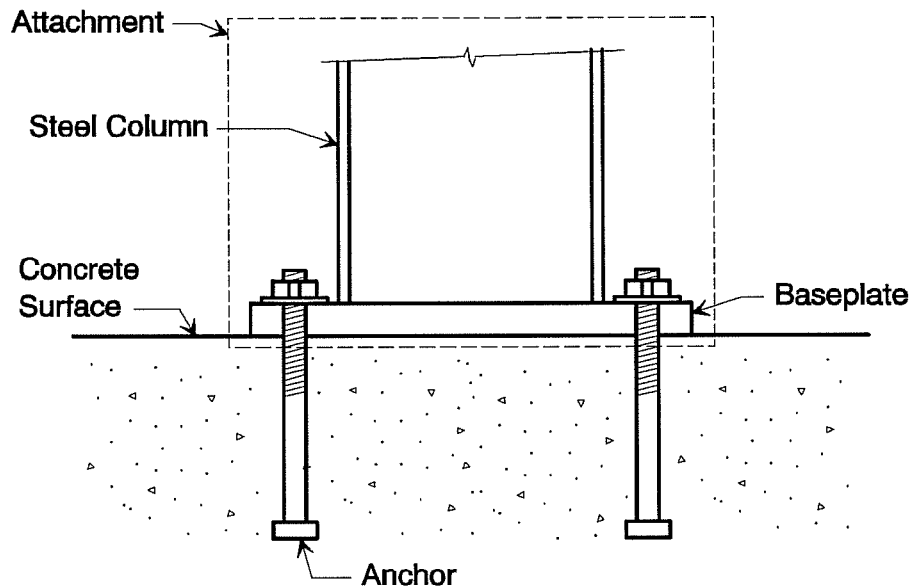


**Figure 1.1 Typical steel-to-concrete connection**

### 1.1.3 Codes and Suitability Criteria

The United States now has only one design code specifically applicable to post-installed anchors; this code is ACI 349-85: *Code Requirements for Nuclear Safety Related Concrete Structures* [1]. Appendix B of that code pertains to steel embedments, of which anchors are a subset. That appendix and other codes under development include provisions for the design of anchors loaded in axial tension, shear, and combined tension and shear.

To use those codes, basic anchor performance must be verified. This is accomplished through the use of suitability criteria for the qualification of anchors. The use of such criteria in a testing program is common in Europe; however, it is relatively new in the United States.

In this country, suitability criteria have been developed for statically loaded expansion anchors by the International Conference of Building Officials Evaluation Service (ICBO ES) [2]. These criteria include concrete requirements, test specimen requirements, testing procedure requirements and report requirements.

Dynamic loading qualification criteria have been proposed by Klingner [3] and others. These criteria consider the importance of anchor preload and concrete cracking. In addition, Klingner suggests that the attachment be required to have a plastic hinging region if the dynamic loads are of unknown magnitude [3].

## **1.2 Objectives of Study**

The main objectives of this study were to conduct tests of anchors under dynamic conditions, and thereby to propose guidelines for dynamic qualification of anchors. The specific objectives of the testing program were:

1. To determine expansion and undercut anchor performance in uncracked concrete under the following types of dynamic loads:
  - a. Seismic
    - i. Tension
    - ii. Shear
  - b. Fatigue

- i. Tension
    - ii. Shear
  - c. Shock (Tension only)
2. To determine the remaining static capacity of the anchors previously subjected to the various loading cases in Objective 1. This objective serves as an indication of possible detrimental effects of the various dynamic load cases on the capacity of the anchor in the case that the anchor did not fail under the dynamic load in question.

### **1.3 Objectives of Thesis**

The main objectives of this thesis are the following:

1. To evaluate the performance of the anchors tested under the objectives listed in Section 1.2.
2. To comment on possible suitability criteria for the dynamic qualification of anchors.

## 2. SCOPE

### 2.1 Anchor Types and Sizes Tested

Many types of post-installed anchors are available commercially for structural and nonstructural applications. Some of these are:

- Expansion
- Undercut
- Adhesive
- Grouted
- Drop-in

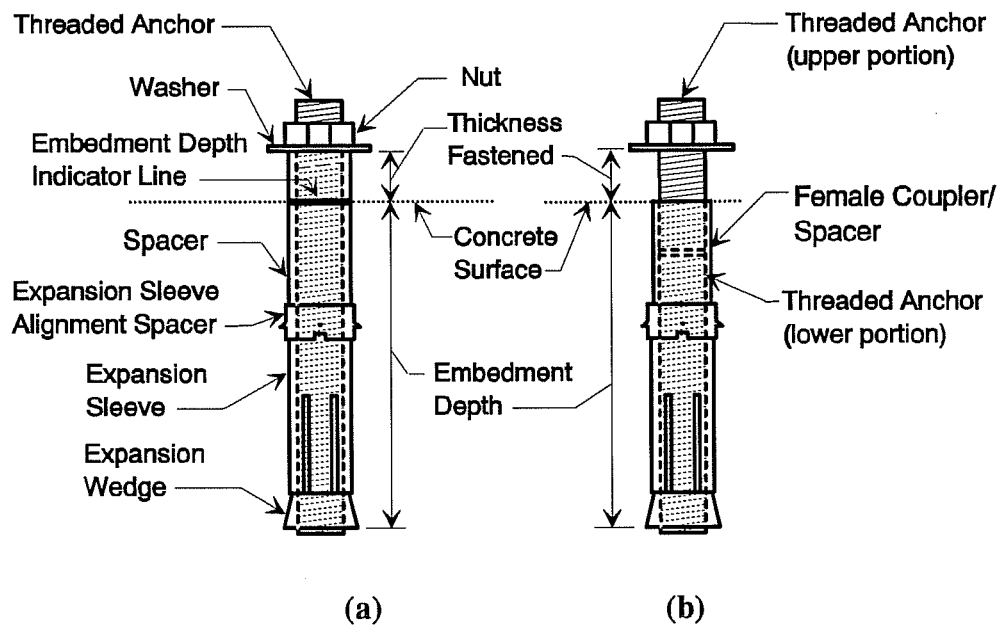
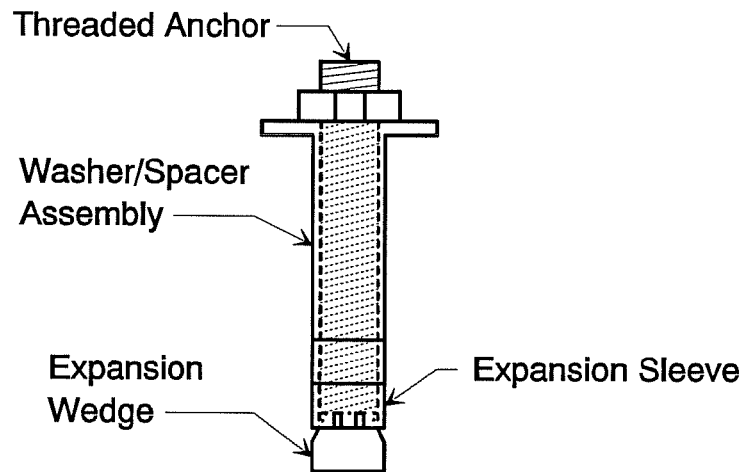


Figure 2.1 Typical torque-controlled expansion anchors:  
(a) standard; (b) flush

Two of the most common types of heavy-duty post-installed anchors, torque-controlled expansion and undercut, were used in this testing program. Figure 2.1 shows typical heavy-duty, torque-controlled expansion anchors, and Figure 2.2 shows a typical undercut anchor.



**Figure 2.2 Typical undercut anchor**

A single embedment depth was used for each type and diameter of anchor tested. In addition, the baseplate thickness was kept constant within each anchor type and diameter. Table 2.1 shows the anchor diameters, embedment depths and baseplate thicknesses used in this testing program.

## **2.2 Test Types**

### **2.2.1 Baseline Tests**

Both anchor types and all anchor diameters shown in Table 2.1 were subjected to baseline tests in static tension and shear. In this phase, anchors

were tested to failure; the results were compared with those from seismic, fatigue, and shock tests. These baseline tests determined the ultimate static load for each type and size of anchor embedded in the particular concrete mix design used in this project. The baseline tests are further discussed in Section 4.2.

### **2.2.2 Seismic Tests**

Both anchor types and all anchor diameters shown in Table 2.1 were subjected to low-cycle fatigue tests in dynamic tension and shear. These tests, intended to simulate seismic effects, are further discussed in Section 4.3.

### **2.2.3 Fatigue Tests**

Selected expansion anchor diameters and all undercut anchor diameters shown in Table 2.1 were subjected to high-cycle fatigue tests in dynamic tension and shear. The expansion anchor diameters tested were 8 mm, 12 mm Flush, 16 mm and 24 mm. The fatigue tests are further discussed in Section 4.4.

### **2.2.4 Shock Tests**

Selected expansion anchor diameters and all undercut anchor diameters shown in Table 2.1 were subjected to shock tests in dynamic tension. The expansion anchor diameters tested were 8 mm, 12 mm Flush, 16 mm and 24 mm. The shock tests are further discussed in Section 4.5.

**Table 2.1 Expansion and Undercut Anchors Used in Testing Program**

<b>EXPANSION ANCHORS</b>		
<b>Diameter (mm)</b>	<b>Embedment Depth (mm)</b>	<b>Baseplate Thickness (mm)</b>
8	65	20
10	75	20
12	80	25
12 Flush	80	25
16	105	25
20	130	30
24	155	30

<b>UNDERCUT ANCHORS</b>		
<b>Diameter (mm)</b>	<b>Embedment Depth (mm)</b>	<b>Baseplate Thickness (mm)</b>
12	125	25
16	170	30
20	220	32

### 2.3 Other Test Variables

All anchors in this project were tested in uncracked concrete. A single mix design for the concrete was used, with a 28-day target compressive



strength of 4500 psi. The concrete strength in all cases was between 4000 psi and 5500 psi at the time of anchor testing. More will be said about the concrete in Section 4.1 of this thesis.

## 2.4 Test Nomenclature

Tests were called out by a five- or six-letter label, followed by a one- or two-digit number. The labelling system was for internal use only and was not intended to indicate a particular product.

The first two or three letters in each label indicate the test type: BT for baseline tension, BV for baseline shear, ST for seismic tension, SV for seismic shear, FT for fatigue tension, FV for fatigue shear, and IT for shock tension. The letter "U" preceding any of these indicates the ultimate test conducted after the anchor was subjected to dynamic loading. The next three letters indicate the anchor type: HSL denotes a torque-controlled expansion anchor, and HUC denotes an undercut anchor. The numbers following the series of letters are the individual test numbers of the expansion or undercut anchor for each test type. For the expansion anchors, numbers 01 through 05 refer to 8 mm; 06 through 10, 10 mm; 11 through 15, 12 mm; 16 through 20, 12 mm Flush; 21 through 25, 16 mm; 26 through 30, 20 mm; and 31 through 35, 24 mm. For the undercut anchors, numbers 01 through 05 refer to 12 mm; 06 through 10, 16 mm; and 11 through 15, 20 mm.

### **3. BACKGROUND**

#### **3.1 Description of Anchor Types Tested**

As shown in Table 2.1, the two anchor types tested in this project were torque-controlled expansion anchors and undercut anchors. While these two anchor types are somewhat similar in appearance (see Figures 2.1 and 2.2), they differ in the way that they transmit forces from the steel attachment to the concrete.

##### **3.1.1 Expansion Anchors**

A standard type of torque-controlled expansion anchor employed in this study is shown in Figure 2.1(a). Expansion anchors transfer load by friction. When the nut is tightened to the specified installation torque, all parts surrounding the anchor shaft, between the nut and the expansion wedge, are placed in compression. The washer reacts against the spacer as well as the steel baseplate placed between the washer and the surface of the concrete. The spacer then transmits the force to the expansion sleeve alignment spacer, whose function is to keep the expansion sleeve straight. The alignment spacer bears against the expansion sleeve, which then slides downward over the expansion wedge. As the sleeve rides over the wedge, the sleeve expands against the sides of the hole in the concrete. In this way, a large frictional force is generated between the expansion sleeve and the concrete, due to the normal force produced by the torque. In addition, the sleeve's outside surface is roughened, which produces a larger coefficient of friction and a proportionately larger available frictional resistance.

A secondary expansion force occurs for this type of expansion anchor. This force is due to the anchor expansion wedge moving into the sleeve, thereby further increasing the available frictional resistance.

### 3.1.2 Undercut Anchors

The typical undercut anchor used in this testing program is shown in Figure 2.2. The load transfer mechanism of undercut anchors is direct bearing. During the installation procedure of an undercut anchor (see Section 4.2.5) an undercut is formed at the bottom of the hole in the concrete. See Figure 3.1. When the anchor is then placed in the hole and tightened, the expansion sleeve slides over the top portion of the expansion wedge and expands into the undercut at a low installation torque. The expansion sleeve then bears directly on the concrete.

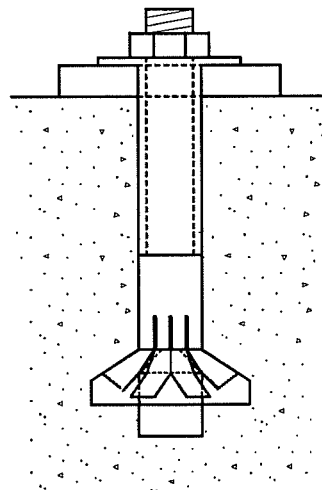


**Figure 3.1 Undercut anchor installed in hole**

## 3.2 General Anchor Failure Modes under Monotonic Loading

### 3.2.1 Tension

The general failure modes observed for anchors under monotonically increasing tensile load are the following:

1. Anchor steel fracture
2. Thread stripping
3. Concrete cone breakout
4. Concrete splitting
5. Anchor pullout
6. Anchor pull-through

Each of these failure mechanisms will now be discussed in more detail.

*Anchor steel fracture:* Figure 3.2 (a) illustrates anchor steel fracture. This failure generally occurs when the anchor is sufficiently embedded in the concrete so that the capacity of the concrete exceeds that of the steel. The failure starts with yielding and necking of the steel followed by steel fracture.

*Thread stripping failure:* This failure mode is shown in Figure 3.2 (b). Thread stripping failure usually occurs when, due to the dimensional tolerances and frictional characteristics of the anchor-nut combination, the threads are stripped out of the nut, leaving the anchor embedded in the concrete.

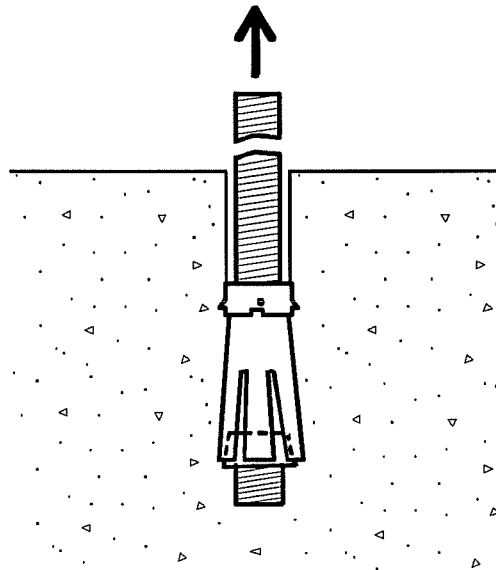


**Figure 3.2 (a) Tensile anchor fracture**

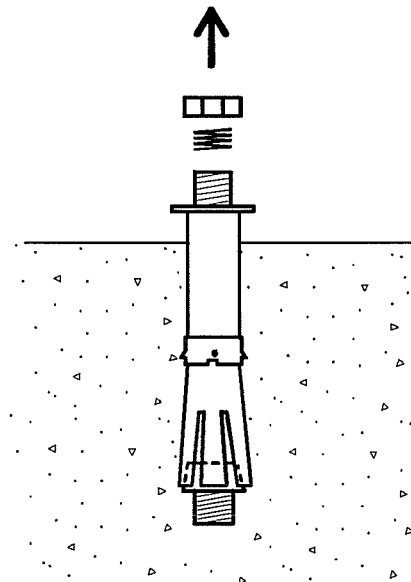


**Figure 3.2 (b) Tensile thread stripping failure**

*Concrete cone breakout:* This failure mode, shown in Figure 3.2 (c), is characteristic of anchors embedded at shallow depths. The failure begins with the formation of microcracks in the concrete surrounding the anchor head. With increasing load, the cracks propagate upward toward the surface of the concrete at an angle of inclination. As a result, a roughly conical piece of concrete becomes detached from the remaining portion of the concrete. The anchor is contained within this breakout cone, since the apex of the cone is at the anchor head. Whether the anchor is physically included in the breakout cone is irrelevant; its ability to carry load ceases with cone failure. The angle of inclination of the concrete cone failure surface is generally about 35 degrees with respect to the free surface and is somewhat dependent on the embedment depth of the anchor.

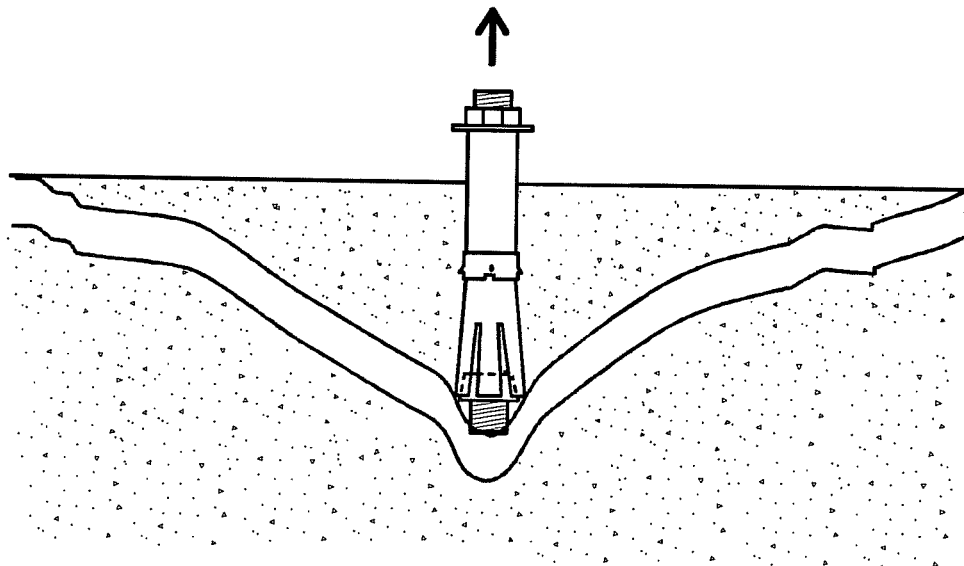


**Figure 3.2 (c) Tensile concrete cone breakout**

*Concrete splitting:* Splitting failure generally occurs when the anchor is located near a free edge or near another anchor. Transverse tensile forces are developed as a result of the proximity of these discontinuities, and the failure mode is similar to that for insufficient cover or spacing of reinforcing bars in concrete.

*Anchor pullout:* Anchor pullout is shown in Figure 3.2 (d). This failure mode occurs when the frictional resistance between the

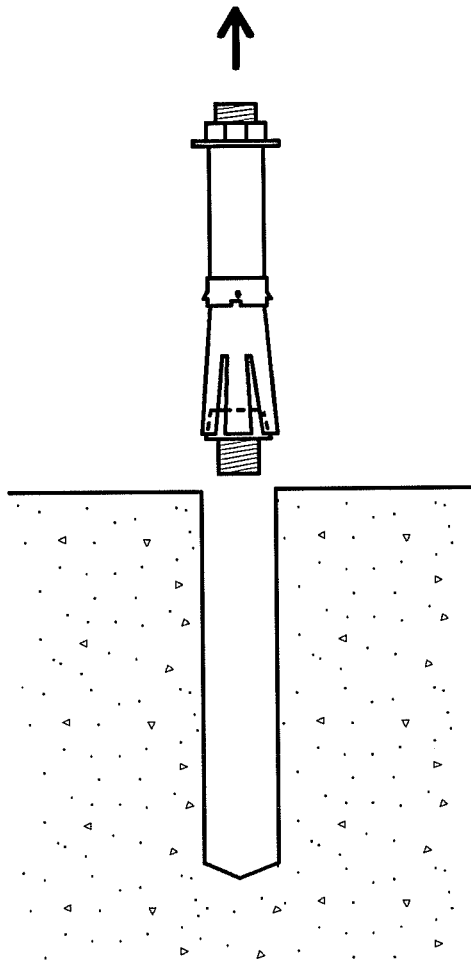


**Figure 3.2 (d) Tensile anchor pullout**

expansion sleeve and the concrete is less than the tensile force in the anchor. Common causes of pullout may be insufficient setting torque, improper hole diameter, or inadequate anchor design.

*Anchor pull-through:* Figure 3.2 (e) shows anchor pull-through. This failure mode occurs when the anchor shaft and wedge pull completely through the expansion sleeve, leaving the sleeve in the hole. Pull-through failures require a relatively deep embedment; if the

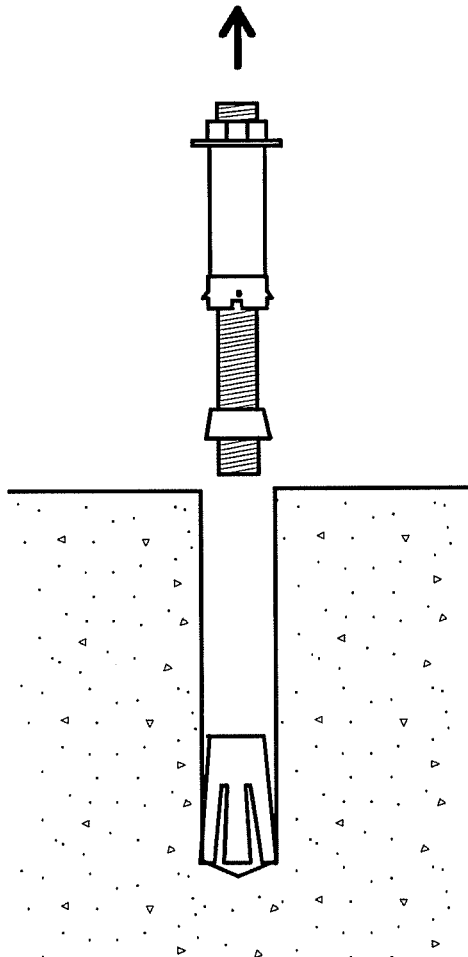


**Figure 3.2 (e) Tensile anchor pull-through**



embedment is shallow, concrete breakout will occur before pull-through.

### 3.2.2 Shear

The following general modes of failure are observed for anchors under monotonically increasing shear load:

1. Anchor steel fracture
2. Concrete breakout
3. Anchor pullout

Each of these failure mechanisms will now be discussed in more detail.

*Anchor steel fracture:* Anchor steel fracture generally occurs when the anchor is placed far from a free edge and the embedment is sufficient to develop a capacity of the concrete greater than that of the steel. Figure 3.3 (a) shows anchor steel fracture.

*Concrete breakout:* Concrete breakout usually occurs when the anchor is loaded towards a nearby free edge. Figure 3.3 (b) illustrates this type of failure. The apex of the cone is typically located near the anchor head for shallow embedment depths, and rises up with respect to the anchor for increasing embedment depths.

*Anchor pullout:* Anchor pullout is shown in Figure 3.3 (c). In this failure mode, the concrete between the anchor and the point of loading crushes. This crushing allows the anchor head to rotate and fail the concrete side of the anchor opposite from the point of loading.

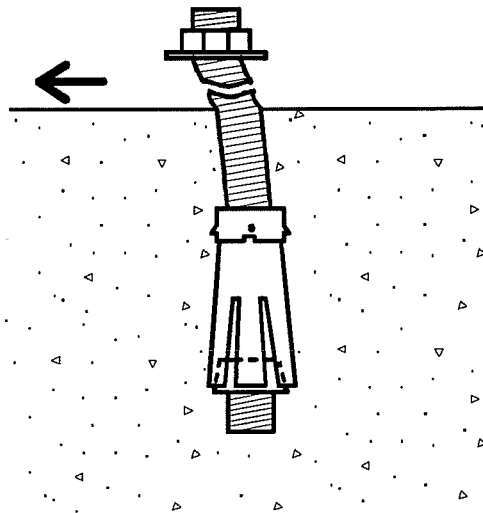


**Figure 3.3 (a) Shear anchor fracture**

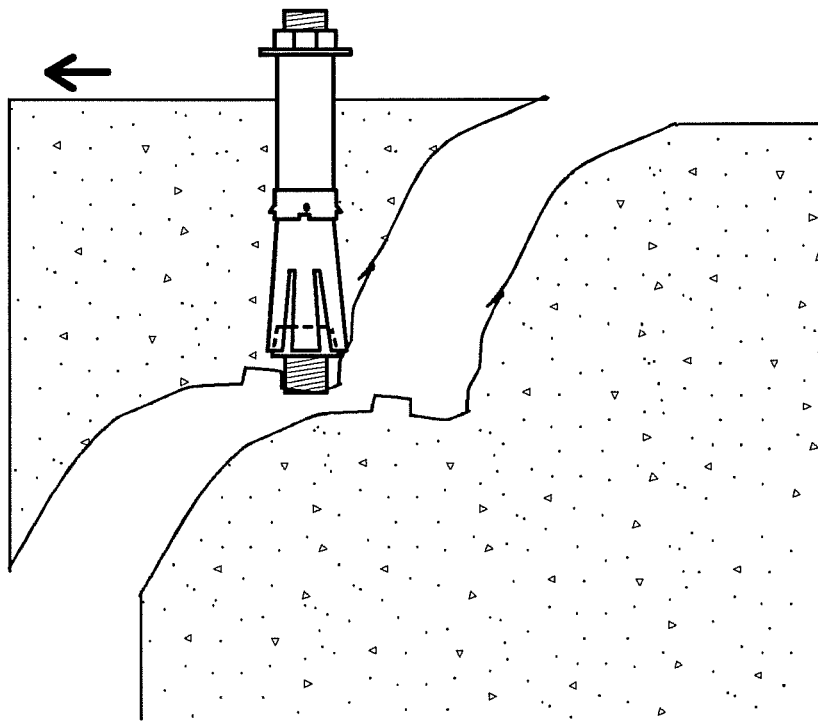


**Figure 3.3 (b) Shear concrete breakout**

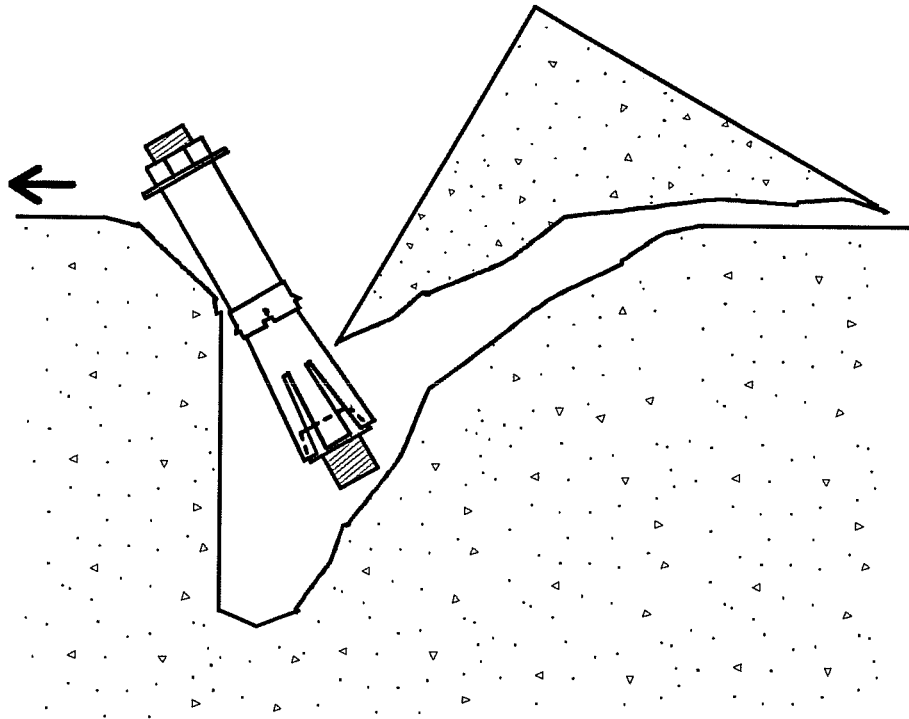


**Figure 3.3 (c) Shear anchor pullout**

### **3.3 Seismic Tests**

#### **3.3.1 Tensile Seismic Tests**

Anchor performance under tensile seismic loads has been assessed by several researchers. From the results published, the following general conclusions may be reached [4]:

1. Anchors failing by steel fracture exhibit better hysteretic behavior than do anchors failing by concrete cone breakout.

2. If fatigue failure does not occur during the application of low-cycle fatigue loads, the maximum load obtained when the anchor is subsequently tested to failure under monotonic loads is similar to the ultimate load obtained in identical anchors subjected to static load only.

Anchor performance under real earthquake-induced tensile loads may be considerably improved by:

1. Embedding the anchor sufficiently far into the concrete to ensure that ductile steel failure precedes brittle concrete failure
2. Placing reinforcing steel around the anchor to intercept potential concrete cone failure surfaces

### **3.3.2 Shear Seismic Tests**

Anchor performance under reversed shear seismic loads is generally characterized by the following [4, 5]:

1. Considerable pinching of hysteresis loops and correspondingly small hysteresis loop areas
2. Substantial stiffness degradation
3. Reduction of shear force for a given displacement as the number of cycles imposed increases

Anchor performance under real earthquake-induced shear loads may be considerably improved by:

1. Embedding the anchor sufficiently far into the concrete to ensure that ductile steel failure precedes brittle concrete failure
2. Placing hairpin-type reinforcing steel in the vicinity of the anchor as close as practical to the concrete surface

### **3.4 Fatigue Tests**

#### **3.4.1 Tensile Fatigue Tests**

Two important factors meriting consideration in a discussion of fatigue loading are the fatigue strength of the concrete and the fatigue strength of the anchor.

Section 3.2.1 describes the formation of a concrete breakout cone under tensile loading. Initially, microcracks form at the anchor head. As these cracks propagate to the concrete surface, the area available for cracking increases due to the conical shape of the failure surface. Thus, the following opposite effects occur: the crack length is increasing, and the area is also increasing. Because the net effect on crack propagation is almost zero, the effects are nearly equal and opposite. Therefore, the crack propagation is said to be stable. If the applied load is a low percentage of the ultimate load, concrete fatigue becomes relatively unimportant [4].

The fatigue strength of the anchor is directly related to the anchor preload. When prestress force is applied to an anchor, the concrete between the anchor head and the baseplate is placed in compression, while the anchor experiences tension. When a tensile load  $N$  is then applied externally, it is distributed according to the relative axial stiffnesses of the anchor and the surrounding concrete. Since the anchor is usually much more

flexible than the surrounding concrete, the force in the anchor is increased only by a small percentage of  $N$ . Thus, the anchor force increases much more slowly than the applied load, until the concrete is no longer in compression. At this point, the externally applied load has overcome the preload. Beyond this, the anchor force will be equal to  $N$  as  $N$  is increased.

The above discussion indicates that if the applied load is a fairly low percentage of the ultimate load and is also less than the anchor preload, the anchors should perform satisfactorily in fatigue, for the following reasons:

1. If the applied load is a fairly low percentage of the ultimate load, fatigue of the concrete itself will not be a problem.
2. If the applied load is less than the anchor preload, the anchor will be subjected to a small percentage of the stress range that otherwise would result from the applied load, and fatigue of the anchor will not be a problem.

Conversely, if the load is large, fatigue of the concrete may become an issue. In addition, if the load is greater than the anchor preload, the anchor will be subjected to the entire stress range resulting from the applied load. In this case, the fatigue performance of the anchor depends on [4]:

1. Anchor diameter
2. Type of thread
3. Type and quality of the anchor material

### 3.4.2 Shear Fatigue Tests

Shear fatigue loads influence the concrete in much the same way as tensile fatigue loads. Since the crack propagation is similar, fatigue of the concrete is typically not a problem if the applied shear load is a fairly low percentage of the ultimate load achieved under monotonically increasing shear load.

In addition, the presence of anchor preload directly affects the fatigue performance of the anchor under shear. An applied shear load,  $V$ , may be resisted either by the anchor or by the frictional resistance,  $F$ , between the baseplate and the concrete surface. If the applied shear is less than the available frictional resistance, the applied shear is resisted entirely by friction. However, if the applied shear exceeds the available frictional resistance, the applied shear is resisted by the anchor as well. This effect is magnified by the presence of locally high bearing stresses on the anchor at its point of contact with the lower surface of the baseplate. This effect is even more pronounced if the anchor does not have a sleeve-type spacer around the threads; notching may then occur.

Thus, the shear fatigue performance of the anchor depends primarily upon the anchor preload and the coefficient of friction between the baseplate and the concrete. If the applied shear exceeds the available frictional resistance, the anchor performance depends on [4]:

1. Anchor type
2. Anchor diameter
3. Type of thread
4. Type and quality of the anchor material

### 3.5 Shock Tests

Anchor performance under shock loads may be divided into two categories: performance of those anchors that are embedded to develop the full capacity of the steel; and performance of those anchors that are not, i.e., those that would otherwise fail by concrete cone breakout, by pullout, or by pull-through.

Fully embedded anchors have been studied by Collins [6], who reached the following conclusions:

1. Expansion and undercut anchors did not exhibit any loss of strength due to the applied shock load.
2. Expansion and undercut anchors exhibited a slight reduction in secant stiffness due to anchor slip; however, this slip was not more than the slip observed for statically loaded anchors, and it had no effect on anchor strength.

Several researchers have produced test results for anchors embedded insufficiently to develop the full capacity of the anchor steel. According to [4], the general conclusions reached are:

1. The ultimate load achieved under shock loading is greater than or equal to the ultimate load achieved by static loading.
2. For anchors tested statically to failure after being subjected to shock loads, the ultimate load achieved under static loading is about the same as would have been achieved if the anchor had not been subjected to the shock loads.



The results described above lead to the conclusion that expansion and undercut anchors perform satisfactorily under tensile shock loads; that is, the ultimate load achieved under this type of load is comparable to that for a monotonically tested anchor. In addition, there is little stiffness degradation due to shock loads. Very little research has been done on shear shock loads.

## **4. DEVELOPMENT OF TEST PROGRAM**

The following sections of this thesis contain information pertaining to all types of tests within the project scope. This chapter was written as if the tests were completed; however, at the time of this writing, some types of tests had not yet been conducted. Therefore, for those test types, a description of the intended setup and procedures is given, and is subject to change.

### **4.1 Concrete**

#### **4.1.1 Characteristics of Concrete Blocks**

A typical concrete block used in this experiment is shown in Figure 4.1. The block measured 3 feet 3-1/2 inches by 7 feet 3-1/2 inches in plan, and had a depth of 2 feet. Seven #6 longitudinal reinforcing bars served to guard against failure in transport. The steel was placed at the midheight of the block to facilitate testing anchors on both the top and bottom surfaces while precluding interference with anchor performance. Four lifting loops located at the midheight and on the sides of the blocks facilitated transportation by an overhead crane.

#### **4.1.2 Mix Design**

All concrete used in this test program was ready-mix concrete of a single mix design. The 28-day target strength was 4500 psi, with a strict requirement that the compressive strength be between 4000 psi and 5500 psi

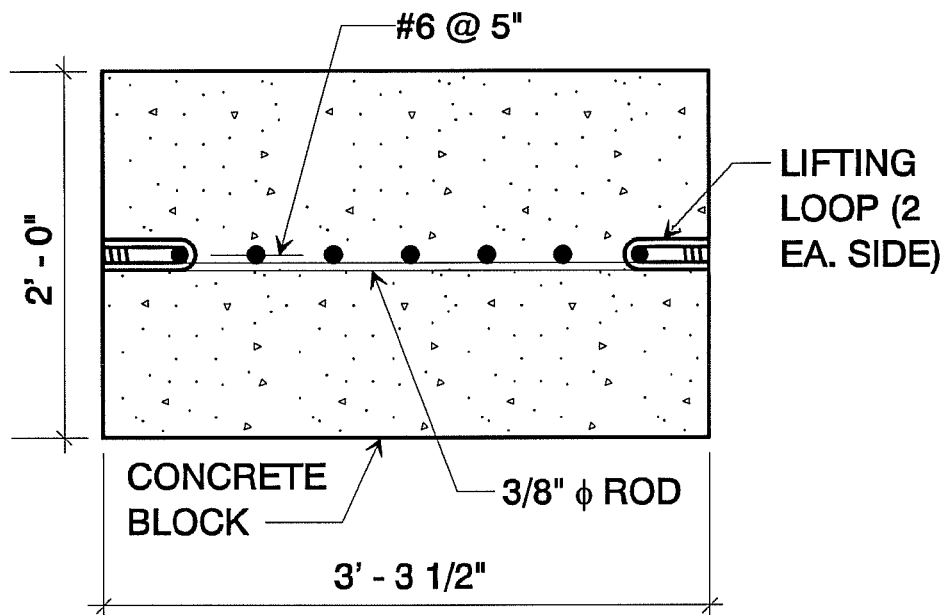


Figure 4.1 Typical concrete block

at the time of anchor testing. The complete mix design is summarized in Table 4.1. Crushed limestone (3/4-inch maximum size) was used as the coarse aggregate because of its low hardness compared to other readily available aggregates, such as gravel. This soft material would represent a "worst-case" scenario for evaluating the performance of anchors in concrete. The water/cement ratio for this mix was kept constant using slump as an indication of amount of water present in the mix. Water was added on site as needed to obtain a 7-inch slump. This procedure was used primarily because of the uncertainty of the moisture content of the coarse aggregate. This concern was addressed by continuous sprinkling of the stockpiled limestone so that near-SSD conditions could be consistently obtained.

**Table 4.1 Concrete Mix Design for Testing Program**

<b>Target Strength</b>	<b>3/4" Crushed Limestone</b>	<b>Type I Portland Cement</b>	<b>Concrete Sand</b>	<b>Rheobuild 1000 Superplasticizer</b>
(psi)	(pounds/yd <sup>3</sup> )	(pounds/yd <sup>3</sup> )	(pounds/yd <sup>3</sup> )	(ounces/yd <sup>3</sup> )
4500	1876	390	1432	48

### 4.1.3 Concrete Casting

Concrete was placed into the formwork directly from an overhead bucket, as shown in Figures 4.2 and 4.3. The concrete blocks were rodded thoroughly instead of vibrated because of the desire to maintain uniformity of concrete strength throughout the block. Figure 4.4 shows a freshly cast block. After casting, the blocks were field-cured under polyethylene sheets for a minimum of 23 days before anchor testing began..

### 4.1.4 Test Cylinders

As shown in Figure 4.5, eighteen test cylinders were cast in accordance with ASTM C31-90a [7] for each set of blocks cast on a given date. These cylinders were field-cured near the blocks. The cylinders were capped using sulfur-based capping compound in accordance with ASTM C617-87 [8], and were tested in compression in accordance with ASTM C39-86 [9]. Three cylinders were tested before and after anchor testing. If both sets of cylinder strengths were within the block strength limits discussed in

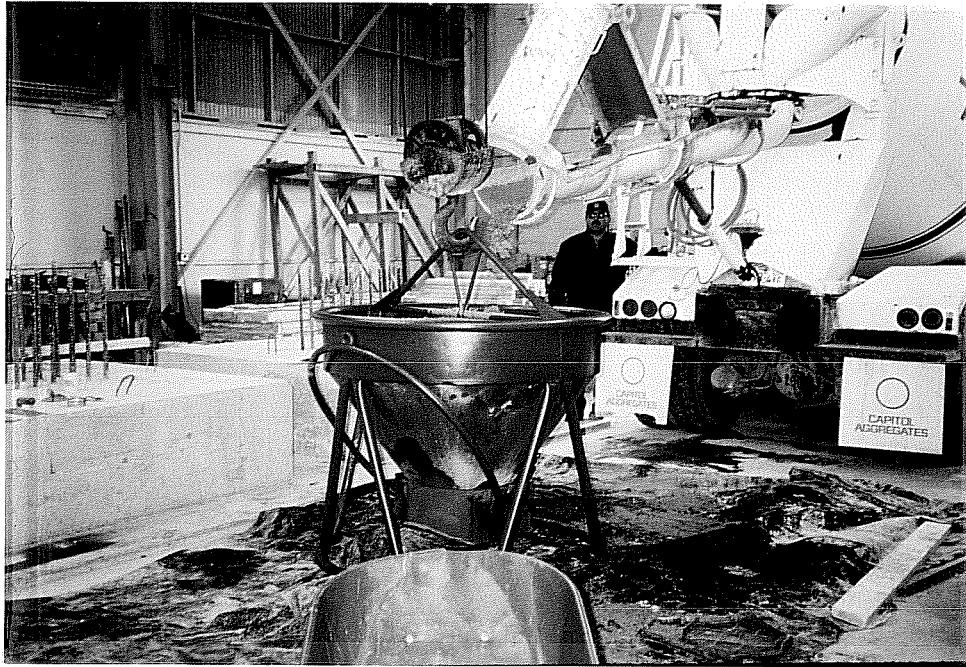


**Figure 4.2 Pouring concrete from truck into bucket**

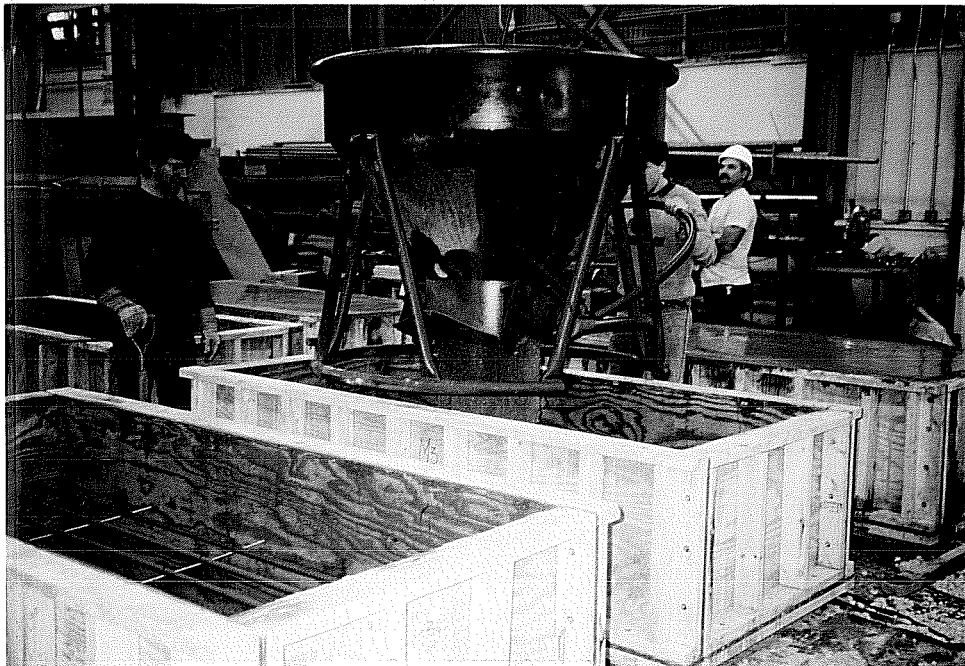


**Figure 4.3 Placing concrete from bucket into forms**

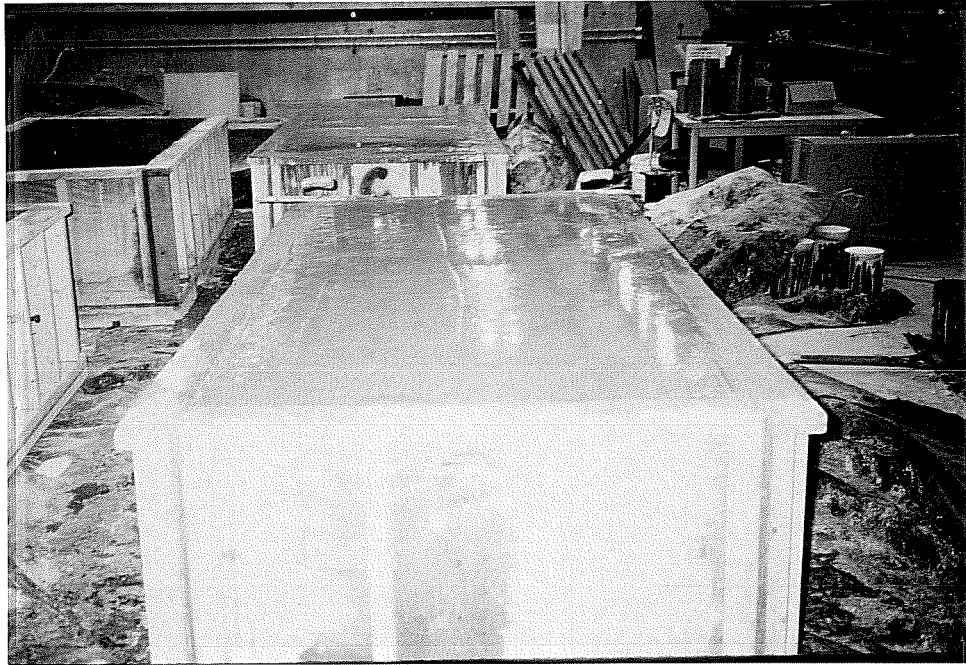


**Figure 4.4** Freshly cast concrete block



**Figure 4.5** Casting concrete test cylinders

Section 4.1.1, the tests were deemed valid. If the second cylinder test did not meet these limits, linear interpolation was used to determine the concrete strength at the time of each individual test, and those tests meeting the strength requirements were deemed valid.

## **4.2 Baseline Tests**

### **4.2.1 Loading for Baseline Tests**

Baseline tests were conducted to determine the ultimate anchor capacity under monotonic loading.

Anchors loaded in tension were loaded concentrically. The loading rate varied between anchor sizes such that the total test time was between two and six minutes after loading commenced. The lower end of the time was the minimum test time prescribed by ASTM E488-90 [10]. The upper end of the time was selected to attempt to include the ultimate displacement on the descending branch of the load-displacement curve. Ultimate displacement values were obtained for all but a few tests.

Anchors loaded in shear were loaded such that the line of force was as close as practicable to the interface of the bottom surface of the baseplate and the concrete. The loading rate was varied so that the total test time for all anchors was between two and six minutes, as for the tension tests.

### **4.2.2 Test Setup for Baseline Tests**

Loads were applied to the anchors by a hand pump connected to either of two centerhole hydraulic rams: a 20-ton ram was used for the

smaller expansion anchors; a 60-ton ram was used for the larger expansion anchors and for all undercut anchors. These rams loaded the anchors in tension or shear via a high-strength threaded rod passing through the centerhole and connected to a loading shoe or plate. The reaction of the ram was resisted by testing fixtures, described below.

In tension, three loading shoe sizes were used: small, medium, and large. A typical shoe is shown in Figure 4.6. Each size shoe consisted of a steel tube welded to a baseplate. The anchor was tightened against the baseplate. A steel cylinder fitted inside the pipe, and a pin was used to connect the cylinder to the pipe. The cylinder had a female thread at the end opposite the loading shoe into which a high-strength threaded rod was inserted; this rod was loaded by the ram as described above.



**Figure 4.6** Typical baseline tensile loading shoe



The basic requirements for a tension testing fixture were the following:

1. The fixture must be capable of sustaining the loads required to fail the anchors.
2. The fixture must be of sufficient stiffness such that the fixture can be assumed to act as a rigid system, i.e. the displacement applied by the hydraulic ram must be entirely transmitted to the anchor. In addition, the fixture should be sufficiently stiff so that the displacement of the anchor is approximately equal to the displacement of the anchor less the displacement of the fixture.
3. The fixture must not impose any reaction against the concrete within a distance  $m$ , given by ASTM E488-90 [10].
4. The reaction of the fixture on the concrete must be applied in such a manner as to prevent damage to the concrete block.
5. Since the blocks were not tied to the laboratory floor, the system must be self-equilibrating.

Given these criteria, two tension testing fixtures were used for this part of the program. The first, shown in Figure 4.7 and Figure 4.8, was used for the smaller expansion anchors. The fixture was essentially a ring of steel, atop which was mounted back-to-back steel channels. A plate, welded on top of the channels, had a hole in it which allowed a 1-inch or 1-1/4 inch diameter high-strength threaded rod to pass through to the surface of the concrete. The hydraulic ram was positioned on top of this plate.

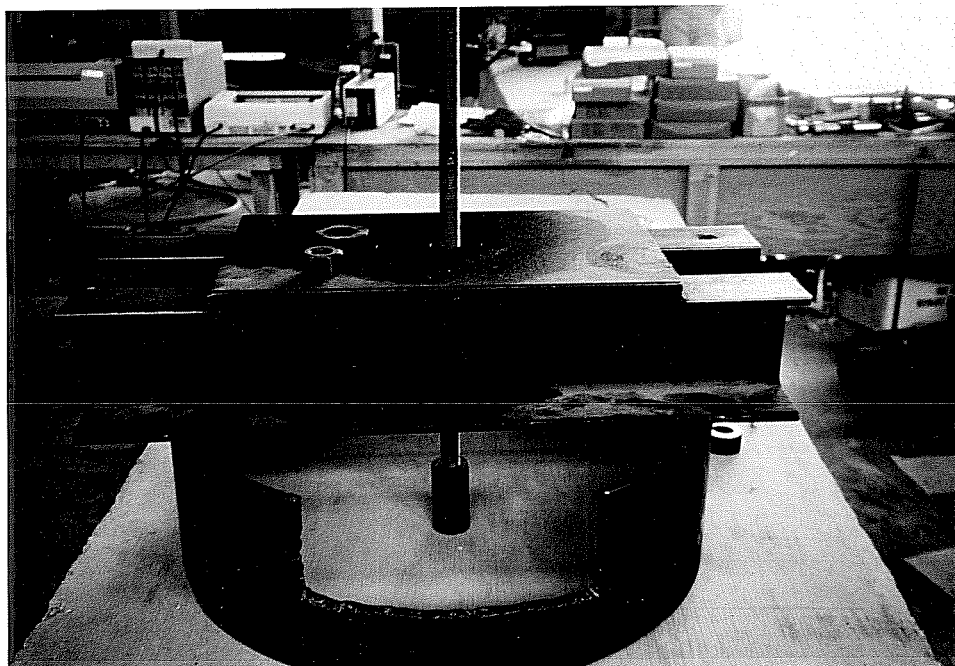


Figure 4.7 Tensile ring testing fixture

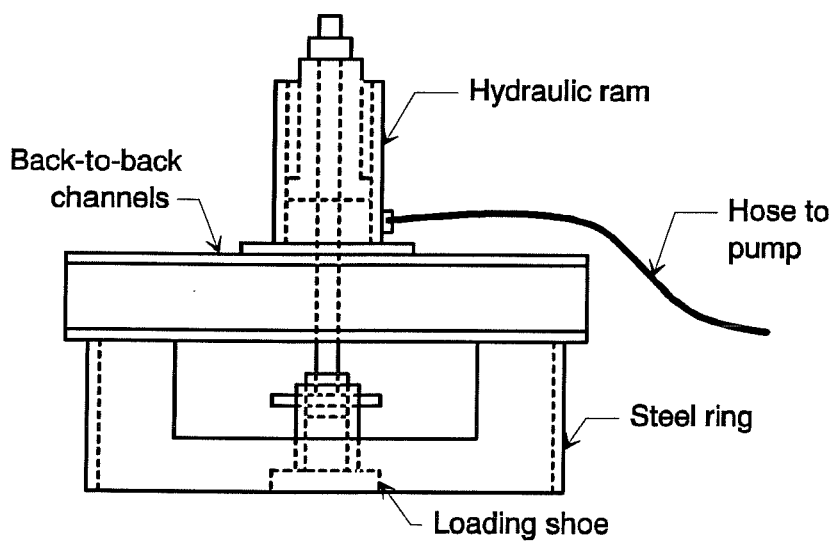
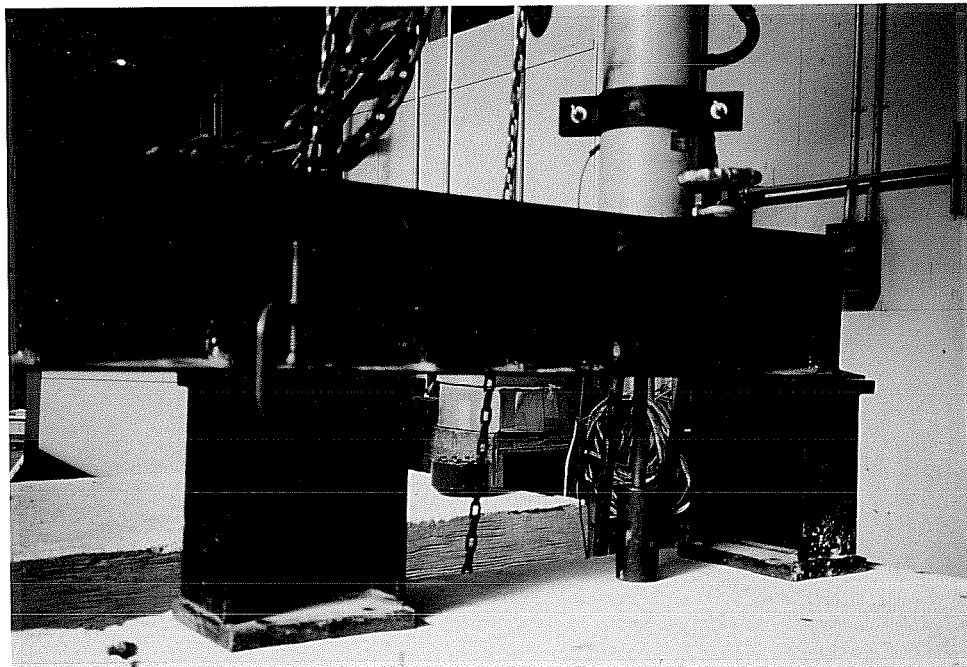


Figure 4.8 Tensile ring testing fixture

The second tension loading fixture, shown in Figure 4.9, was a stiff steel beam. This fixture was used to load the larger expansion anchors and all of the undercut anchors. The beam was composed of back-to-back channels, mounted on short wide-flange columns. A threaded rod passed between the channels to the surface of the concrete. The hydraulic ram was positioned on top of the beam.

In shear, three loading plate sizes were used: small, medium, and large. The sizes were selected to comply with the area requirements set forth in ASTM E488-90 [10]. These requirements are based primarily on the amount of friction generated between the loading plate and the concrete. Since friction increases with increased preload (and therefore with increasing anchor size), the area requirements are a function of anchor diameter. Additionally, a sheet of polytetrafluoroethylene was placed between the plate



**Figure 4.9 Tensile beam testing fixture**

and the concrete, in accordance with ASTM E488-90 [10], to aid in the reduction of this friction. A typical shear loading plate is shown in Figure 4.10. The plate is essentially a two-inch thick block of steel which has at one end a female thread to accept a high-strength threaded rod. The loading plate had a 2-1/4 inch diameter threaded hole perpendicular to its plan. Various 2-1/4 inch diameter threaded baseplates were used to accommodate all types and sizes of anchors.

The same basic requirements for the tension fixture apply to the shear testing fixture. The shear fixture used in this testing program is shown in Figure 4.11. The fixture consisted of back-to-back channels (which served as a beam) mounted to two L-shaped reaction brackets. Two different beams were used: the beam described in the paragraph above was used for larger anchors, and a similar but smaller beam was used for smaller anchors. In either case, a threaded rod passed between the channels to the loading plate. As the anchor was loaded, the L-shaped brackets bore against the side of the concrete block. The hydraulic ram was positioned horizontally on the flanges of the beam, and was supported by a wooden stand until loading began.

### **4.2.3 Instrumentation for Baseline Tests**

Load and displacement data were required for all tests. These data were recorded electronically (see Section 4.2.4) to facilitate the subsequent generation of computer-generated graphs.

A 10,000 psi pressure transducer was used to obtain pressure values. The transducer was connected to the pump in parallel with the ram, so that the load could be calculated using the ram area.



**Figure 4.10 Typical shear loading plate**



**Figure 4.11 Shear testing fixture**

Displacement was measured by a 2-inch or a 6-inch linear potentiometer. In tension tests, the potentiometer was placed on the top surface of the baseplate part of the loading shoe. In shear tests, the potentiometer was placed on the side of the loading plate opposite the testing fixture.

#### 4.2.4 Data Acquisition and Reduction for Baseline Tests

The complete data acquisition system is shown schematically in Figure 4.12. Data for the pressure transducer were gathered by first applying a 10-volt excitation to the amplified transducer signal, then feeding the signal to a Hewlett Packard HP 7090A plotter/data acquisition system (DAS), where the data were recorded and temporarily stored in the buffer. Data for the linear potentiometer were gathered by feeding the signal directly to the DAS, where the data were recorded and temporarily stored in the buffer. After each test, the buffer was downloaded to an IBM XT/370 personal computer. Data were then stored on diskettes in comma-separated value format. Data were then reduced from voltages to load and displacement values:

$$P = 10,000 \text{ psi} \left( \frac{V_{pt}}{10V} \right) A$$

where

$P$  = load, pounds

$v_{pt}$  = voltage from pressure transducer after excitation, volts

$A$  = hydraulic ram area, square inches

$$\Delta = x \left( \frac{v_{lp}}{10V} \right)$$

where

$\Delta$  = displacement, inches

$v_{lp}$  = voltage from linear potentiometer, volts

$x$  = total travel of potentiometer, inches

Load versus displacement curves were then plotted using commercially available micro-computer software.

#### 4.2.5 Test Procedures for Baseline Tests

Four basic steps were carried out to test anchors under monotonically increasing load in either tension or shear:

1. Anchor installation
2. Testing equipment and instrumentation setup
3. Anchor loading
4. Information recording

##### *Anchor installation:*

First, the location of the anchor on the concrete block was determined. The anchors were located at least a distance  $m$  away from any

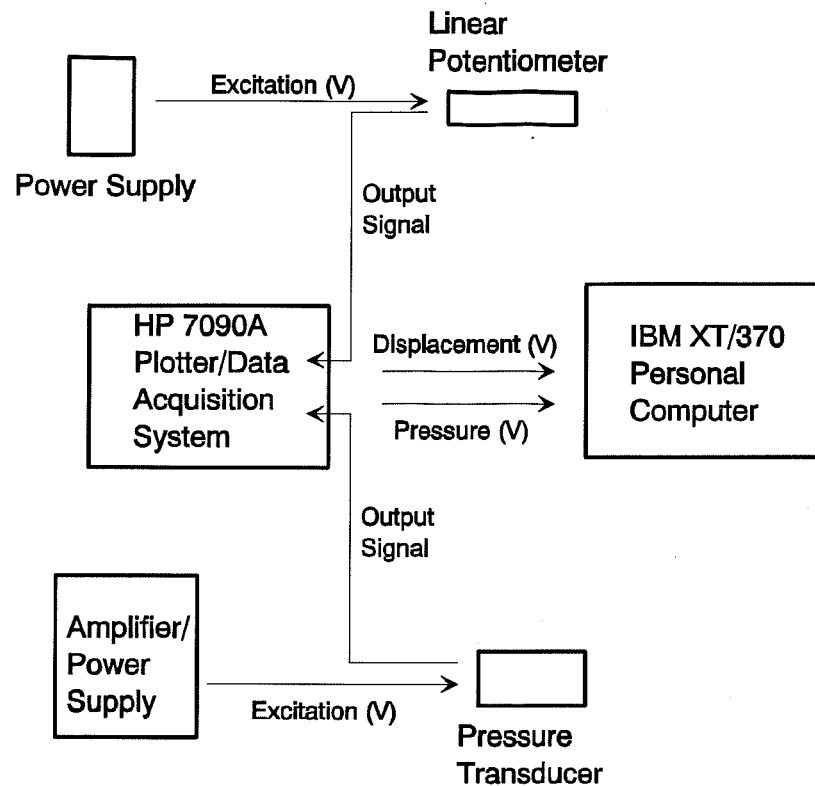


**Figure 4.12 Schematic of data acquisition system for baseline tests**

discontinuities, as prescribed by ASTM E488-90 [10]. In addition, the anchor location had to be such that the testing fixture could be placed in an appropriate position for anchor loading.

Second, the hole was drilled. For the expansion anchors, this was accomplished by a hammer drill. For the undercut anchors, hole drilling was a two-step process: the hole was cored using a coring machine, then an



undercut was formed at the base of the cored hole using an undercutting tool (Figure 4.13).

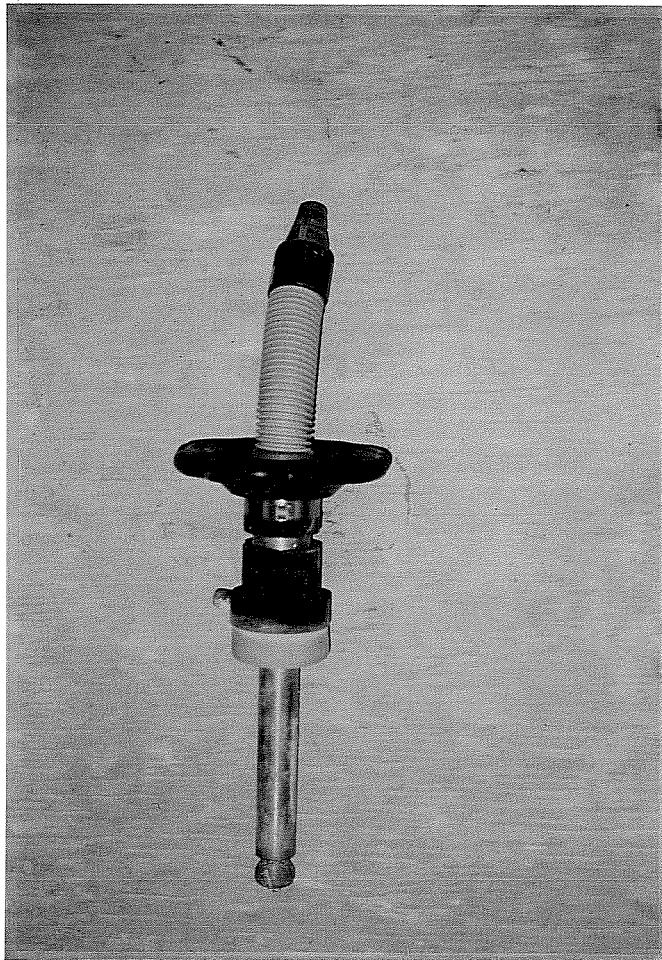


**Figure 4.13 Undercutting tool for installation of undercut anchors**

Third, the hole was cleaned. For expansion anchors, compressed air was used to free the hole of excess concrete dust created by the drilling process. For the undercut anchors, a vacuum cleaner was used to remove excess cooling water from the hole.

Fourth, the anchor was tapped into the hole with a hammer. For the undercut anchors, a tightening tool was used at this point to expand the sleeve into the undercut.

Fifth, the loading shoe or plate was placed over the anchor. A washer and nut were then placed on the anchor over the shoe, and the nut was tightened to a specified installation torque [4].

Sixth, the nut was loosed and retightened to 50% of the specified installation torque. This step was conducted in order to account for preload relaxation, as test results have shown that the preload drops significantly within the first few hours after tightening, and then asymptotically approaches about half of the original torque.

#### *Testing equipment and instrumentation setup:*

After the anchor was installed, the fixture was placed in the appropriate position for testing, and the threaded rod was attached to the loading shoe or plate. Then, the linear potentiometer was placed in its proper position (Section 4.2.3). The initial voltage values corresponding to pressure and displacement were checked to ensure non-zero initial values. Initial values of zero would indicate either that the transducer or potentiometer was positioned below the level at which it could record data, or that there was a misconnection in the wiring.

*Anchor loading:*

After the correct settings on the data acquisition system were verified, the system was activated and loading commenced. Load was applied at the rate specified in ASTM E488-90 [10] (Section 4.2.1). Load application was stopped when the anchor failed, or after six minutes, whichever came first.

*Information recording:*

The load and displacement values were then downloaded to the computer and stored in comma-separated value format for later conversion to engineering units. In addition, the following information was recorded by hand for each test:

- Anchor type and diameter
- Concrete block number
- Total test time
- Failure mode
- Ram area
- Potentiometer travel

### **4.3 Seismic Tests**

#### **4.3.1 Loading for Seismic Tests**

Seismic tests involved low-cycle sinusoidal loading intended to represent typical earthquake-induced loads. The waveform, shown for tension in Figure 4.14 and for shear in Figure 4.15, was stepped and lasted a total of 270 cycles. The first portion of the test consisted of 60 cycles to a peak load of 60% of the maximum service load expected on the anchor. The

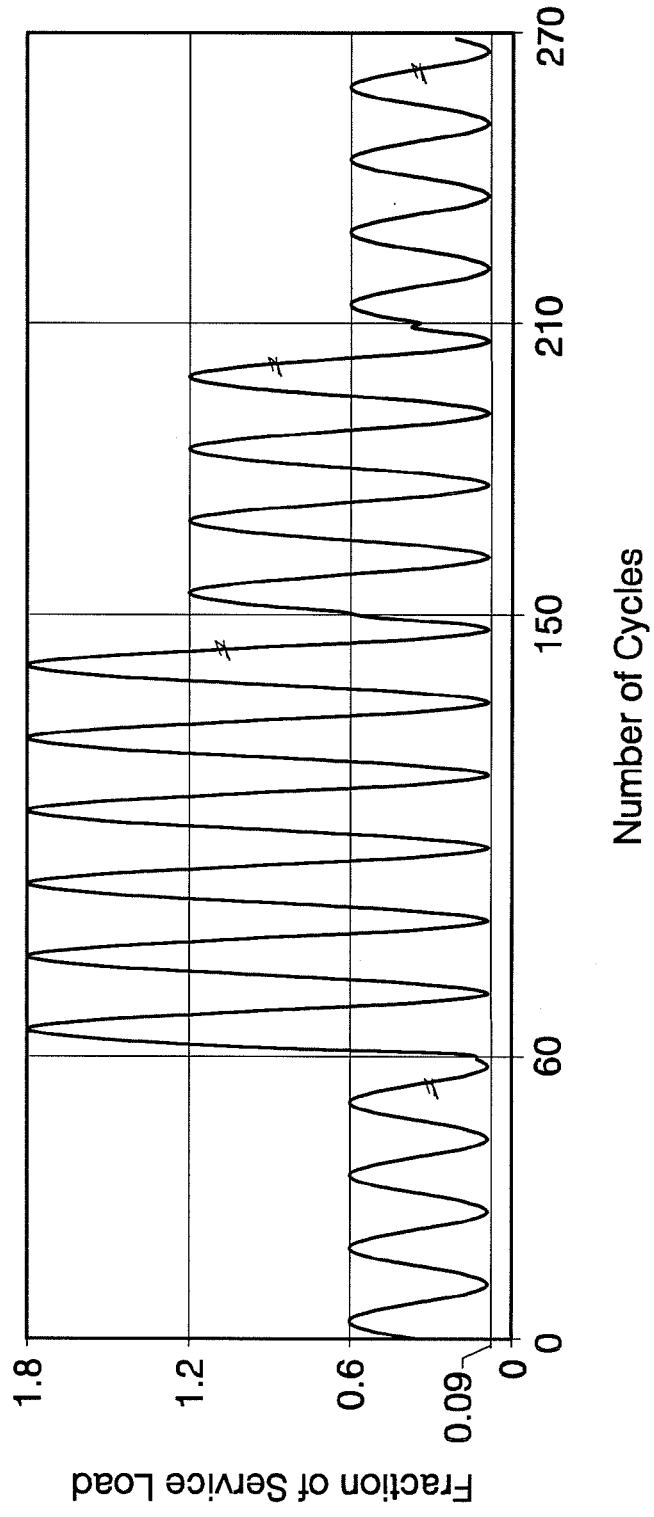


Figure 4.14 Tensile seismic waveform used in testing program

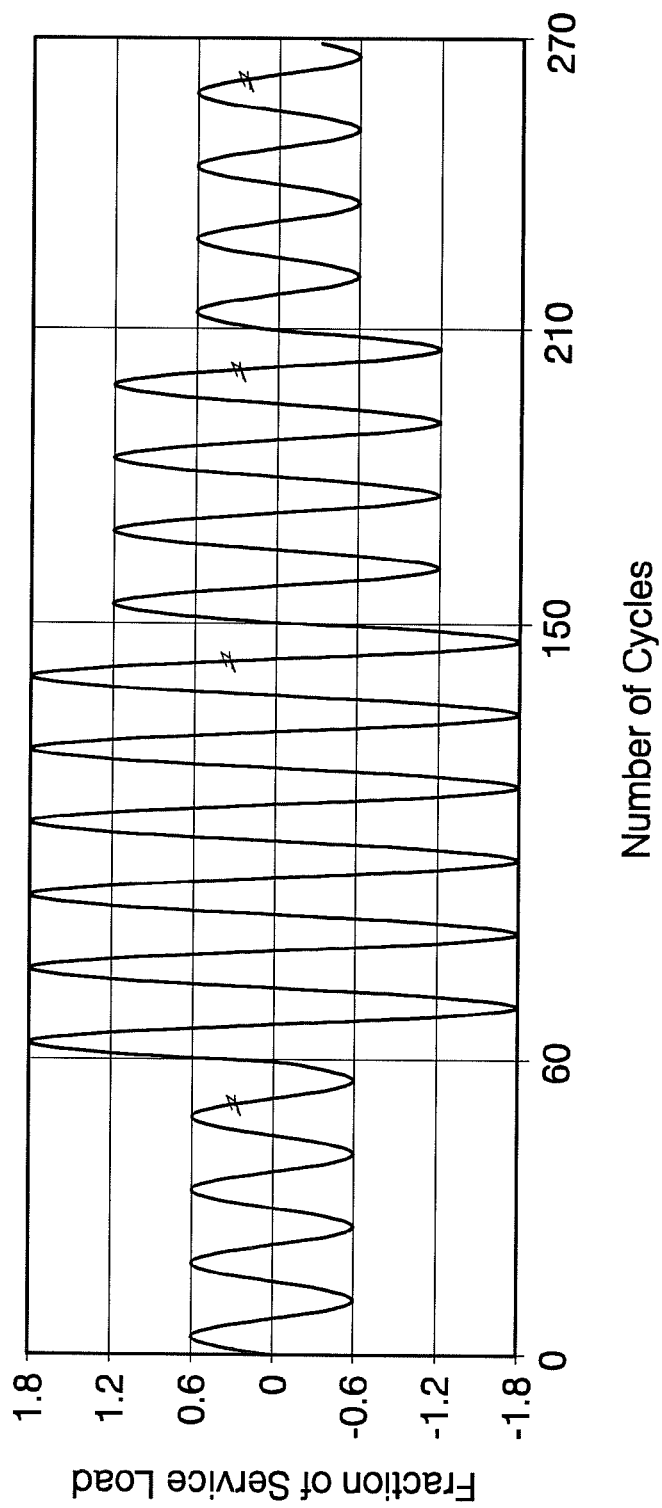


Figure 4.15 Shear seismic waveform used in testing program

second portion of the loading consisted of 90 cycles to a peak load of 1.8 times the service load. The next loading portion was 60 cycles to a peak load of 1.2 times the service load. The remaining 60 cycles had a peak load of 60% of the service load. Anchors that did not fail under this seismic loading were then tested monotonically to failure.

For tensile tests, the minimum load for the entire test was 9% of the service load. For shear tests, the direction of loading was reversed, so the peak loads described above were attained in both directions for each cycle. The desired frequency of the waveforms was 5 Hertz.

#### **4.3.2 Test Setup for Seismic Tests**

For the tensile seismic tests, the loads were applied by a 60-ton Enerpac double-action hydraulic centerhole ram. Oil was supplied to the ram from a 27 gallon per minute (gpm) electric pump. The oil passed through a 20 gpm line tamer and entered a 15 gpm servo-valve. The amount of oil flowing to and from the ram depended on the position of the valve, which was controlled to operate in a sinusoidal fashion by a Pegasus servo-controller. An MTS function generator supplied the function signal to the controller.

The tensile loading shoe used for these tests is shown in Figure 4.16. It consists of two parts: a 2-3/4 inch diameter, 6-inch high cylindrical portion and a 2-1/4 inch diameter threaded baseplate. The cylindrical portion had a threaded hole at the top to allow the connection of a high-strength threaded rod. A 2-1/4 inch diameter section was hollowed out of the lower four inches of the cylinder, and the bottom 1-1/4 inch of the

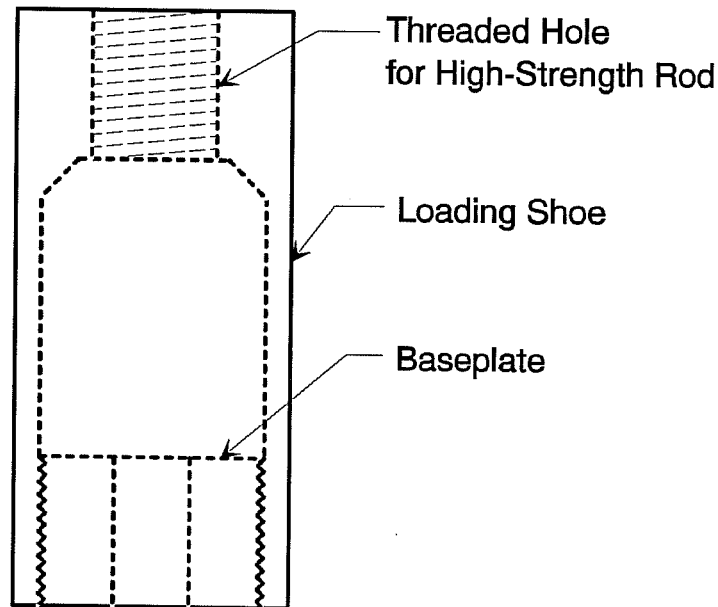


**Figure 4.16 Tensile loading shoe for dynamic tests**

hollow portion was threaded. The baseplate could then be threaded directly into the cylinder.

The testing fixture used for the tensile seismic tests was identical to the large fixture used for the tensile baseline tests (Section 4.2.2).

The shear loading plates used were identical to those used for the shear baseline tests (Section 4.2.2).

For the shear seismic tests, the loads were applied by a large capacity double-action hydraulic tension ram. The hydraulics of the system were the same as for seismic tension tests, and the loading plates used were the same ones as were used for the baseline shear tests.

To test the anchors under reversed loading, it was necessary to tie the concrete blocks to the laboratory floor. This was done with high strength

threaded rods, which passed through holes in the blocks and were threaded into the floor.

The anchors were tested using a high-strength threaded rod, which was connected to the loading plate. This rod was coupled to a larger diameter threaded rod which was screwed into the tension ram. The ram was bolted to a beam, which was fabricated from back-to-back channels. Four sets of back-to-back channels formed two angles, which were bolted into the laboratory floor and served as reactions. Therefore, the ram could be moved between sets of bolt holes along the length of the beam to test anchors along the length of a block.

#### **4.3.3 Instrumentation for Seismic Tests**

For tensile seismic tests, 60-kip fatigue-rated load cell was placed atop the beam. The Pegasus controller fed the command signal to the servo-valve as described above, and the load cell returned the feedback signal to the controller. The controller then read the error, or difference between the two signals. If the error exceeded user-specified limits, the system would shut down. The load on the anchor was monitored continuously by the load cell.

The closed-loop control system for the shear seismic tests was similar, except that a pressure transducer was used in place of the load cell.

For both tensile and shear seismic tests, the displacement was recorded in the same manner as for the baseline tests.



#### 4.3.4 Data Acquisition and Reduction for Seismic Tests

Data were recorded and reduced for tensile and shear seismic tests in the same manner as the baseline tests (Section 4.2.4), except that, for the tensile seismic tests, the DAS received input from the load cell instead of the pressure transducer.

#### 4.3.5 Test Procedures for Seismic Tests

Four basic steps were carried out to test anchors under seismic load in either tension or shear:

1. Anchor installation
2. Testing equipment and instrumentation setup
3. Anchor loading
4. Information recording

##### *Anchor installation:*

Anchors were installed for either tensile or shear seismic tests as described in Section 4.2.5, except that the cylindrical part of the tensile seismic loading shoe had to be screwed on after retightening the anchor to 50% of the specified installation torque.

##### *Testing equipment and instrumentation setup:*

For tensile seismic tests, the beam was positioned on the concrete, and the hydraulic ram was placed on the beam. A high-strength threaded

rod was then fed through the centerhole in the ram to the loading shoe and was screwed into the shoe. The load cell was placed atop the ram, and the potentiometer was positioned on the loading shoe. The data acquisition system preparation was similar to that for the baseline tests (Section 4.2.5). The electric pump, water pump, and fan were then turned on, and testing was ready to begin.

*Anchor loading:*

For the tensile seismic tests, the minimum load of the waveform shown in Figure 4.14 was applied statically. This step was unnecessary for the shear seismic tests because of the reversed loading application. Then, the testing frequency was selected. The command function was input to the function generator, and the servo-valve was activated. The load span was increased, and the static load (for tensile tests) and span were adjusted iteratively until the correct load values were obtained. The feedback waveform was observed on an oscilloscope and compared with the command waveform. The test was run for 270 cycles and stopped manually.

*Information recording:*

The data for the tensile and shear seismic tests were recorded in a similar manner as for the baseline tests.

## **4.4 Fatigue Tests**

### **4.4.1 Loading for Fatigue Tests**

Fatigue loading consisted of 2,000,000 load cycles for each anchor. Anchors that did not fail under this cyclic loading were then tested monotonically to failure.

Anchors were loaded in fatigue using a sinusoidal waveform. The amplitude of the waveform was 90% of the allowable service load for the particular type and diameter anchor being tested, with the maximum load corresponding to the allowable load and the minimum load corresponding to 10% of this value.

The frequency of the waveform depended primarily on the limitations of the testing equipment, the direction of loading (tension or shear), and the anchor type and diameter. In general, anchors were tested as fast as practical given the above limitations.

### **4.4.2 Test Setup for Fatigue Tests**

Loads were applied to the anchors by either of two hydraulic rams, which rested on the concrete surface: a 60-ton Enerpac double-action ram was used for the smaller anchors; a larger capacity double-action ram was used for the larger anchors. The hydraulics of the system were similar to those for the seismic tests (Section 4.3.2), except a Pegasus function generator supplied the function signal to the controller.

The loading shoes and plates used for the fatigue tests were identical to those used for the seismic tests (Section 4.3.2).

Due to the duration of fatigue tests and the number of anchors to be tested under this program, it was desirable to test more than one anchor at a time. Thus, the requirements of the loading fixture were:

1. The fixture must load the anchors concentrically.
2. The fixture must be capable of sustaining the loads required to test the anchors under service loads.
3. The fixture must be capable of withstanding the cyclic fatigue resulting from the application of load.
4. The fixture must be of sufficient stiffness so that it can be assumed to act as a rigid system, i.e. the displacement applied by the hydraulic ram must be entirely transmitted to the anchor.
5. The reaction of the fixture on the concrete must be applied in such a manner so as to prevent damage to the concrete block.
6. Since the blocks were not tied to the laboratory floor, the system must be self-equilibrating.

In tension, three anchors were loaded simultaneously with the fixture shown in Figures 4.17 and 4.18. This fixture is comprised of a 1-inch thick hexagonal steel plate. The plate has six 1-inch stiffeners, and six 1-5/16 inch diameter holes were drilled between the stiffeners near the vertices of the plate. A 1/2-inch thick steel pipe was welded on the bottom surface of the plate. Partial penetration welds were used throughout to connect the various pieces of the fixture together. This fixture was placed atop the ram, and a high-strength threaded rod was passed from the fixture to each of three

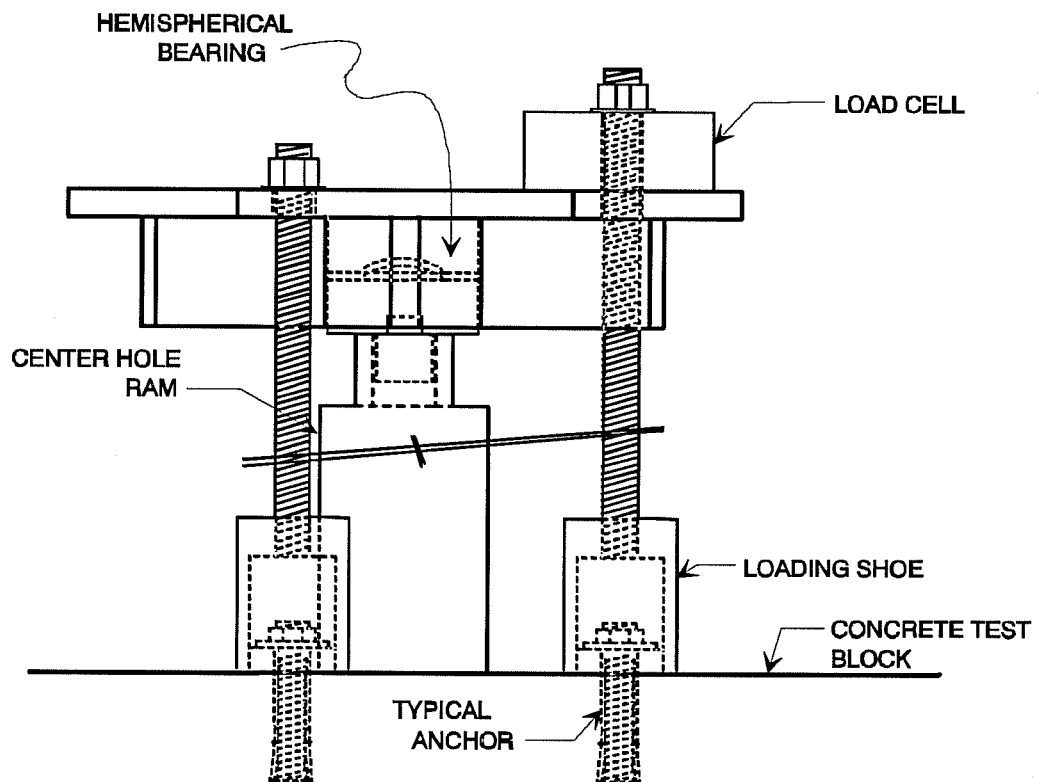
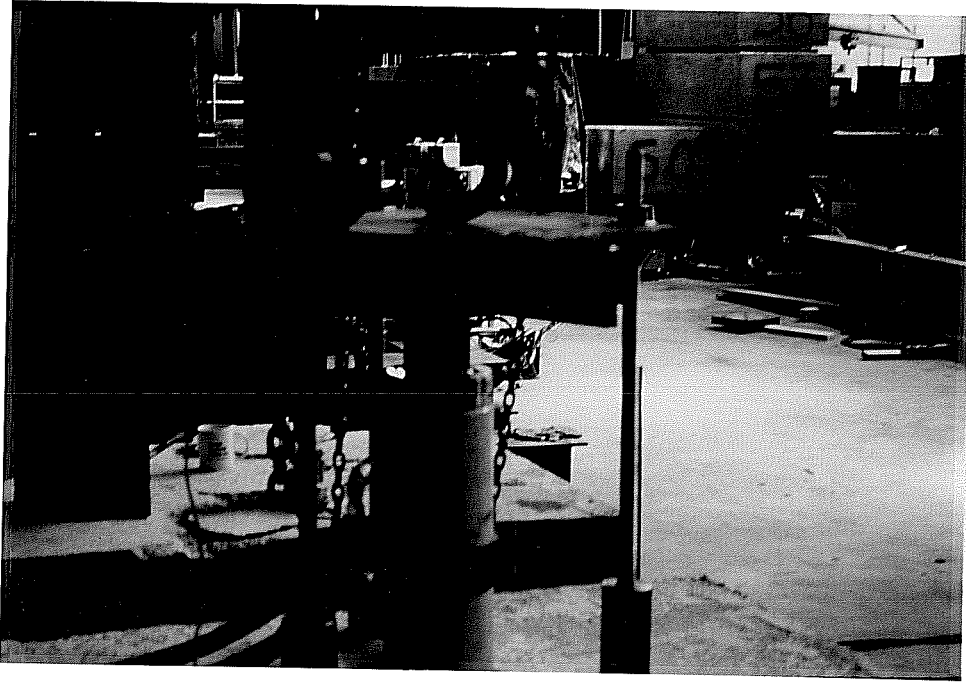


Figure 4.17 Tensile fatigue testing apparatus



**Figure 4.18 Tensile fatigue testing fixture (testing in progress)**

loading shoes. Note that in case one anchor failed, the plate could be turned around and a new anchor installed at the vertex opposite to the one corresponding to anchor failure (see Figure 4.19). This feature would enable the remaining anchors to be tested to the completion of the 2,000,000 cycles.

During tensile fatigue loading, load was monitored using a load cell on only one of three anchors. Due to the statical determinacy of the system, the load on the remaining two anchors was equal to the load on the anchor with the load cell. Due to the slight mass imbalance produced by the load cell, it was calculated that the forces in the anchors would differ by at most 0.14%. This difference was judged to be insignificant. If the loads on the three anchors were significantly unequal at any time during the test, the result would be out-of-limit readings from the load cell, and the system

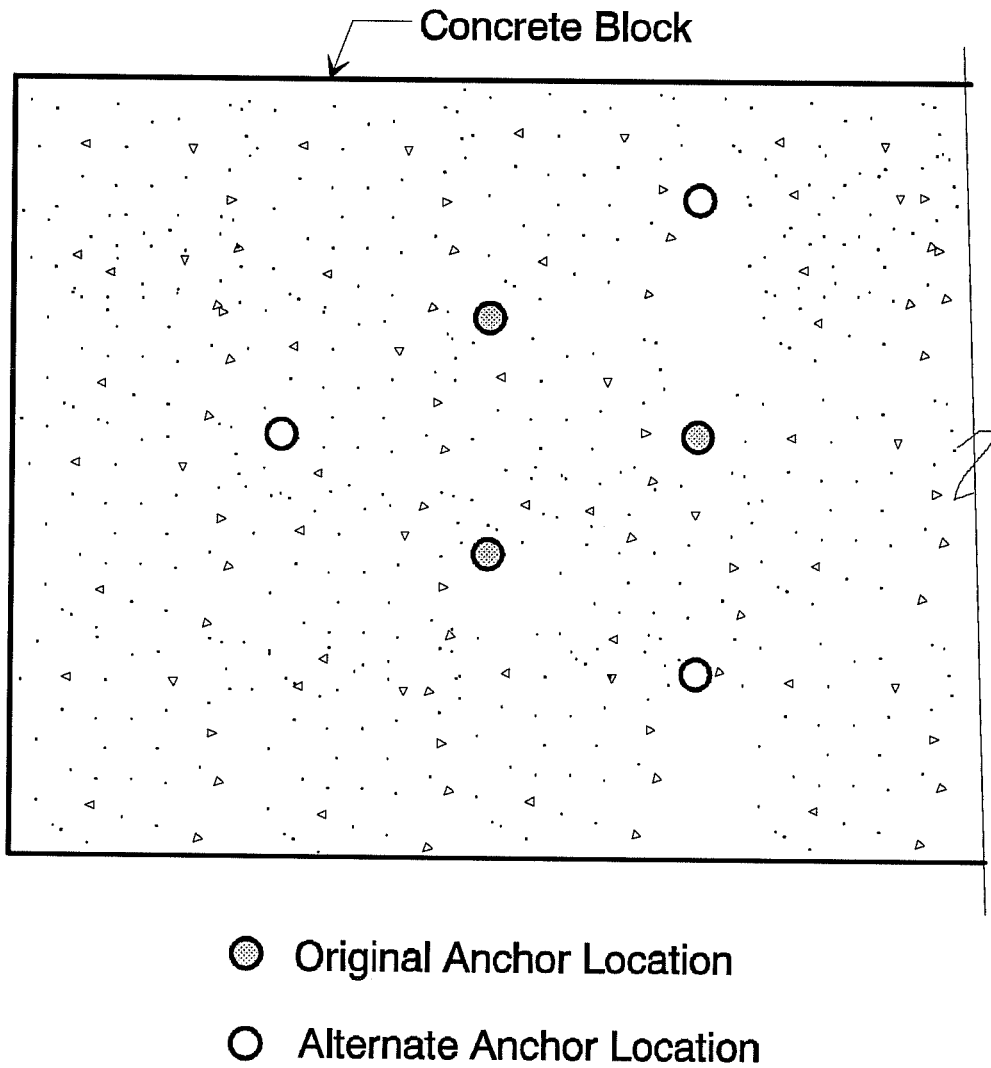


**Figure 5.19** Alternate anchor locations for tensile fatigue failure

would shut down.

For the reasons given above, it was desirable to test more than one anchor simultaneously in shear fatigue. The shear fatigue testing fixture was

For the reasons given above, it was desirable to test more than one anchor simultaneously in shear fatigue. The shear fatigue testing fixture was essentially a stiff beam. An hydraulic ram rested on the beam, and the hexagonal plate fixture described above was positioned on top of the ram.

Two anchors were simultaneously tested in shear fatigue. Two concrete blocks were positioned on their sides and were placed next to each other. An anchor was installed in the facing surfaces of each block at equal distances from the laboratory floor, and were loaded using the shear plates via threaded rods passing to the hexagonal fixture.

If the anchors survived the entire cyclic loading, they were tested monotonically to failure. The test setup for these tests was identical to that used for the baseline tests, except that the tensile loading shoes described in this section were used instead of the shoes described in Section 4.2.2.

#### **4.4.3 Instrumentation for Fatigue Tests**

For tensile fatigue tests, a 50-kip load cell or a 60-kip fatigue-rated load cell was placed atop the loading fixture over one of the three threaded rods. The feedback circuit for the fatigue tests was the same as the one used for the seismic tests (Section 4.3.3).

For shear fatigue tests, the 60-kip fatigue-rated load cell was placed atop one of the threaded rods. The load and function signals were then commanded and monitored as for the tensile fatigue tests.

Due to the length of the tests, no continuous displacement readings were taken for the fatigue tests. However, final displacement readings were taken when possible. If the anchors survived the entire cyclic loading, the final monotonic tests were instrumented identically to the baseline tests.



#### **4.4.4 Data Acquisition and Reduction for Fatigue Tests**

No data were continuously recorded for the fatigue tests. Data for the subsequent monotonic tests, if conducted, were recorded and reduced in exactly the same manner as for the baseline tests.

#### **4.4.5 Test Procedures for Fatigue Tests**

Four basic steps were carried out to test anchors under fatigue load in either tension or shear:

1. Anchor installation
2. Testing equipment and instrumentation setup
3. Anchor loading
4. Information monitoring

##### *Anchor installation:*

For multiple anchors tested simultaneously from a common fixture, layout was crucial. The anchors were arranged so that if any of the anchors failed in fatigue before reaching 2,000,000 cycles of load, cycling could be completed on the remaining anchors. That is, a suitable location on the concrete surface would be needed to install another anchor at the opposite vertex as described in Section 4.4.2 for tensile fatigue tests.

The remainder of the anchor installation was conducted similarly to that described in Section 4.2.5, except that the cylindrical part of the tensile fatigue loading shoe had to be screwed on after retightening the anchor to 50% of the specified installation torque.

*Testing equipment and instrumentation setup:*

For tensile fatigue tests, the hydraulic ram was then placed in the center of the bolt group to keep the loads on the anchors equal. For shear tests, the beam was placed on the concrete, and the ram was then positioned at midspan of the beam.

In either case, the hemispherical bearing was then placed on the ram and lubricated with anti-seize compound. The hexagonal fixture was placed on the bearing and levelled. The load cell was positioned over one threaded rod, all nuts on the rods were tightened until snug, and the fixture was checked to make sure it was level.

The dial gauges were then placed in their appropriate positions, zeroed, and taped up until the end of the test to prevent damage to them. The cycle counter was zeroed and set to shut down the system when the test reached 2,000,000 cycles. The electric pump, water pump, and fan were then turned on, and testing was ready to begin.

*Anchor loading:*

Initially, the mean load was applied statically to the anchors. Then, an initial low frequency was chosen, and the servo-valve was activated. The load span was then increased, and the mean load and amplitude were adjusted iteratively until the correct maximum and minimum loads were obtained. The feedback waveform was observed on an oscilloscope and compared with the command waveform. The frequency was increased to the maximum that could be obtained for the given anchor size and configuration. The error was checked, and the upper and lower limits and override were set so that the system would shut down if any of these were exceeded.

*Information monitoring:*

Tests were monitored at intervals throughout to observe the performance of the system. Among the items checked:

- Load maintained at the appropriate levels
- Error not approaching the limiting error
- Counter functioning properly
- General performance of the system, i.e. level plate, little or no threaded rod vibrations, no oil leaks, pump not overheating, etc.

## **4.5 Shock Tests**

### **4.5.1 Loading for Shock Tests**

Shock tests were conducted on anchors to determine their performance both during and after being subjected to impact loads. Shock loading consisted of the application of two shock pulses. Anchors that did not fail under these pulses were tested monotonically to failure.

Anchors were shock-tested using a waveform similar to that shown in Figure 4.20. The amplitude of the waveform was 2.5 times the maximum service load expected on the anchor, with a maximum load of 3 times the service load, and a minimum of 0.5 times the service load.

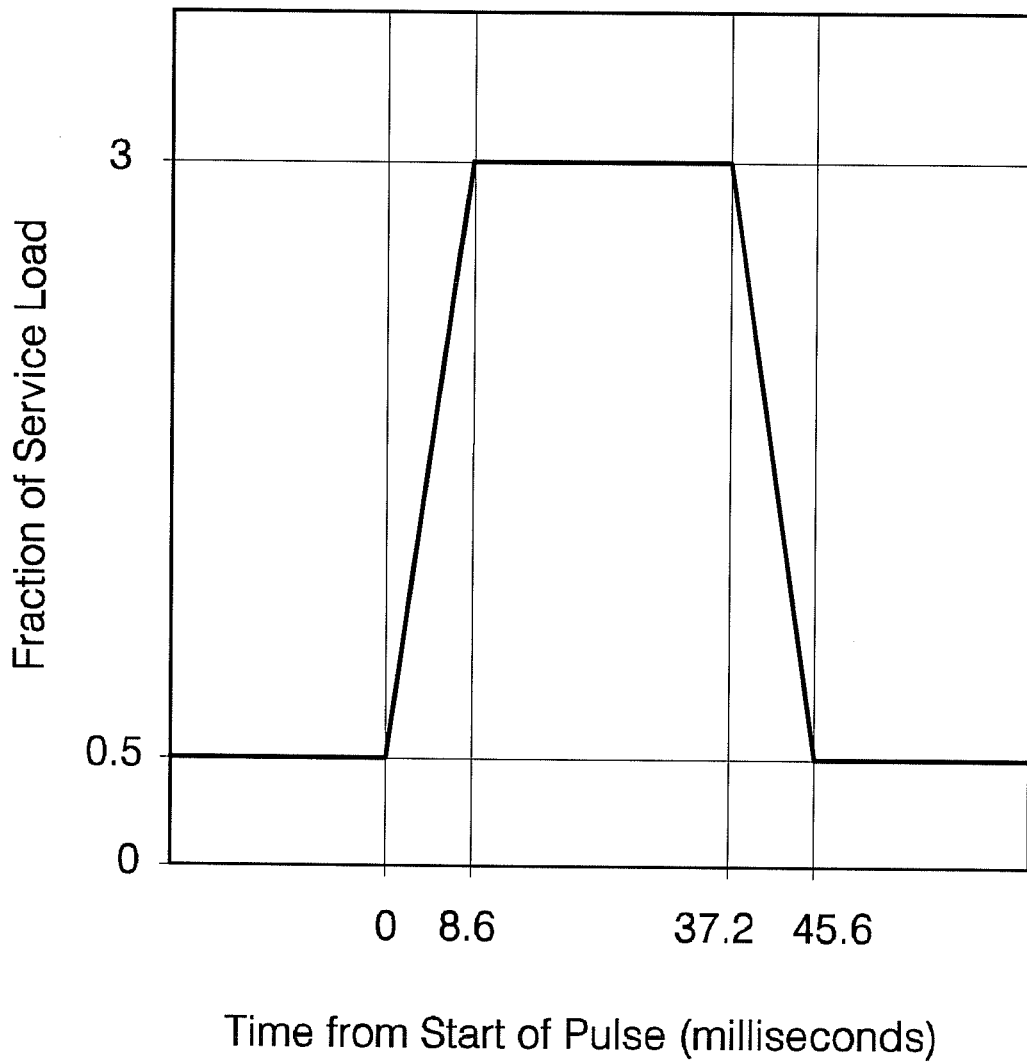


**Figure 4.20 Shock waveform used in testing program**

#### **4.5.2 Test Setup for Shock Tests**

The test setup for shock tests was the same as for the tensile seismic tests (Section 4.3.2), except that an Exact function generator was used to create the command waveform, and the DAS had to be triggered due to the short duration of the tests. The DAS was triggered by the function generator; when the voltage exceeded a specified value, the DAS recorded all subsequent data. In addition, data from a specified interval before the trigger was stored in the buffer, so that the complete feedback waveform could be later reproduced.

#### **4.5.3 Instrumentation for Shock Tests**

The instrumentation for the shock tests was identical to that used for the tensile seismic tests (Section 4.3.3), except that a 25-kip load cell was used for the smaller expansion anchors.

#### **4.5.4 Data Acquisition and Reduction for Shock Tests**

The procedures for data acquisition and reduction for the shock tests were identical to those for the tensile seismic tests.

#### **4.5.5 Test Procedures for Shock Tests**

The steps involved in testing anchors in shock were similar to those for the tensile seismic tests (Section 4.3.5). There were only three differences between these types of tests. First, an Exact function generator

was used for the shock tests instead of the MTS function generator. Second, since the shock tests consisted of only two cycles, the span had to be read before testing began. Third, since the duration of the shock tests was so short, the function generator was triggered manually for both cycles.

## 5. TYPICAL RESULTS AND SIGNIFICANCE

### 5.1 Baseline Tests

#### 5.1.1 Tensile Baseline Tests

At the time of this writing, all expansion anchor tensile baseline tests had been completed except for the 12 mm Flush size. More than half of the undercut anchor tensile baseline tests had been completed. The following failure modes were observed for these tests:

- Anchor fracture
- Thread stripping
- Concrete cone breakout
- Anchor pullout
- Anchor pull-through

The characteristics of each failure mode will now be described in detail, with reference to typical results for each mode.

*Anchor fracture:* Anchor fracture is shown in Figure 5.1. The smallest expansion anchor size and all undercut anchor sizes exhibited this failure mode. A typical load-displacement curve is shown for an 8 mm expansion anchor in Figure 5.2. The very high initial stiffness is due to the large anchor preload; the anchor itself received very little of the applied load until the preload was overcome. Figure 5.3 shows the same failure mode for the same anchor type and size; however, the anchor slipped somewhat upon the

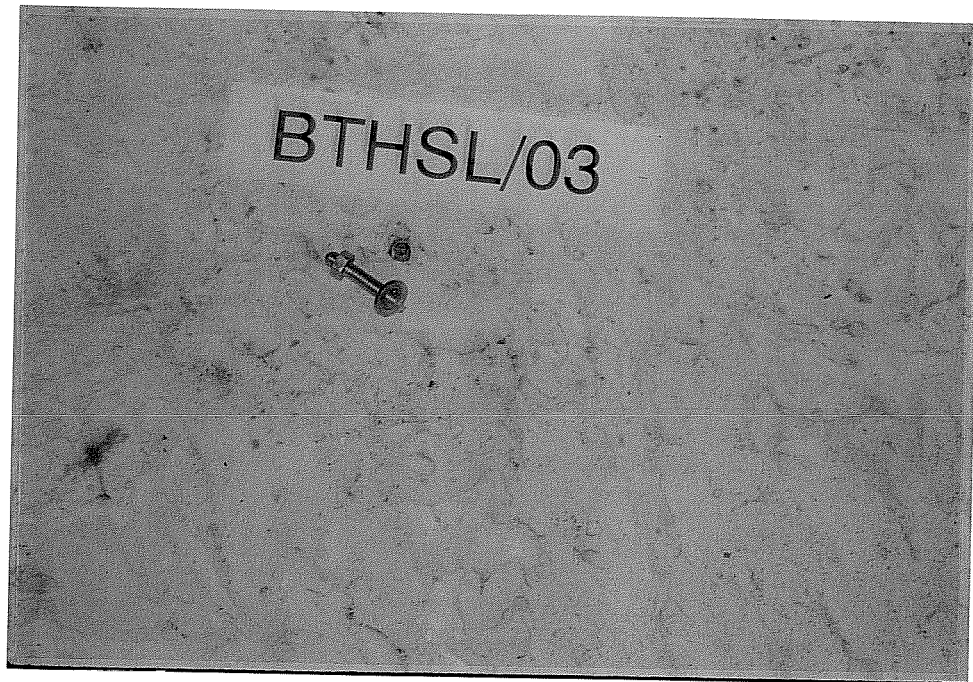


**Figure 5.1 Tensile baseline expansion anchor fracture**

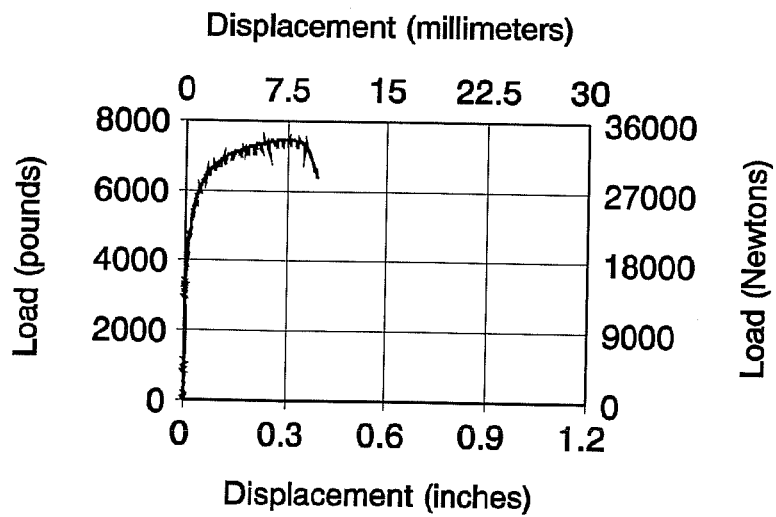


**Figure 5.2 Load-displacement curve for tensile baseline expansion anchor fracture (no slip)**



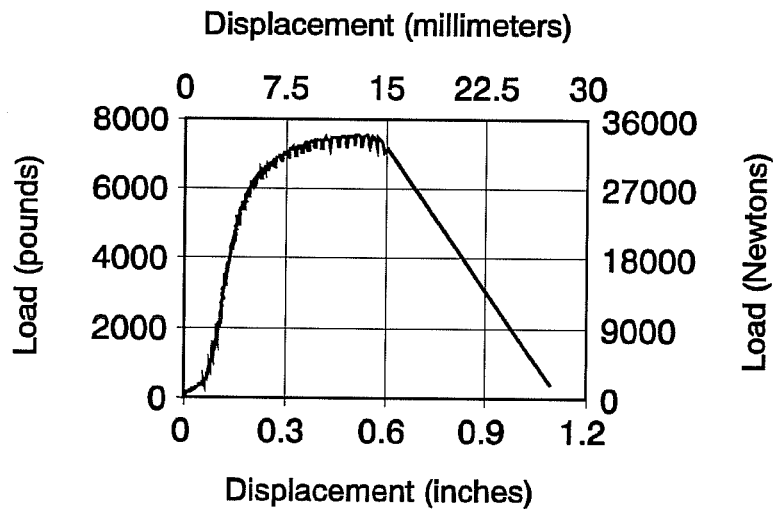


**Figure 5.3 Load-displacement curve for tensile baseline expansion anchor fracture (slip)**

initial application of load before exhibiting very stiff behavior. In both cases, initial yield was about 6 kips, and the ultimate load was about 7.5 kips. Therefore, the only effect that initial slip had on the anchor was to produce greater displacement for a given load; it had no effect on ultimate capacity.

A typical load-displacement curve for an undercut anchor displaying anchor fracture is shown for a 20 mm anchor in Figure 5.4. Note that the initial stiffness for the undercut anchors is not as large as that for the expansion anchors, due to the undercut anchors' lower preload. The undercut anchors have a well-defined yield point and typically exhibit high ductility; that is, they are able to undergo large displacements after first yield without a significant decrease in load-carrying capability.

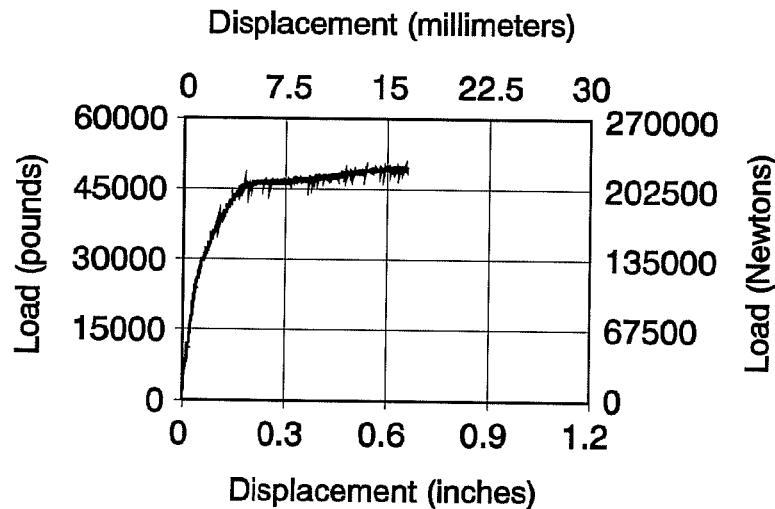


**Figure 5.4 Load-displacement curve for tensile baseline undercut anchor fracture**

*Thread stripping:* This failure mode is generally considered unacceptable behavior for anchors in concrete, mainly because the results are neither reproducible nor predictable. Nonetheless, thread stripping was observed in this testing program for both expansion anchors and undercut anchors. Only one expansion anchor (a 16 mm) exhibited this mode of failure. The failure is shown in Figure 5.5, and the anchor's load-displacement curve is shown in Figure 5.6. The anchor failed at a much lower load than the average for the anchor type and size, and demonstrated no ductility.

Several undercut anchors exhibited thread stripping. A typical failure is shown in Figure 5.7, and the corresponding load-displacement curve is shown in Figure 5.8. This failure mode was not observed on the 20 mm

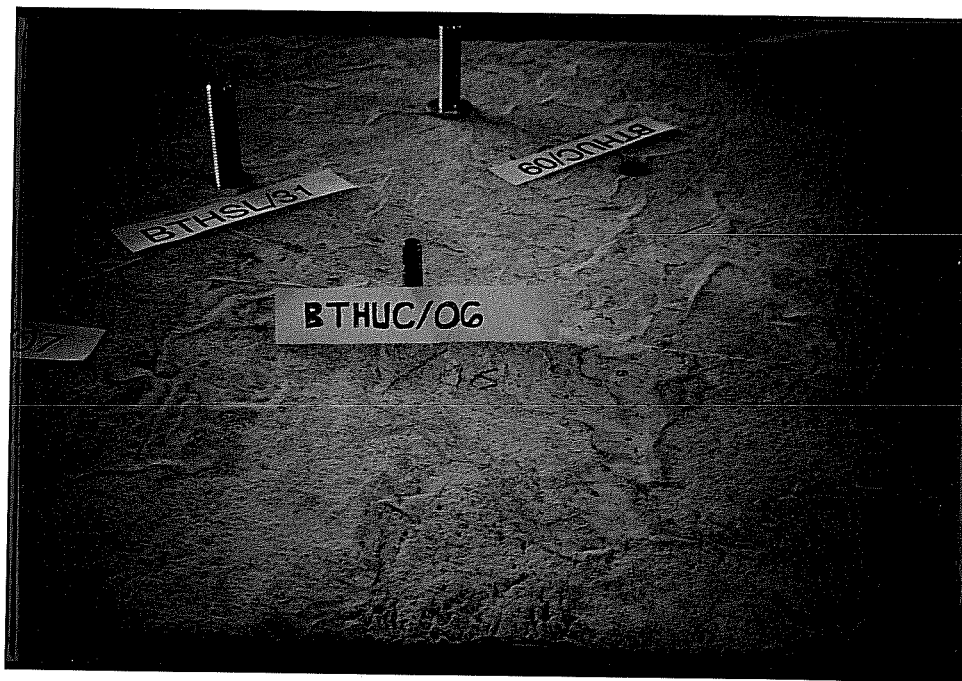


Figure 5.7 Tensile baseline undercut anchor thread stripping

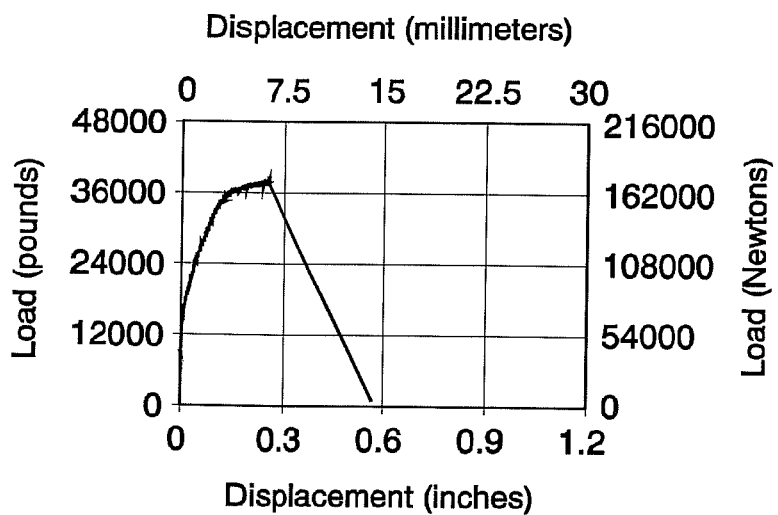


Figure 5.8 Load-displacement curve for tensile baseline undercut anchor thread stripping

anchors, because these anchors were fabricated from a lower strength steel than the 12 mm and 16 mm sizes; therefore, the 20 mm anchor fractured before the threads stripped. The thread stripping problem was investigated by the sponsor, and the sponsor decided to manufacture thicker nuts for the undercut anchors in an attempt to preclude thread stripping. At the time of this writing, the anchors with the thicker nuts had yet not been tested.

*Concrete cone breakout:* This failure mode was observed for most of the expansion anchors; however, no undercut anchors exhibited any concrete failure. A typical concrete cone breakout failure is shown in Figure 5.9, and a typical load-displacement curve is shown in Figure 5.10 for a 16 mm anchor. Typically, the anchors exhibited a very high initial stiffness, for the same reasons as described above for anchor fracture. In addition, a few of the smaller anchors slipped somewhat upon the initial application of load, as for the anchor fracture mode. The anchors failing by the concrete failure mode, however, exhibited an increase in load-carrying capability through a secondary expansion force. This secondary expansion force is due to the bottom of the expansion wedge moving into the expansion sleeve, thereby increasing the available frictional force. As shown in Figure 5.10, the anchor began to displace at a load of about 12 kips, and the curve started to bend in a manner indicative of insipient failure. At a load of about 18 kips, however, the secondary expansion force enabled the anchor to carry load up to its ultimate of 27.8 kips.

*Anchor pullout:* This failure mode occurred in only a few expansion anchor tests, and in no undercut anchor tests. One reason for the small number of anchors failing in this mode is the difficulty in detecting the failure. As an



**Figure 5.9 Tensile baseline expansion anchor concrete cone breakout**

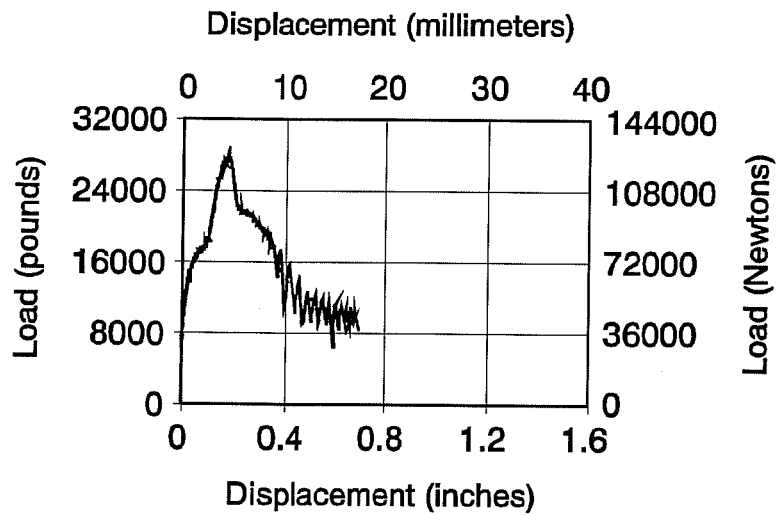


**Figure 5.10 Load-displacement curve for tensile baseline expansion anchor concrete cone breakout**

anchor starts to pull out of its hole in the concrete, the area available for cracking in a conical shape decreases, and a shallow cone usually forms. Anchor pullout is shown in Figure 5.11, and a load-displacement curve for a 24 mm anchor is shown in Figure 5.12. The curves for pullout exhibit the same characteristics as those for concrete breakout, except that the pullout curves reflect the large displacements (slip) at ultimate load.

*Anchor pull-through:* Only one anchor in this testing program failed by anchor pull-through. This failure, which occurred for an 8 mm expansion anchor, is shown in Figure 5.13, and the load-displacement curve is shown in Figure 5.14. Note that the high initial stiffness typical of other expansion anchor failure modes was not present in this test. Therefore, the anchor preload was probably not present, either because of improper torquing or improper operation of the anchor's expansion mechanism. The ultimate load for this anchor was significantly less than that for the other 8 mm expansion anchors; it failed prematurely, as shown by its load-displacement characteristics. This emphasizes the importance of preload to proper expansion anchor performance.

Table 5.1 summarizes typical statistical characteristics (mean and coefficient of variation) of the results obtained for the tensile baseline tests. Generally, the most consistent mode of failure (least scatter in the data) is anchor fracture. Concrete cone breakout is the next consistent mode; other modes of failure (pullout, pull-through, thread stripping) have the most scatter because of their unpredictability.



**Figure 5.13 Tensile baseline expansion anchor pull-through**

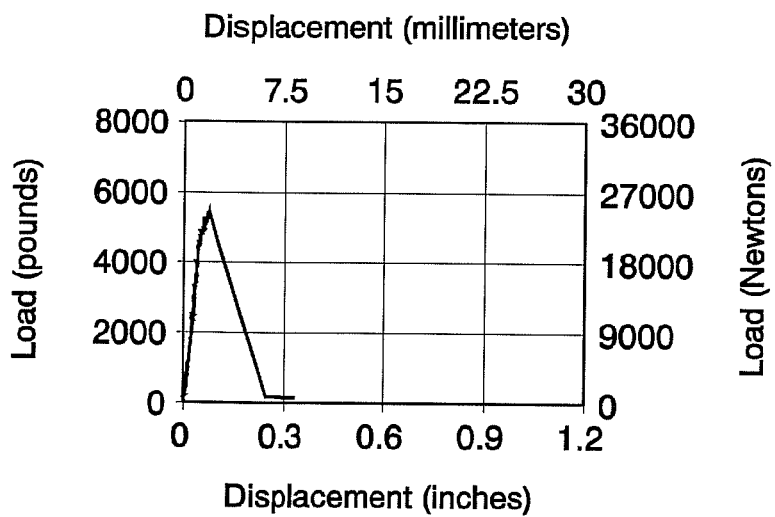


**Figure 5.14 Load-displacement curve for tensile baseline expansion anchor pull-through**

**Table 5.1 Statistical Data for Tensile Baseline Test Failures**

ANCHOR TYPE	SIZE (mm)	ALL FAILURE MODES			ANCHOR FRACTURE			CONCRETE BREAKOUT FAILURE			OTHER FAILURE MODES		
		n	mean (lb.)	COV	n	mean (lb.)	COV	n	mean (lb.)	COV	n	mean (lb.)	COV
Expansion	8	5	6834	0.127	2	7504	0.009	2	6868	0.053	1	5426	--
	10	5	10960	0.116	--	--	--	4	10927	0.134	1	11092	--
	12	5	13970	0.087	--	--	--	5	13970	0.087	--	--	--
	16	5	24338	0.257	--	--	--	4	26160	0.209	1	17050	--
	20	5	34733	0.174	--	--	--	5	34733	0.174	--	--	--
Undercut	24	5	32478	0.274	--	--	--	4	32691	0.313	1	31626	--
	12	2	23651	0.058	1	22688	--	--	--	--	1	24613	--
	16	4	38191	0.058	1	40150	--	--	--	--	3	37538	0.058
	20	5	54725	0.056	5	54725	0.056	--	--	--	--	--	--



### **5.1.2 Shear Baseline Tests**

As of this writing, the data for shear baseline tests has not been sufficiently reduced and evaluated.

## **5.2 Seismic Tests**

No seismic tests had been completed at the time of this writing.

## **5.3 Fatigue Tests**

### **5.3.1 Tensile Fatigue Tests**

Anchors were fatigue-tested for 2,000,000 cycles as described in Section 4.4. At the time of this writing, tensile fatigue tests had been run on the 8 mm and 16 mm expansion anchors. One of the 8 mm anchors failed in fatigue at 1,931,480 cycles. This size anchor had the highest stress range (31.5 ksi, based on its effective tensile stress area) of the expansion anchors tested in fatigue, and therefore would be the most likely expansion anchor size to fail. All other anchors tested to date have survived the 2,000,000 cycles of load application.

When the nine anchors that survived the fatigue loading were subsequently tested to failure under monotonic loads, the following failure modes were observed:

- Anchor fracture
- Concrete cone breakout

- Anchor pullout

The characteristics of each failure mode will now be described in detail, with reference to typical results for each mode.

*Anchor fracture:* Anchor fracture occurred for the four 8 mm anchors that survived the fatigue loading. This failure mode is shown in Figure 5.15, and a typical load-displacement curve is shown in Figure 5.16. Note that the very high initial stiffness discussed in Section 5.1.1 is still present after fatigue loading. However, the ductility of the anchor is very low. Given the fact that one 8 mm anchor fractured during the fatigue cycling, the loss of ductility of the remaining anchors could be due to a microcrack forming in the anchors during the application of cyclic load. Once the anchors began to yield during monotonic testing, the cracks could have propagated very quickly until anchor fracture was reached.

*Concrete cone breakout:* Concrete cone breakout failure occurred for three of the 16 mm anchors. This mode is shown in Figure 5.17, and a typical load-displacement curve is shown in Figure 5.18 (UFTHSL23). This curve is similar in all respects to the concrete cone breakout curve for the baseline anchors (Figure 5.10).

*Anchor pullout:* Anchor pullout occurred for two of the 16 mm anchors. This mode is shown in Figure 5.19, and a typical load-displacement curve is shown in Figure 5.20 (UFTHSL21). This curve is qualitatively similar to the curve for concrete cone breakout (Figure 5.18), except for the large displacement achieved after ultimate load for the anchors failing by pullout.

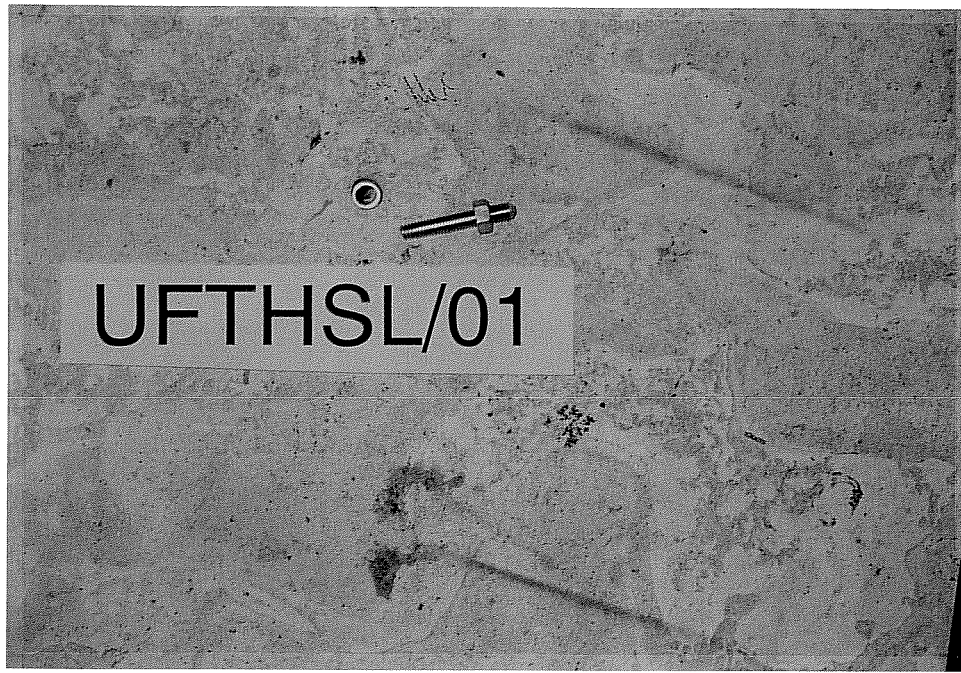


**Figure 5.15 Tensile fatigue expansion anchor fracture**

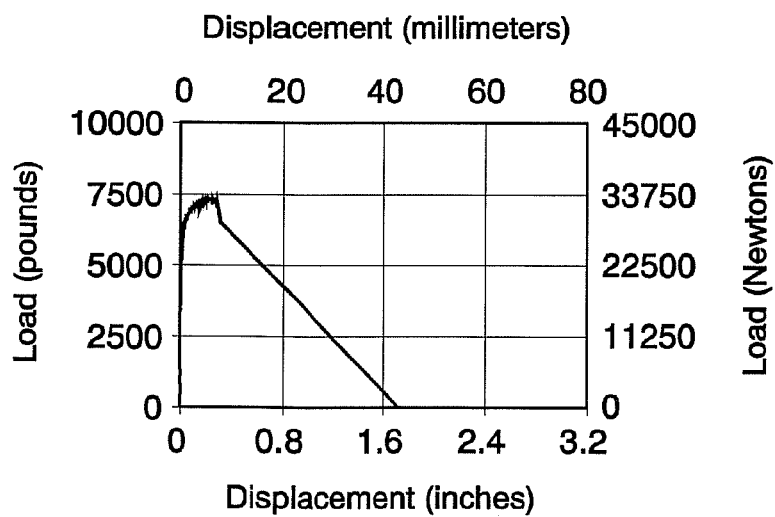


**Figure 5.16 Load-displacement curve for tensile fatigue expansion anchor fracture**

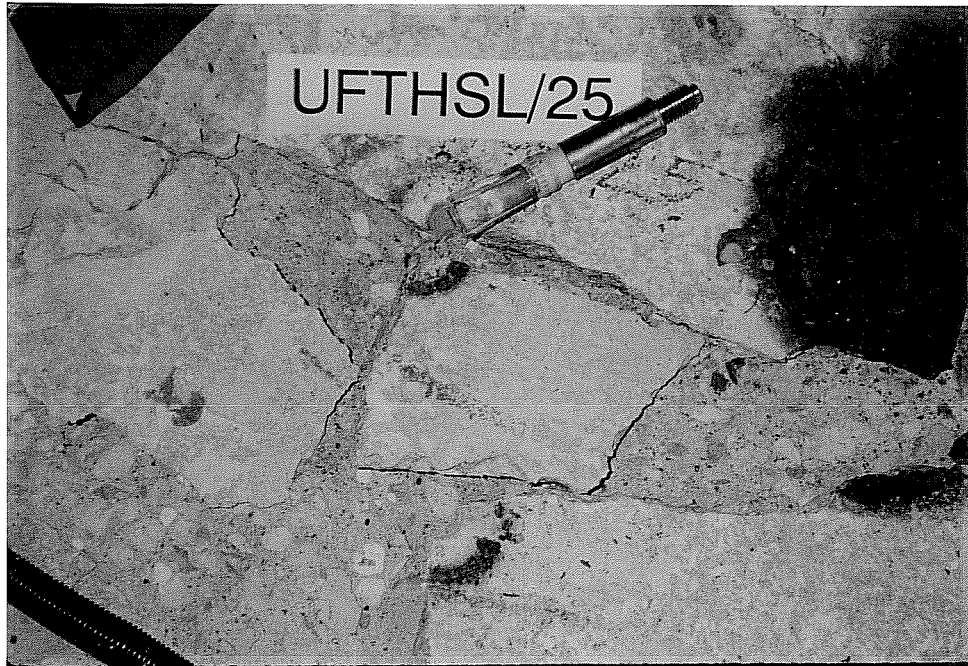


**Figure 5.17 Tensile fatigue expansion anchor concrete cone breakout**

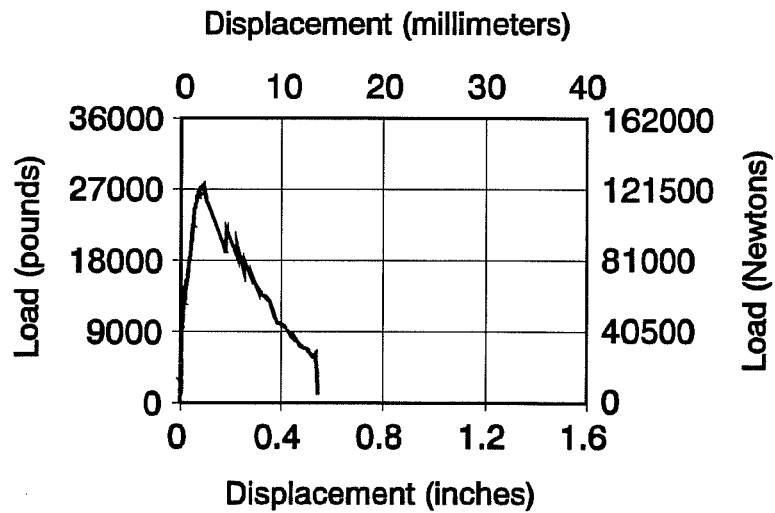


**Figure 5.18 Load-displacement curve for tensile fatigue expansion anchor concrete cone breakout**



**Figure 5.19 Tensile fatigue expansion anchor pullout**

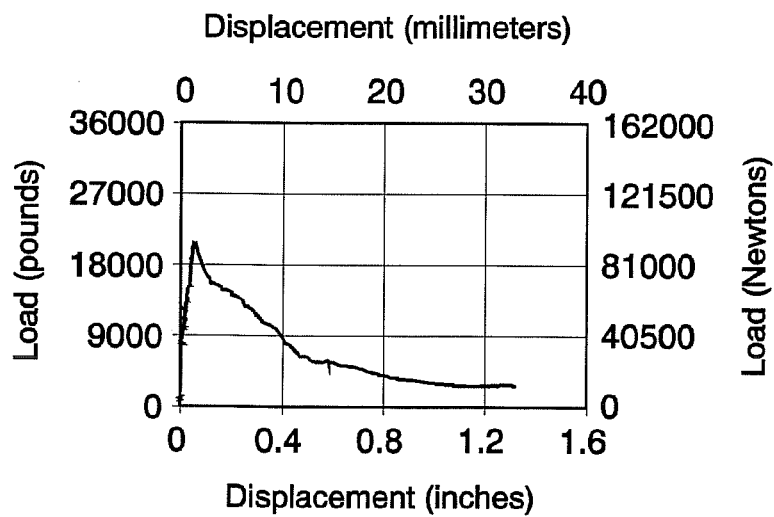


**Figure 5.20 Load-displacement curve for tensile fatigue expansion anchor pullout**

The foregoing discussion indicates that, for anchors surviving the 2,000,000 cycles of fatigue loading, the cycling had no effect on the ultimate loads achieved by the anchors in monotonic tension. In fact, for the 8 mm expansion anchors, the average ultimate load achieved for anchors monotonically tested to failure after being subjected to cycling was actually greater than that for the baseline tensile tests. However, this can probably be attributed to the larger coefficient of variation (Table 5.1) for the baseline anchors due to the very low ultimate load achieved by the anchor failing by pull-through.

The fatigue cycling had a marked detrimental effect on the ductility achieved by the 8 mm expansion anchors (Figure 5.16). This detrimental effect was not observed for the 16 mm expansion anchors.

### **5.3.2 Shear Fatigue Tests**

No shear fatigue tests had been completed at the time of this writing.

## **5.4 Shock Tests**

No shock tests had been completed at the time of this writing. However, the shock test setup had been completed and tested.

## **5.5 Comparison of Baseline Tensile Test Results with Predicted Values**

Predicted ultimate load values for monotonic tensile tests may be obtained for the anchor fracture and concrete cone breakout failure mode.

Nominal ultimate capacities for the anchor fracture mode may be calculated by the following equation:

$$N_{n \text{ steel}} = f_{ult} A_t$$

where:

$N_{n \text{ steel}}$  = Predicted nominal capacity based on anchor fracture, kips

$f_{ult}$  = Minimum specified ultimate tensile strength of the anchor material, ksi

$A_t$  = Tensile stress area of threaded anchor, in<sup>2</sup>

The minimum specified ultimate tensile strength for the expansion anchor material used in this testing program was 116 ksi. The minimum specified ultimate tensile strength for the undercut anchors used in this testing program was about 150 ksi for the 12 mm and 16 mm anchors, and about 120 ksi for the 20 mm anchor [11].

Experimental results and fracture mechanics theory provide a basis for the Concrete Capacity method, which can be used to calculate the ultimate capacity of an anchor as governed by concrete cone breakout. This method assumes the ultimate load is proportional to the embedment depth raised to the 1.5 power. The following empirical equation was developed to calculate the capacity, based on concrete cone breakout, of expansion or undercut anchors located at least a distance of 1.5 times their embedment depth away from any discontinuities [12]:

$$N_{n \text{ conc}} = 0.0350 \sqrt{f_c} h_e^{1.5}$$

where:

- $N_{n\ conc}$  = Predicted nominal capacity based on concrete cone breakout, kips
- $f_c$  = Concrete compressive strength at time of testing, psi
- $h_e$  = Anchor embedment depth, inches

In Table 5.2, predicted mean capacities as governed by steel failure and by concrete cone breakout are computed, and the lower of those two values is the predicted capacity of the anchor. For the purpose of computing the capacities as governed concrete cone breakout, the concrete strength was assumed to be 4500 psi.

Table 5.3 compares the predicted failure modes for each anchor tested in baseline tension with the experimentally obtained failure mode, and compare the predicted ultimate capacities with those obtained experimentally.

All tensile baseline tests produced results higher than predicted except for the 24 mm expansion anchor. The Concrete Capacity method agrees rather well with the results obtained for the anchors that failed by concrete breakout (see Table 5.1). Therefore, this method can be used to obtain a fairly reliable estimate of ultimate strength of an anchor when the failure mode is concrete cone breakout.

The anchors that failed by anchor fracture failed at a higher load than predicted, because the true ultimate strength of the steel was probably somewhat higher than the minimum specified ultimate strength of the steel. The difference between predicted and experimentally obtained ultimate loads is not as great for the 16 mm undercut anchors as for other anchor types and sizes failing by anchor fracture because most of the 16 mm undercut anchors failed by thread stripping.



**Table 5.2 Predicted Ultimate Tensile Capacities for Anchors in Testing Program**

<b>Anchor type and diameter</b>	$A_t$ in <sup>2</sup>	$N_{n \text{ steel}}$ kips	$h_e$ inches	$N_{n \text{ conc}}$ kips	$N_{n \text{ pred}}$ kips
<b>Expansion Anchors</b>					
8 mm	0.0534	6.2	2.56	9.6	6.2
10 mm	0.0870	10.1	2.95	11.9	10.1
12 mm	0.1241	14.4	3.15	13.1	13.1
16 mm	0.2302	26.7	4.13	19.7	19.7
20 mm	0.3739	43.4	5.12	27.2	27.2
24 mm	0.5321	61.7	6.10	35.4	35.4
<b>Undercut Anchors</b>					
12 mm	0.1164	17.8	4.92	25.7	17.8
16 mm	0.2232	33.7	6.69	40.6	33.7
20 mm	0.3519	42.3	8.66	59.8	42.3

**Table 5.3 Comparison of Predicted Failure Modes and Ultimate Capacities with Those Obtained Experimentally**

**(a) 8 mm Expansion Anchor**

<b>Test</b>	<b><math>N_{n \text{ exp}}</math> (kips)</b>	<b>Failure Mode</b>	<b>Predicted Failure Mode</b>	<b><math>\frac{N_{n \text{ exp}}}{N_{n \text{ pred}}}</math></b>
1	6.6	Concrete Cone Breakout	Anchor Fracture	1.07
2	7.1	Concrete Cone Breakout	Anchor Fracture	1.15
3	7.6	Anchor Fracture	Anchor Fracture	1.22
4	7.5	Anchor Fracture	Anchor Fracture	1.20
5	5.4	Pull-through	Anchor Fracture	0.88
Average	6.8			1.10

## (b) 10 mm Expansion Anchor

<b>Test</b>	<b><math>N_{n \text{ exp}}</math> (kips)</b>	<b>Failure Mode</b>	<b>Predicted Failure Mode</b>	<b><math>\frac{N_{n \text{ exp}}}{N_{n \text{ pred}}}</math></b>
1	11.4	Concrete Cone Breakout	Anchor Fracture	1.13
2	11.1	Pullout	Anchor Fracture	1.10
3	10.3	Concrete Cone Breakout	Anchor Fracture	1.02
4	12.7	Concrete Cone Breakout	Anchor Fracture	1.26
5	9.3	Concrete Cone Breakout	Anchor Fracture	0.92
Average	11.0			1.09

## (c) 12 mm Expansion Anchor

<b>Test</b>	<b><math>N_{n \text{ exp}}</math> (kips)</b>	<b>Failure Mode</b>	<b>Predicted Failure Mode</b>	<b><math>\frac{N_{n \text{ exp}}}{N_{n \text{ pred}}}</math></b>
1	14.4	Concrete Cone Breakout	Concrete Cone Breakout	1.10
2	12.1	Concrete Cone Breakout	Concrete Cone Breakout	0.92
3	13.5	Concrete Cone Breakout	Concrete Cone Breakout	1.03
4	15.1	Concrete Cone Breakout	Concrete Cone Breakout	1.15
5	14.7	Concrete Cone Breakout	Concrete Cone Breakout	1.12
Average	14.0			1.07

## (d) 16 mm Expansion Anchor

Test	$N_{n \text{ exp}}$ (kips)	Failure Mode	Predicted Failure Mode	$\frac{N_{n \text{ exp}}}{N_{n \text{ pred}}}$
1	17.1	Thread Stripping	Concrete Cone Breakout	0.87
2	30.5	Concrete Cone Breakout	Concrete Cone Breakout	1.55
3	27.8	Concrete Cone Breakout	Concrete Cone Breakout	1.41
4	28.2	Concrete Cone Breakout	Concrete Cone Breakout	1.43
5	18.2	Concrete Cone Breakout	Concrete Cone Breakout	0.92
Average	24.3			1.23

## (e) 20 mm Expansion Anchor

Test	$N_{n \text{ exp}}$ (kips)	Failure Mode	Predicted Failure Mode	$\frac{N_{n \text{ exp}}}{N_{n \text{ pred}}}$
1	39.3	Concrete Cone Breakout	Concrete Cone Breakout	1.45
2	24.3	Concrete Cone Breakout	Concrete Cone Breakout	0.89
3	36.7	Concrete Cone Breakout	Concrete Cone Breakout	1.35
4	35.1	Concrete Cone Breakout	Concrete Cone Breakout	1.29
5	38.2	Concrete Cone Breakout	Concrete Cone Breakout	1.41
Average	34.7			1.28

**(f) 24 mm Expansion Anchor**

<b>Test</b>	<b><math>N_{n \text{ exp}}</math> (kips)</b>	<b>Failure Mode</b>	<b>Predicted Failure Mode</b>	<b><math>\frac{N_{n \text{ exp}}}{N_{n \text{ pred}}}</math></b>
1	31.6	Pullout	Concrete Cone Breakout	0.89
2	29.6	Concrete Cone Breakout	Concrete Cone Breakout	0.84
3	38.4	Concrete Cone Breakout	Concrete Cone Breakout	1.08
4	19.8	Concrete Cone Breakout	Concrete Cone Breakout	0.56
5	43.0	Concrete Cone Breakout	Concrete Cone Breakout	1.22
<b>Average</b>	<b>32.5</b>			<b>0.92</b>

**(g) 12 mm Undercut Anchor**

<b>Test</b>	<b><math>N_{n \text{ exp}}</math> (kips)</b>	<b>Failure Mode</b>	<b>Predicted Failure Mode</b>	<b><math>\frac{N_{n \text{ exp}}}{N_{n \text{ pred}}}</math></b>
1	22.7	Anchor Fracture	Anchor Fracture	1.27
2	24.6	Thread Stripping	Anchor Fracture	1.38
Average	23.7			1.33

**(h) 16 mm Undercut Anchor**

<b>Test</b>	<b><math>N_{n \text{ exp}}</math> (kips)</b>	<b>Failure Mode</b>	<b>Predicted Failure Mode</b>	<b><math>\frac{N_{n \text{ exp}}}{N_{n \text{ pred}}}</math></b>
1	38.4	Thread Stripping	Anchor Fracture	1.14
2	40.2	Anchor Fracture	Anchor Fracture	1.19
3	35.1	Thread Stripping	Anchor Fracture	1.04
4	39.2	Thread Stripping	Anchor Fracture	1.16
Average	38.2			1.13



## (i) 20 mm Undercut Anchor

Test	$N_{n \text{ exp}}$ (kips)	Failure Mode	Predicted Failure Mode	$\frac{N_{n \text{ exp}}}{N_{n \text{ pred}}}$
1	50.1	Anchor Fracture	Anchor Fracture	1.18
2	55.1	Anchor Fracture	Anchor Fracture	1.30
3	56.4	Anchor Fracture	Anchor Fracture	1.33
4	53.9	Anchor Fracture	Anchor Fracture	1.27
5	58.2	Anchor Fracture	Anchor Fracture	1.38
Average	54.7			1.29

## **6. SUMMARY, CONCLUSIONS AND RECOMMENDATIONS**

### **6.1 Summary**

Torque-controlled expansion anchors and undercut anchors are currently being tested in this ongoing testing program. These anchors are being tested in uncracked concrete of a single mix design under the following loading conditions:

1. Baseline
  - a. Tension
  - b. Shear
2. Seismic
  - a. Tension
  - b. Shear
3. Fatigue
  - a. Tension
  - b. Shear
4. Shock (tension only)

This thesis has described the anchors, given background information, described the testing program and discussed the results obtained so far. Results were obtained for at least some anchors for both of the following test types:

1. Baseline (tension only)
2. Fatigue (tension only)

## 6.2 Conclusions

### 6.2.1 Anchor Installation and Concrete

Conclusions relating to the installation of anchors and adequacy of concrete are the following:

1. The installation of undercut anchors is time-consuming. Two people are required to install these anchors in the laboratory: one to operate the coring machine and one to vacuum up excess cooling water, so as to maintain cleanliness. This would be important in sensitive retrofit jobs. In addition, the amount of time required for two people to install an undercut anchor is about 25 minutes, compared to about 5 to 10 minutes for one person to install an expansion anchor. Thus, about five to ten times more man-hours are required to install undercut anchors.
2. The undercut anchor installation process has a lower success rate than the expansion anchor installation process. This is due to two factors: first, the core may break off at midheight if not drilled deep enough; second, for proper installation, the undercut in the hole must be made at a specific height; the height at which the undercut is actually made may vary by as much as 1/4 inch due to the compressibility of the sponge-like retaining ring on the undercutting tool.
3. When an expansion anchor hole is drilled deeper than the anchor's specified embedment depth and the anchor is subsequently installed, the anchor's shank and wedge

mechanism may slide down through the sleeve. This makes installation of the baseplate and nut difficult.

4. The concrete strengths satisfied the project specifications. The strength was relatively consistent due to the sprinkling of the limestone aggregate.

### **6.2.2 Baseline Tests**

So far, data have been reduced and examined for tensile baseline tests only. The conclusions that can be drawn from the results are as follows:

1. Anchor fracture has the least amount of scatter in the tensile baseline test data, followed by concrete cone breakout. Other failure modes, such as pullout and pull-through, are slightly less predictable. Thread stripping is the least predictable failure mode.
2. Thread stripping failure is neither predictable nor reproducible, and has the most scatter in the data. Therefore, it is an unacceptable failure mode.
3. The Concrete Capacity method of predicting ultimate capacities of concrete breakout failures provides a reliable estimate of the ultimate strength of an anchor failing in this mode. The method used to predict the ultimate capacity based on steel failure slightly underestimated the actual capacity due to the use of the minimum specified tensile strength of the anchor instead of the average actual strength.

4. In most cases, the mode of failure predicted by comparison of the steel capacity and Concrete Capacity calculations was fairly accurate. However, some anchors experienced cone breakout at loads lower than those predicted by the Concrete Capacity method. This is probably due to the inherent scatter in this failure mode. However, it may also be due to slip of the anchor prior to cone breakout. This suggests that there is a need for a method to predict anchor pullout failure.

### **6.2.3 Seismic Tests**

At the time of this writing, no seismic tests had been conducted.

### **6.2.4 Fatigue Tests**

So far, data have been reduced and examined for tensile fatigue tests only. The conclusions that can be drawn from those results are as follows:

1. The test setup involving the simultaneous testing of three anchors in fatigue worked very well; there have been no problems so far.
2. Limited results suggest that small expansion anchors are weakened by fatigue cycling, as evidenced by the occurrence of anchor fracture at less than 2,000,000 cycles, and by the degradation of displacement response and hence ductility.
3. Based on the results obtained in this testing program, the 16 mm expansion anchors performed satisfactorily in fatigue.

There were no instances of failure during cycling, and the failure mode observed after subsequent monotonic testing was concrete cone breakout, which was the same mode as was predominant in the tensile baseline tests.

### **6.2.5 Shock Tests**

At the time of this writing, the results of the shock tests had not been sufficiently evaluated.

## **6.3 Recommendations**

### **6.3.1 Applications**

Anchors such those tested in this program have applications both in new construction and in retrofit projects. Some of these applications are the following:

1. New construction
  - Tilt-up wall connections
  - Precast wall panel to cast-in-place concrete member connections
2. Retrofit
  - Steel column to concrete footing/column connections
  - Flagpole, light pole, and highway sign connections to concrete
  - Shelf angle connections to concrete

- Machine tie-downs

Note that the machine tie-down application implies high-cycle fatigue loading; therefore, small-diameter expansion anchors such as those tested in this testing program should be used with caution in this application.

### 6.3.2 Suitability Criteria

The following suitability criteria for dynamic testing are proposed. It should be noted that these criteria are preliminary and are based on the limited results obtained so far. Generally, the following items merit consideration:

1. *Ductility*: Ductility is defined as the displacement at a certain percentage of the ultimate capacity divided by the displacement at the first occurrence of either yielding or capacity. Therefore, two displacements need to be defined. The displacement at 80% of the maximum load is commonly used for the numerator. The definition of the displacement to use in the denominator depends on the characteristics of the load-displacement curve of the anchor. If the curve is approximately elasto-plastic, the displacement at an "equivalent yield" point is determined. This point is located by the intersection of the elastic modulus with a horizontal line passing through the point of maximum load. If the load-displacement curve is not approximately elasto-plastic, the displacement to be used in the denominator is the

displacement at maximum load. Ductility is important to dynamic suitability criteria because it can be used as an indication of whether previous dynamic loading had a degrading effect on the displacement response of the anchor, and thus suggest whether anchor fracture would be likely to occur if cycling were to have continued.

2. *Preload retention:* For torque-controlled expansion anchors, the presence of preload is essential to anchor performance. Generally, the level of preload must be consistent with the plastic capacity of the attachment, because the connection should be designed for the attachment to yield before the anchors. As noted in Section 4.2.5, the anchor preload drops significantly (to about half the installation preload) within a short period after installation. Therefore, since the allowable service load is equal to the anchor capacity reduced by a factor of safety, the installation preload should be greater than twice the capacity reduced by a factor of safety.
3. *Thread stripping:* Thread stripping should not be allowed as an acceptable failure mode in determining dynamic suitability criteria. The results are neither reproducible nor predictable and thread stripping is not contemplated by current anchor design formulas.
4. *Pullout and Pull-through:* The preload retention requirement addresses these if pullout and pull-through are predictable. However, note that pullout reduces the effective embedment depth, which can lead to concrete cone breakout at loads less than those predicted by the Concrete Capacity method. In



addition, pull-through is generally unpredictable and is highly dependent on the geometry of the anchor, wedge, and expansion sleeve, as well as on the characteristics of the particular hole into which the anchor was installed. Therefore, given the unpredictability of these failure modes, the pullout or pull-through capacity must satisfy the following:

$$\begin{aligned} N_{po,pt} &> \phi_1 N_{n\ steel} \\ N_{po,pt} &> \phi_2 N_{n\ conc} \end{aligned}$$

where:

$$\begin{aligned} N_{po,pt} &= \text{capacity based on pullout or pull-through} \\ \phi_1, \phi_2 &= \text{capacity reduction factors} \end{aligned}$$

6. *Steel fatigue and fracture*: The allowable service load for anchors subjected to fatigue should include a stipulation that the stress range be less than the endurance limit of the anchor, including the effects of the anchor threads as stress risers.

### 6.3.3 Further Research

Recommendations for further research on expansion and undercut anchors, in addition to the ongoing testing under this program, include the following:

1. Dynamic testing of anchors in uncracked concrete, especially under seismic loads
2. Dynamic testing of anchors in low-strength concrete

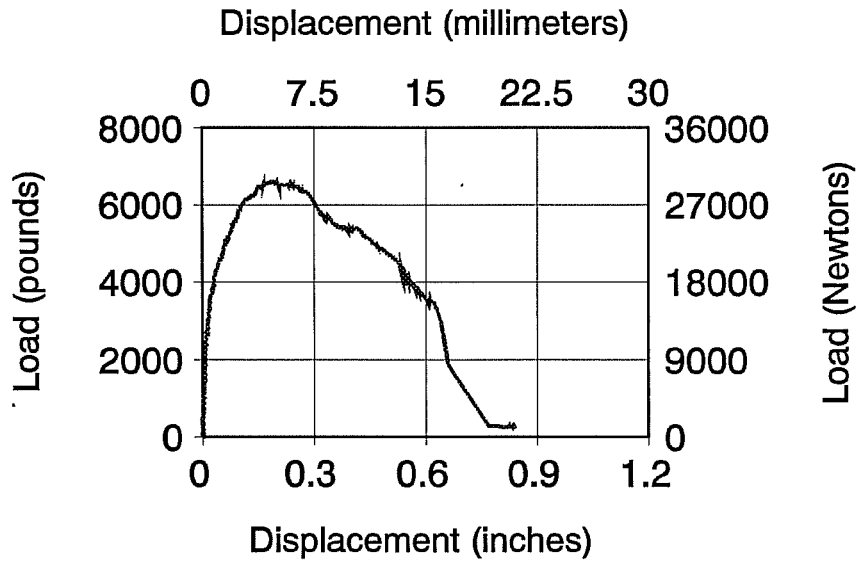
3. Dynamic testing of anchors in high-strength concrete
4. Testing of anchors subjected to shear shock loading

## **APPENDIX**

**Load-Displacement Results of all Tests**

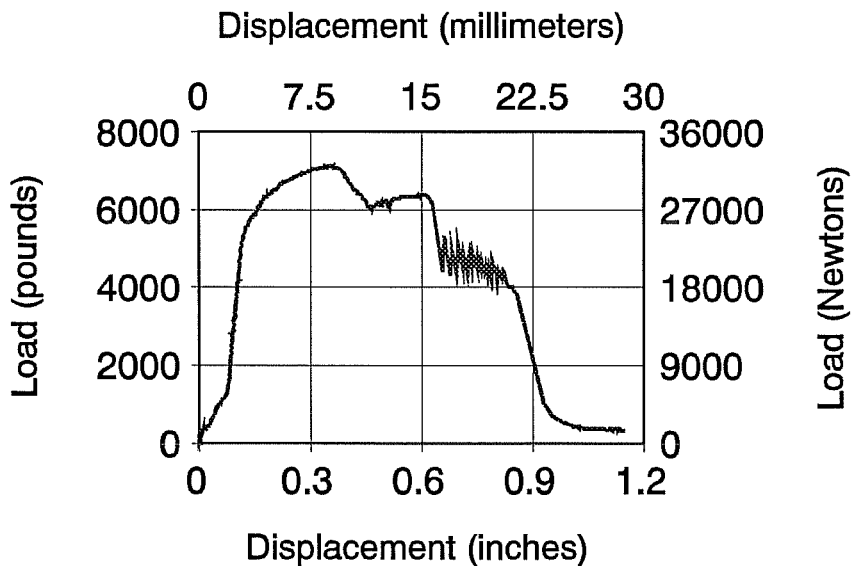
### BTHSL/01

Ultimate Load = 6608 lbs  
29394 N



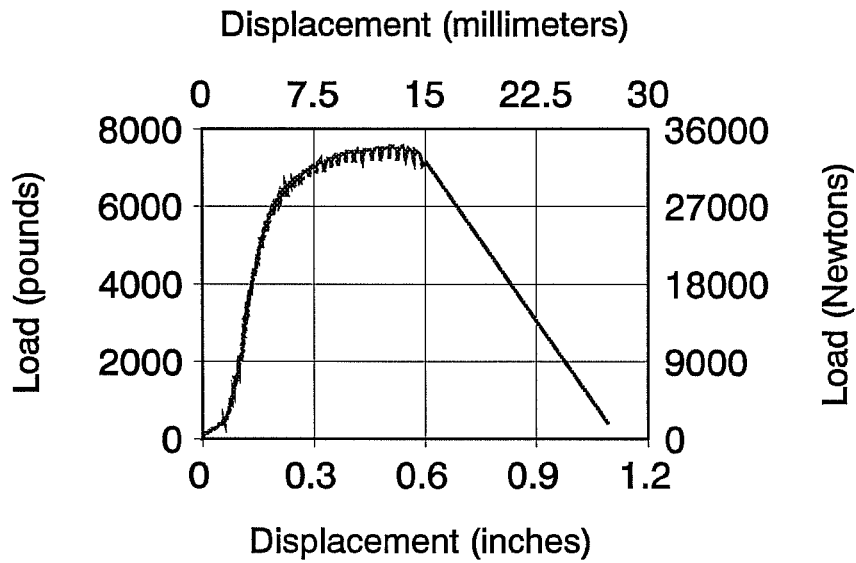
### BTHSL/02

Ultimate Load = 7127 lbs  
31703 N



### BTHSL/03

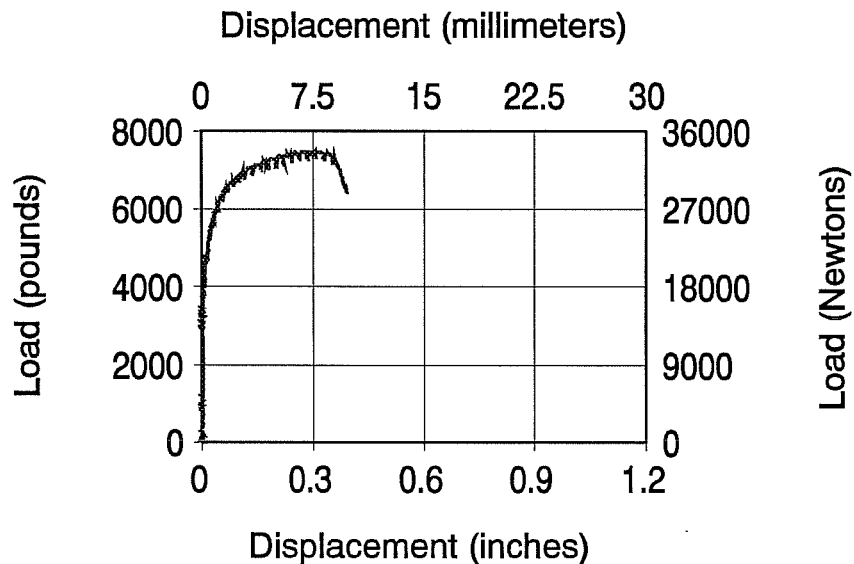
Ultimate Load = 7552 lbs  
33593 N



---

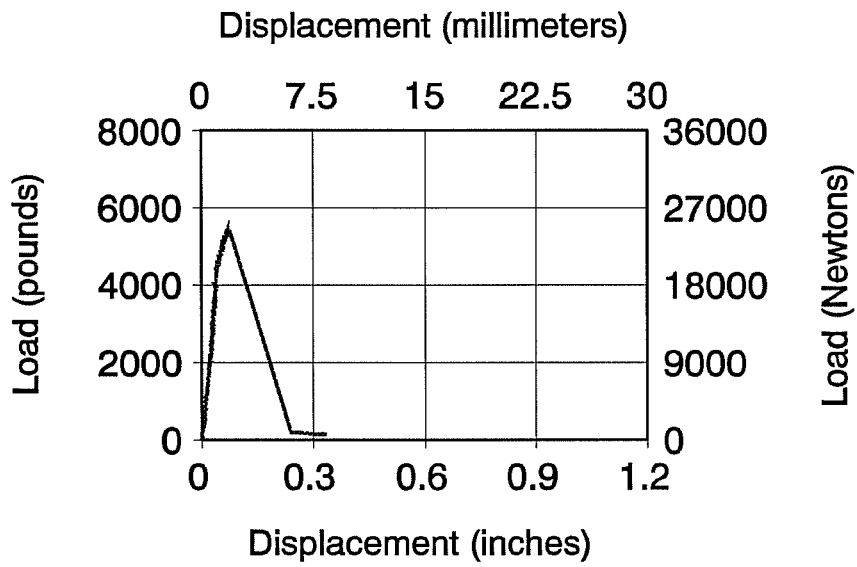
### BTHSL/04

Ultimate Load = 7455 lbs  
33173 N



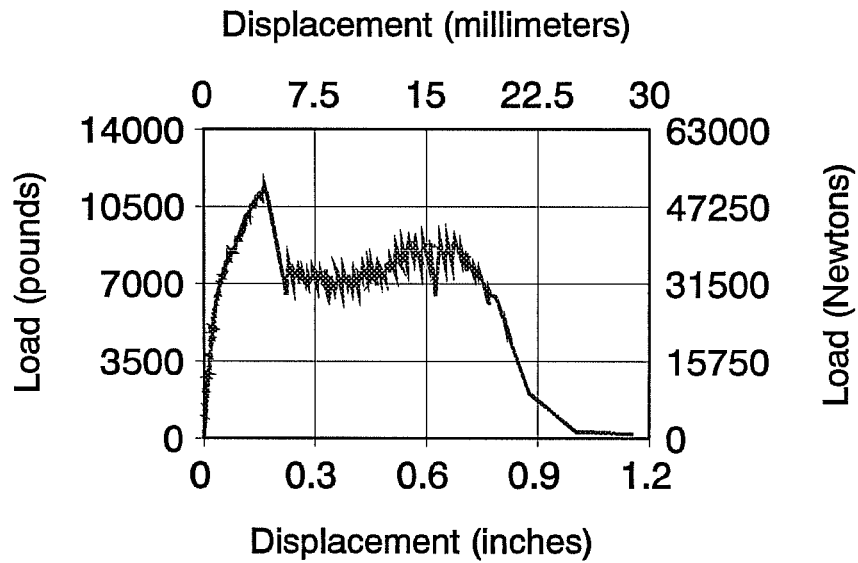
# BTHSL/05

Ultimate Load = 5428 lbs  
24145 N



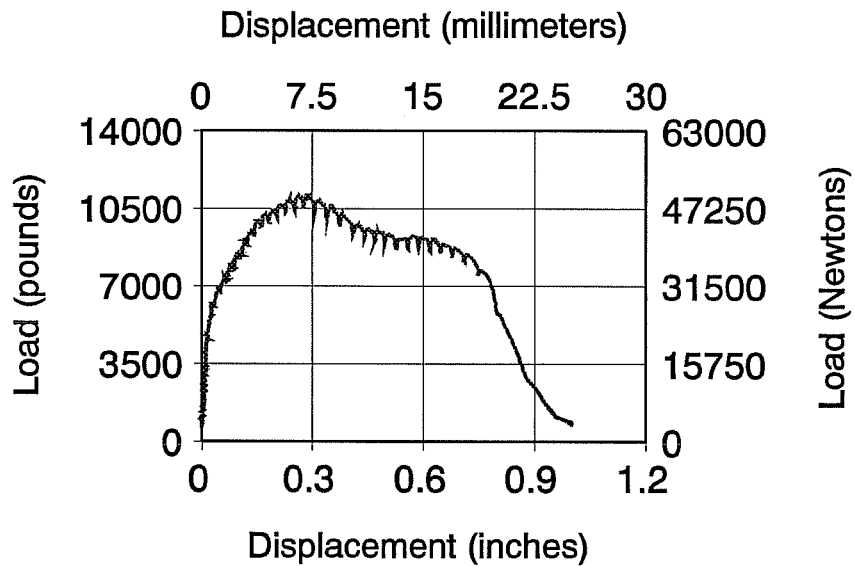
### BTHSL/06

Ultimate Load = 11422 lbs  
50809 N



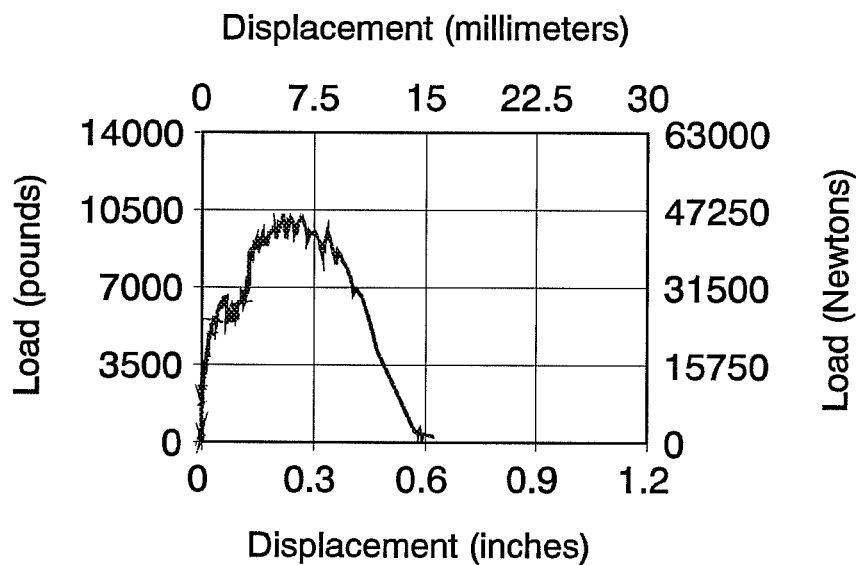
### BTHSL/07

Ultimate Load = 11092 lbs  
49340 N

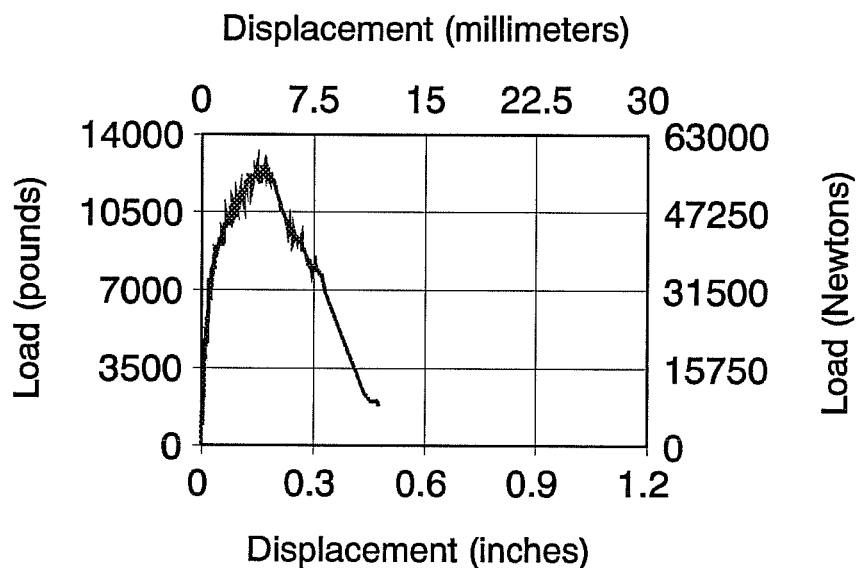


**BTHSL/08**

Ultimate Load = 10290 lbs  
45770 N

**BTHSL/09**

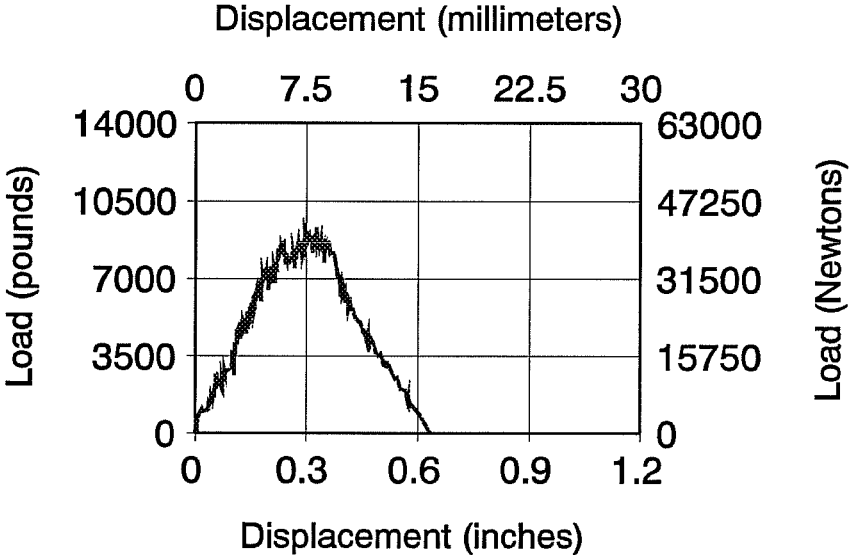
Ultimate Load = 12697 lbs  
56478 N





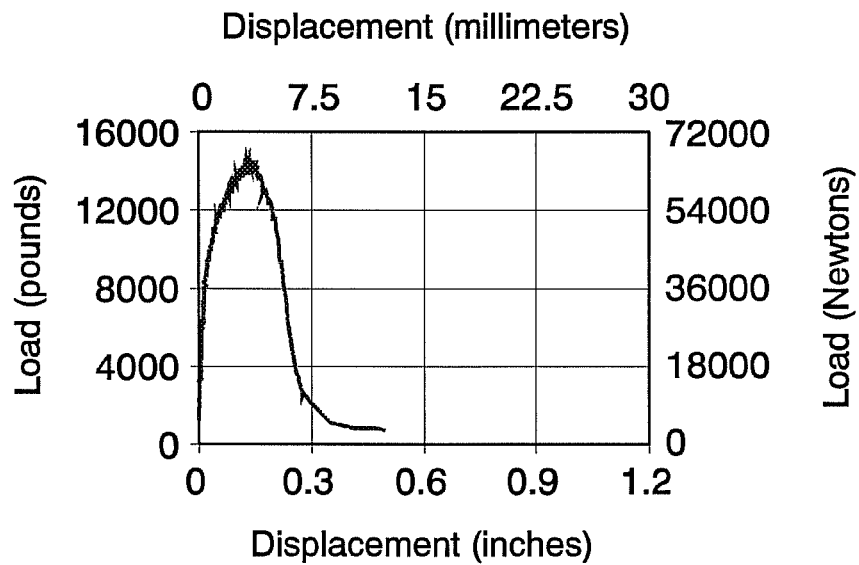
# BTHSL/10

Ultimate Load = 9298 lbs  
41361 N

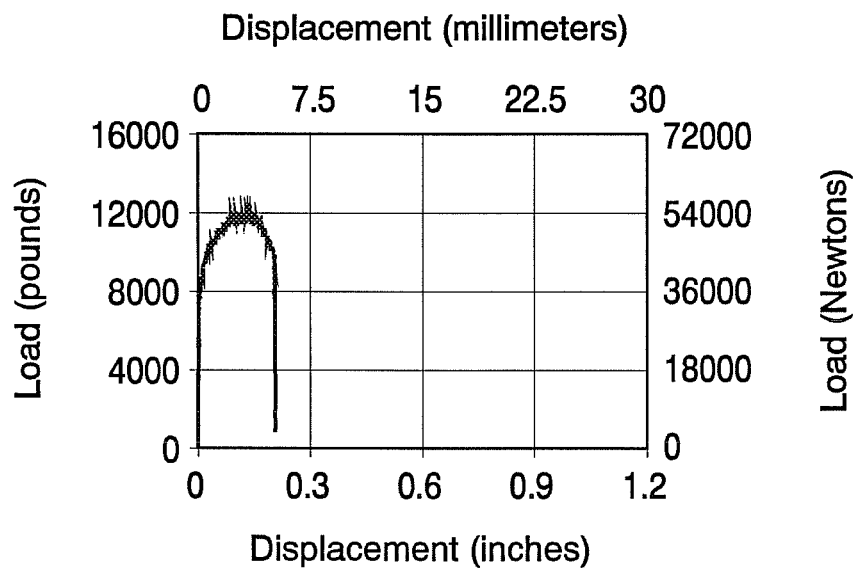


**BTHSL/11**

Ultimate Load = 14438 lbs  
64221 N

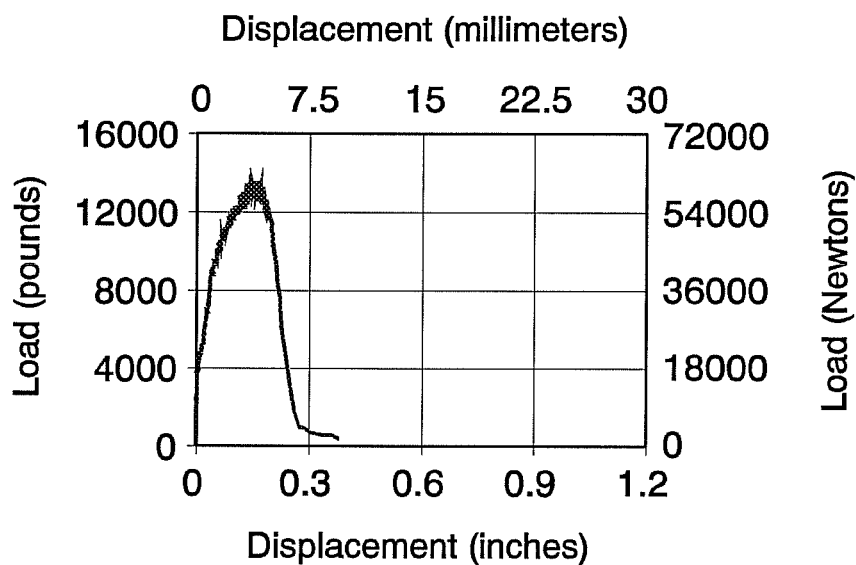
**BTHSL/12**

Ultimate Load = 12100 lbs  
53823 N

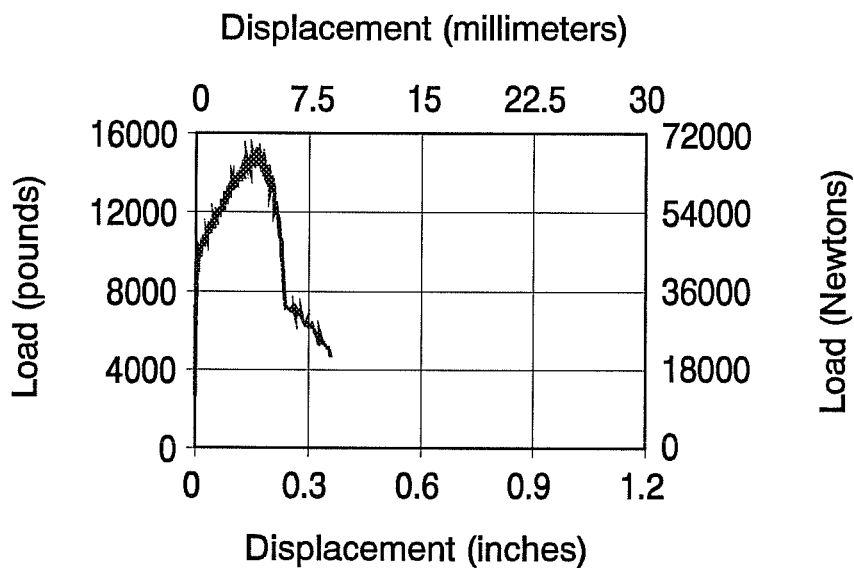


**BTHSL/13**

Ultimate Load = 13475 lbs  
59940 N

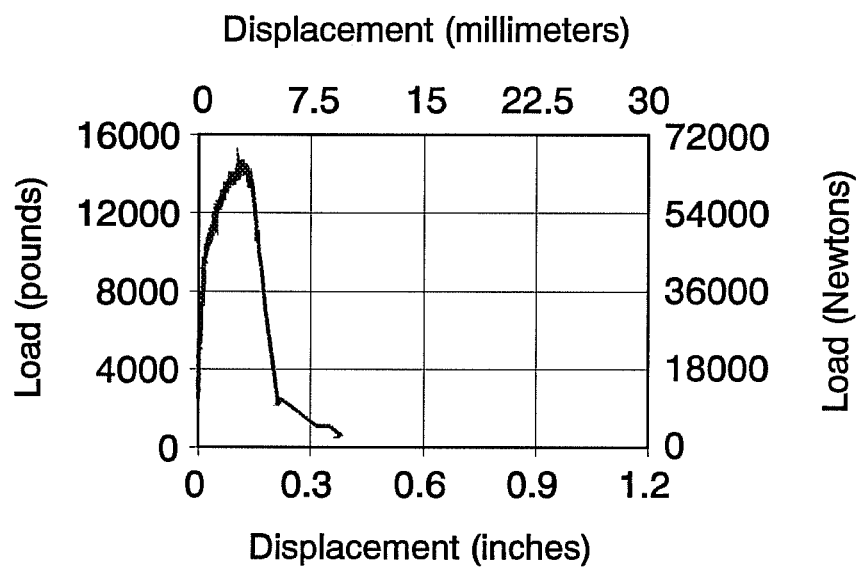
**BTHSL/14**

Ultimate Load = 15125 lbs  
67279 N



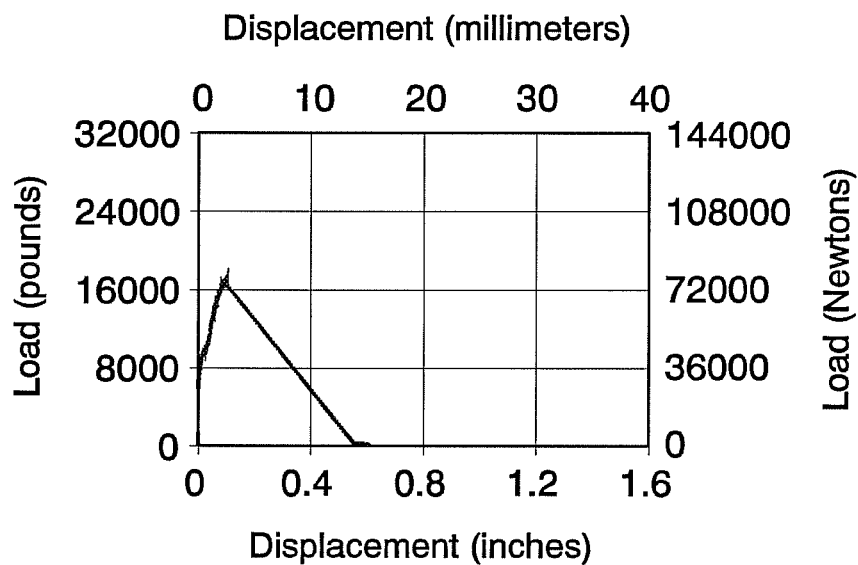
**BTHSL/15**

Ultimate Load = 14713 lbs  
65444 N

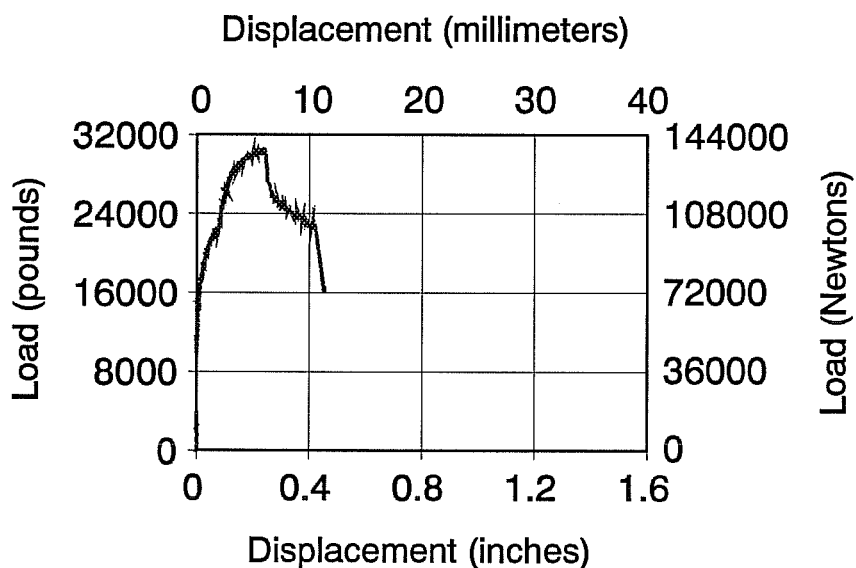


**BTHSL/21**

Ultimate Load = 17050 lbs  
75842 N

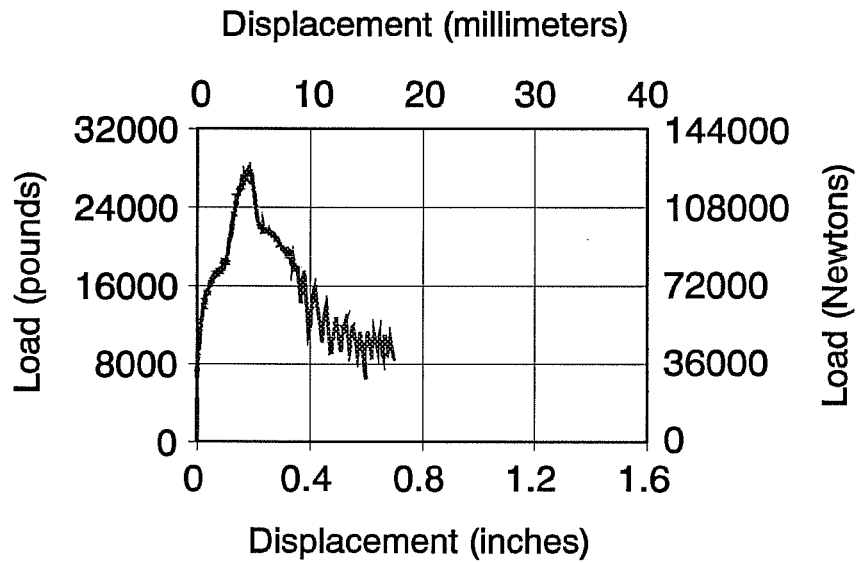
**BTHSL/22**

Ultimate Load = 30525 lbs  
135782 N



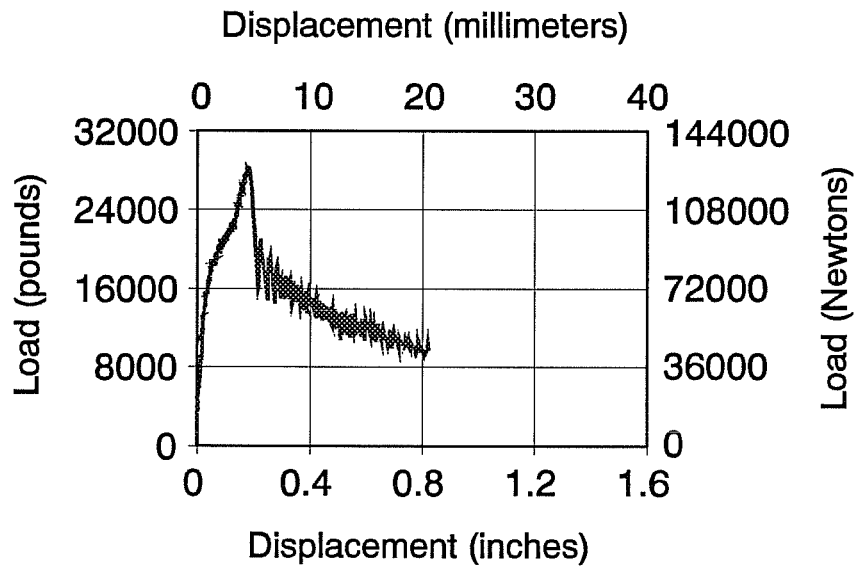
### BTHSL/23

Ultimate Load = 27775 lbs  
123549 N



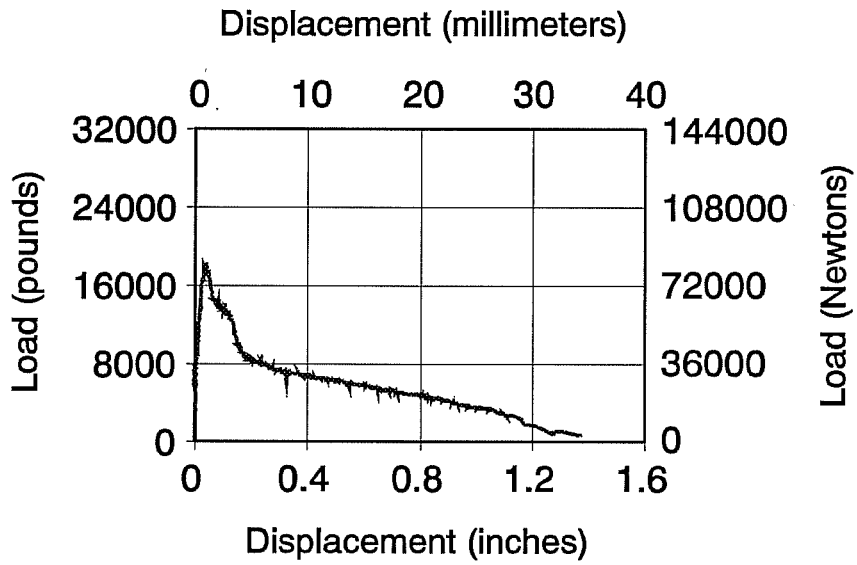
### BTHSL/24

Ultimate Load = 28188 lbs  
125384 N



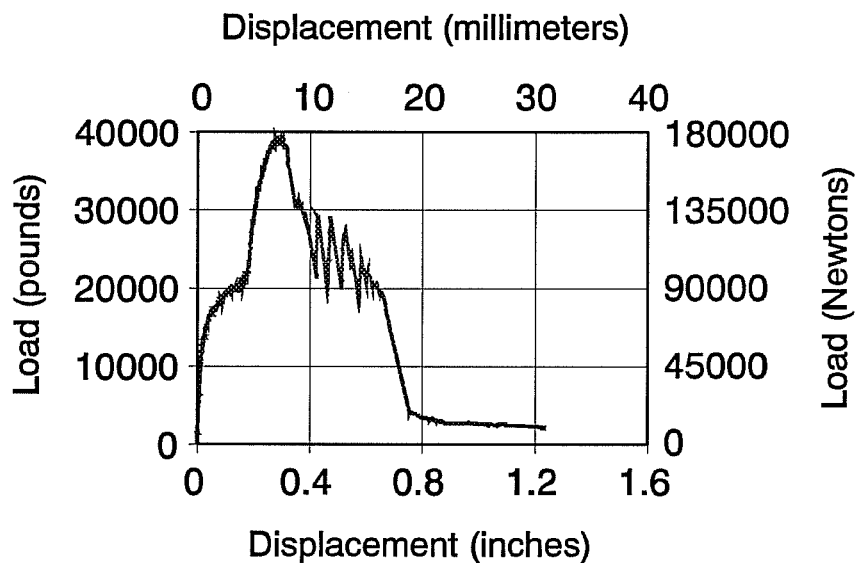
# BTHSL/25

Ultimate Load = 18150 lbs  
80735 N

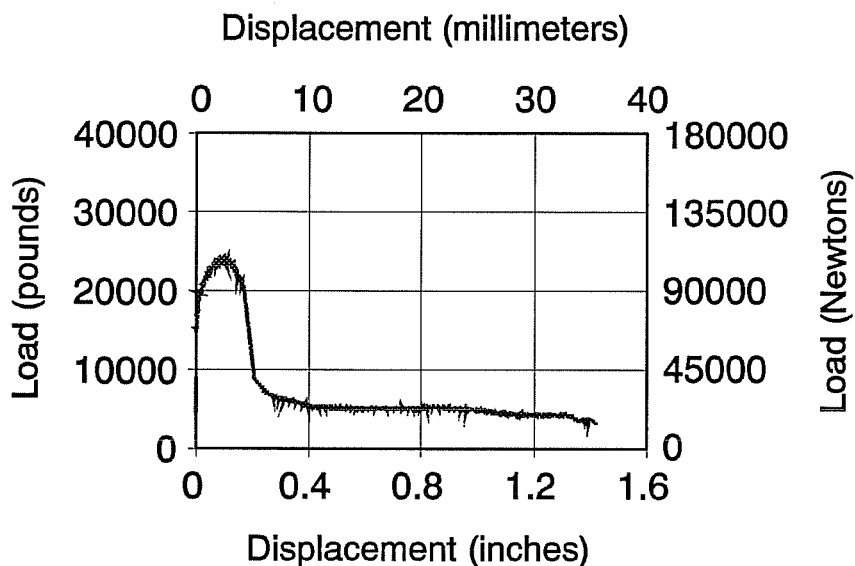


**BTHSL/26**

Ultimate Load = 39325 lbs  
174926 N

**BTHSL/27**

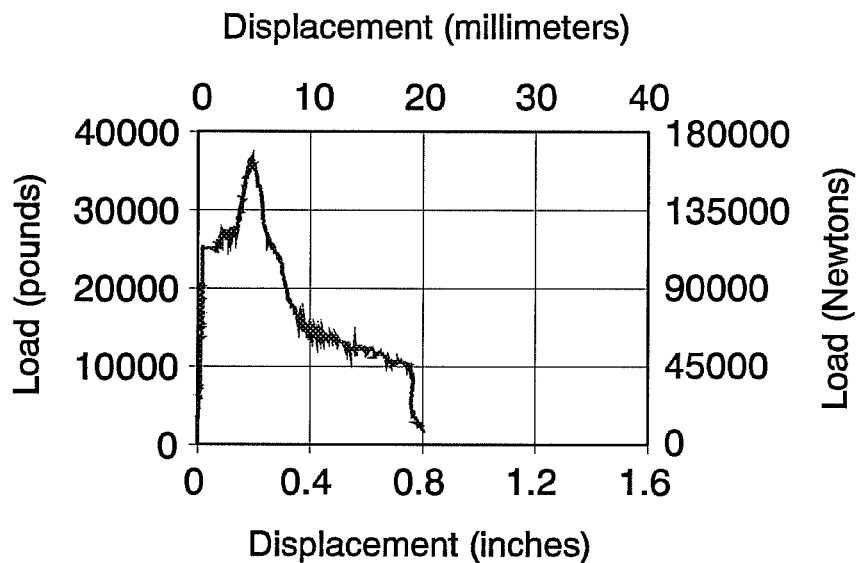
Ultimate Load = 24338 lbs  
108259 N





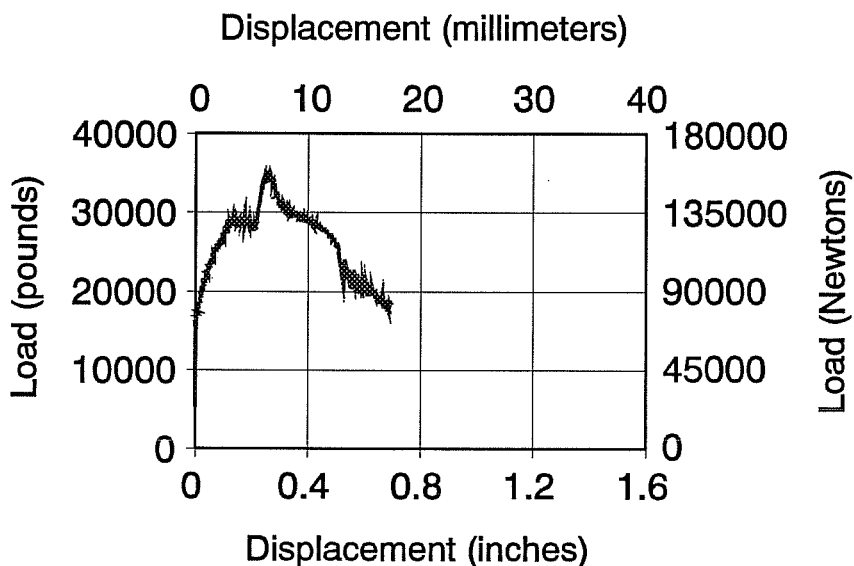
### BTHSL/28

Ultimate Load = 36713 lbs  
163305 N



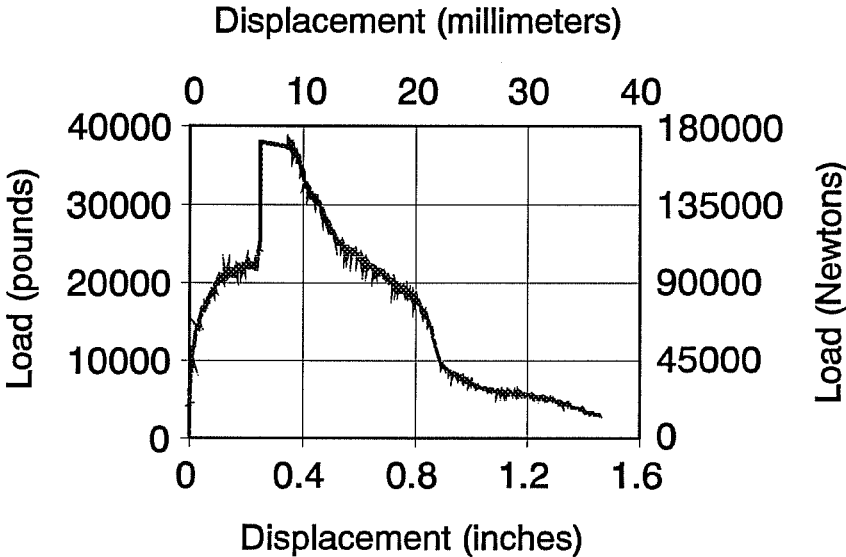
### BTHSL/29

Ultimate Load = 35063 lbs  
155966 N



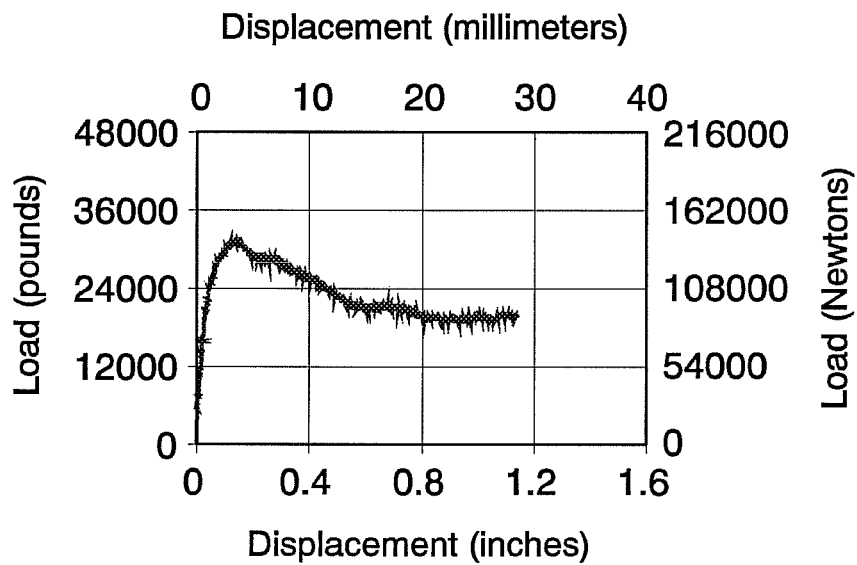
# BTHSL/30

Ultimate Load = 38225 lbs  
170033 N

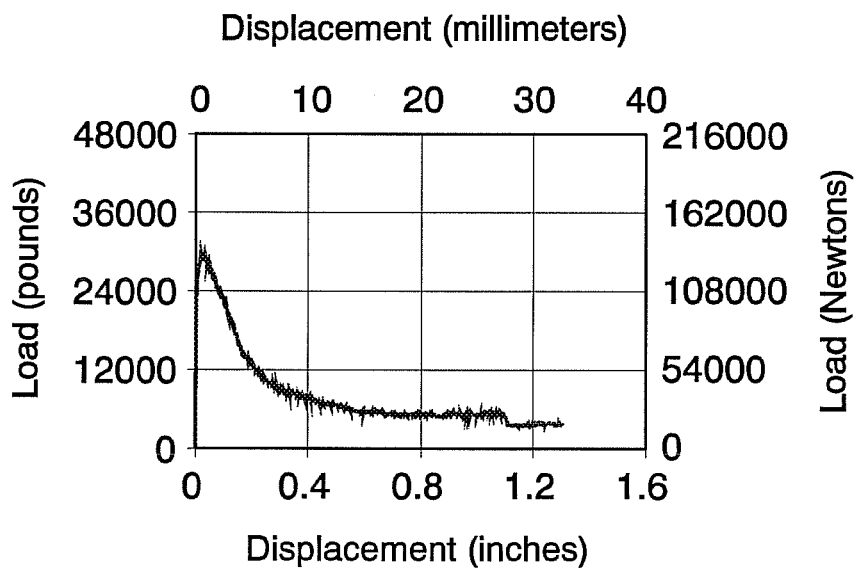


**BTHSL/31**

Ultimate Load = 31625 lbs  
140675 N

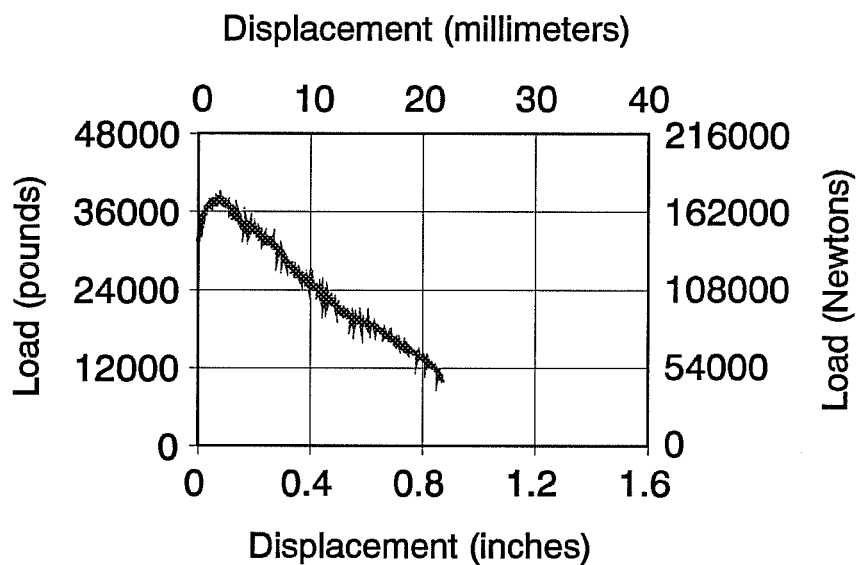
**BTHSL/32**

Ultimate Load = 29563 lbs  
131501 N

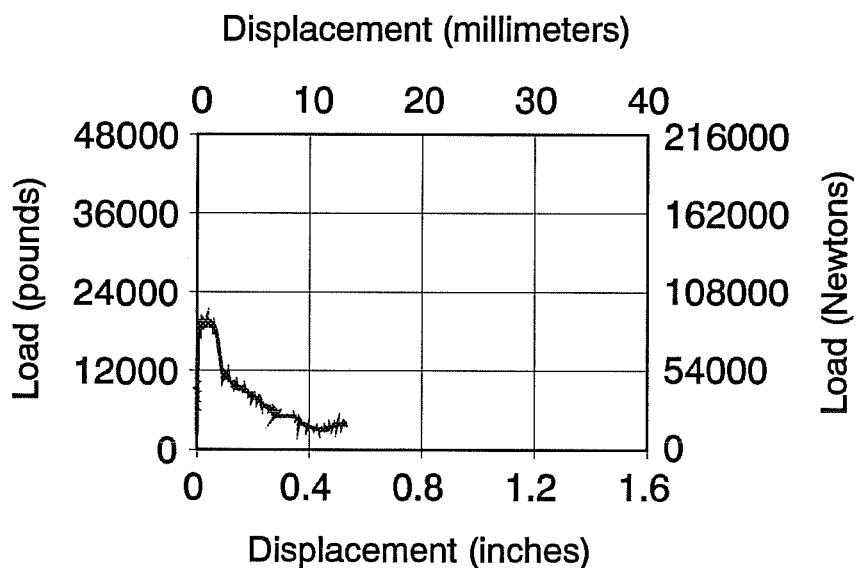


**BTHSL/33**

Ultimate Load = 38363 lbs  
170645 N

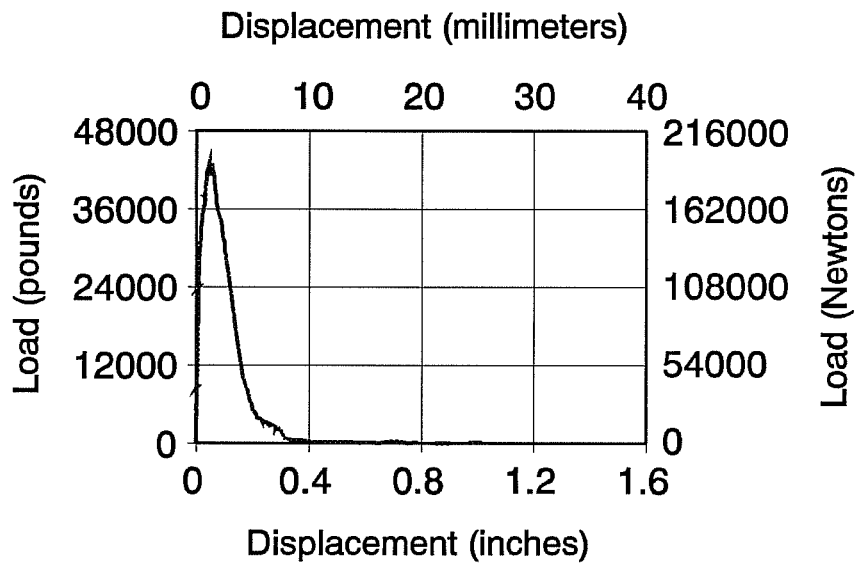
**BTHSL/34**

Ultimate Load = 19800 lbs  
88075 N



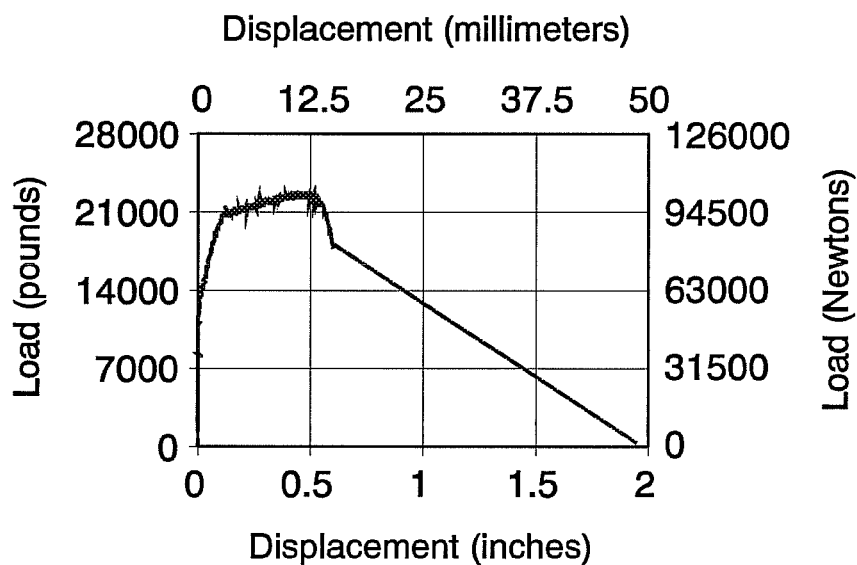
# BTHSL/35

Ultimate Load = 43038 lbs  
191440 N

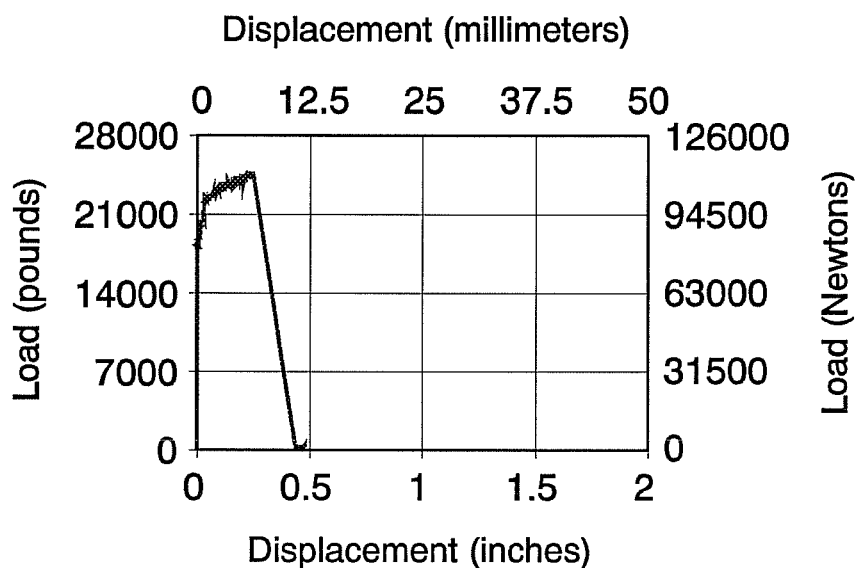


**BTHUC/01**

Ultimate Load = 22688 lbs  
100919 N

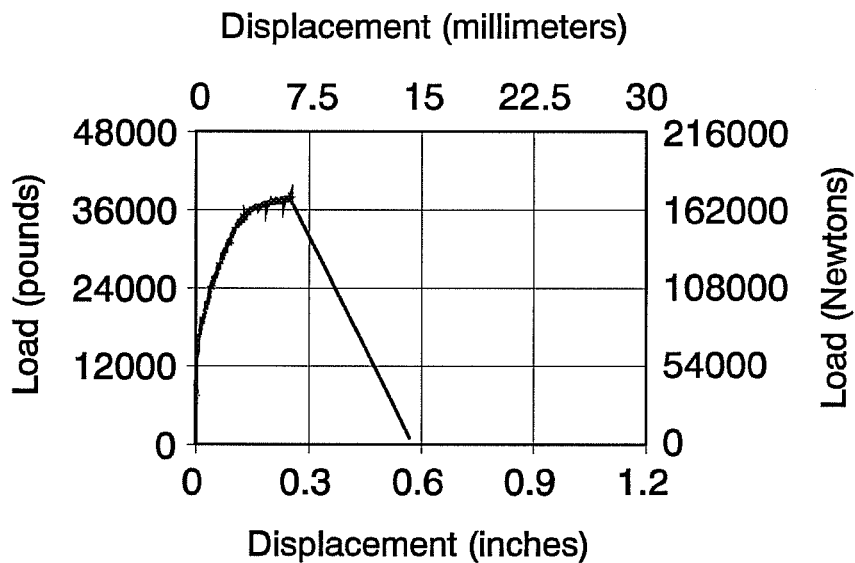
**BTHUC/02**

Ultimate Load = 24613 lbs  
109482 N



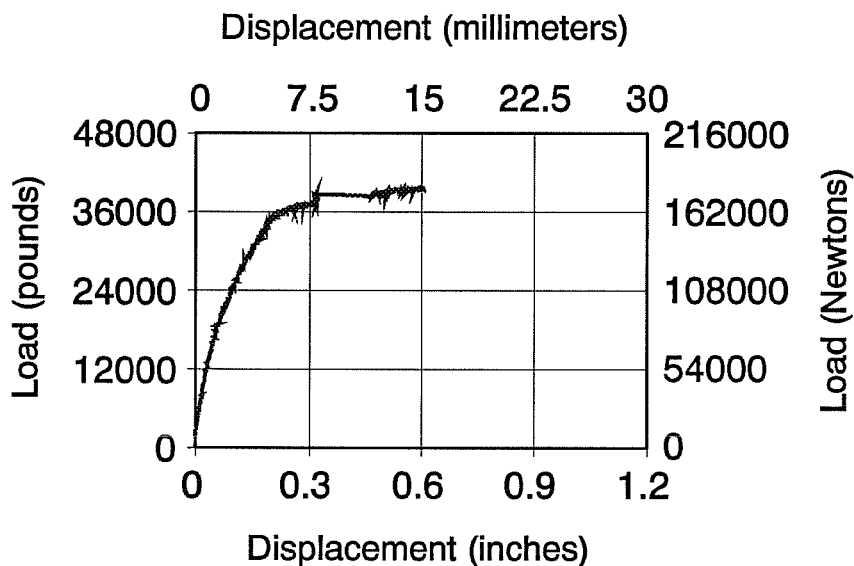
### BTHUC/06

Ultimate Load = 38363 lbs  
170645 N



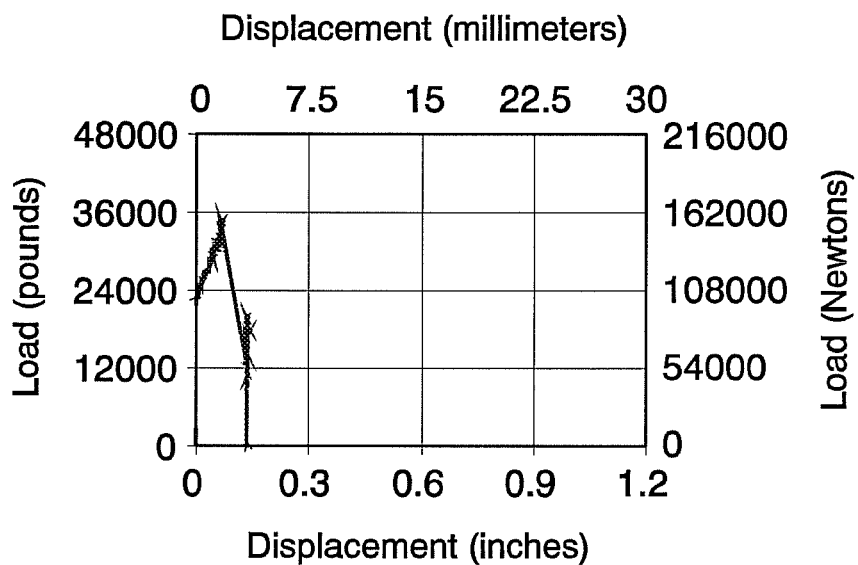
### BTHUC/07

Ultimate Load = 40150 lbs  
178596 N



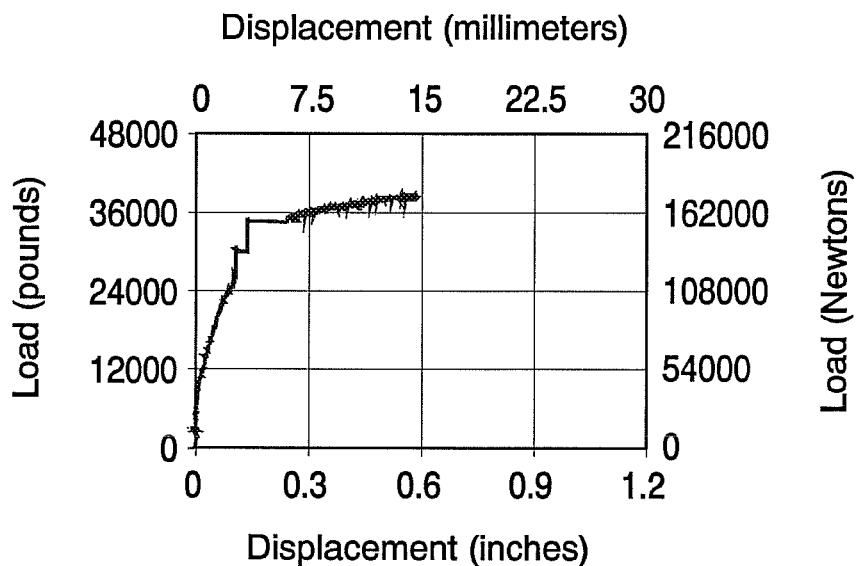
### BTHUC/08

Ultimate Load = 35063 lbs  
155966 N



### BTHUC/09

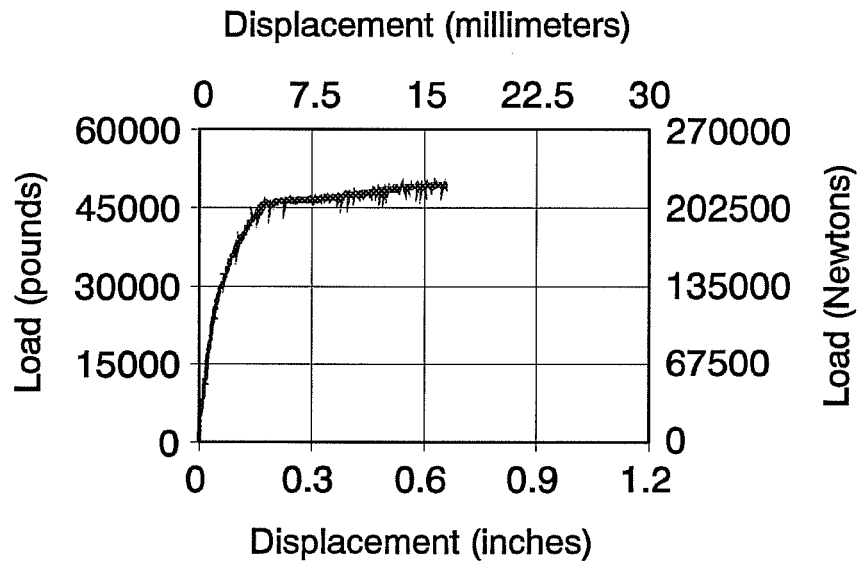
Ultimate Load = 39188 lbs  
174315 N



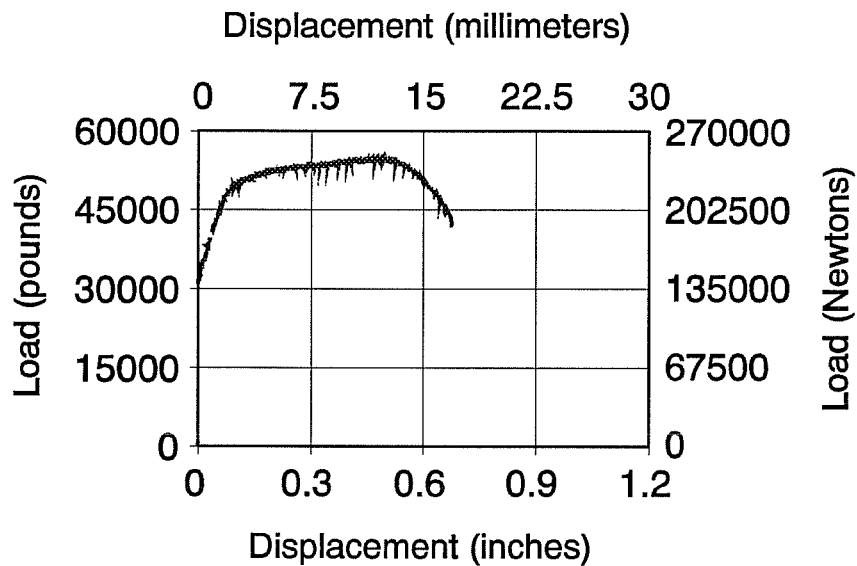


**BTHUC/11**

Ultimate Load = 50050 lbs  
222633 N

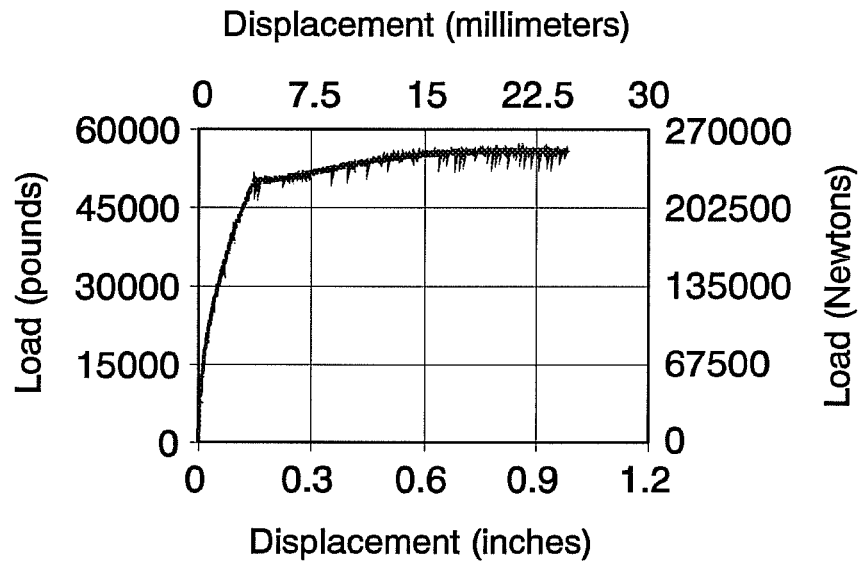
**BTHUC/12**

Ultimate Load = 55138 lbs  
245264 N

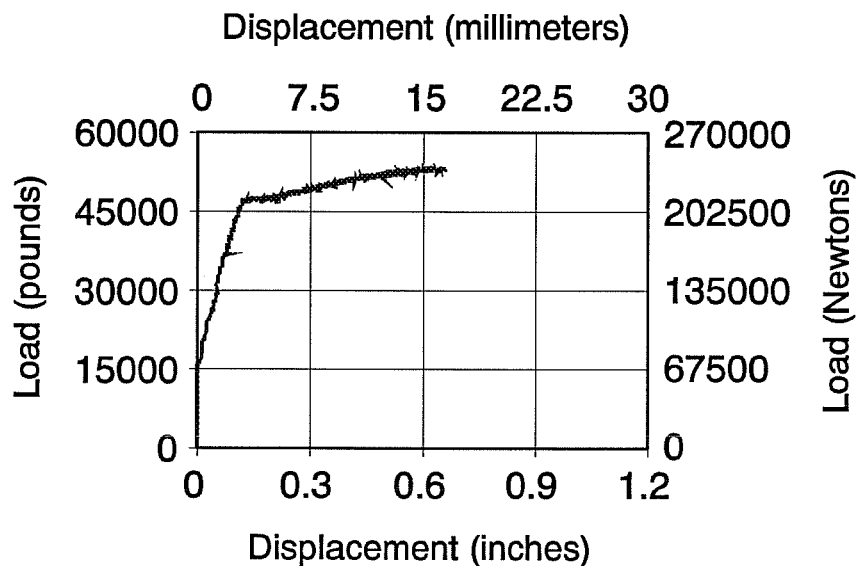


**BTHUC/13**

Ultimate Load = 56375 lbs  
250768 N

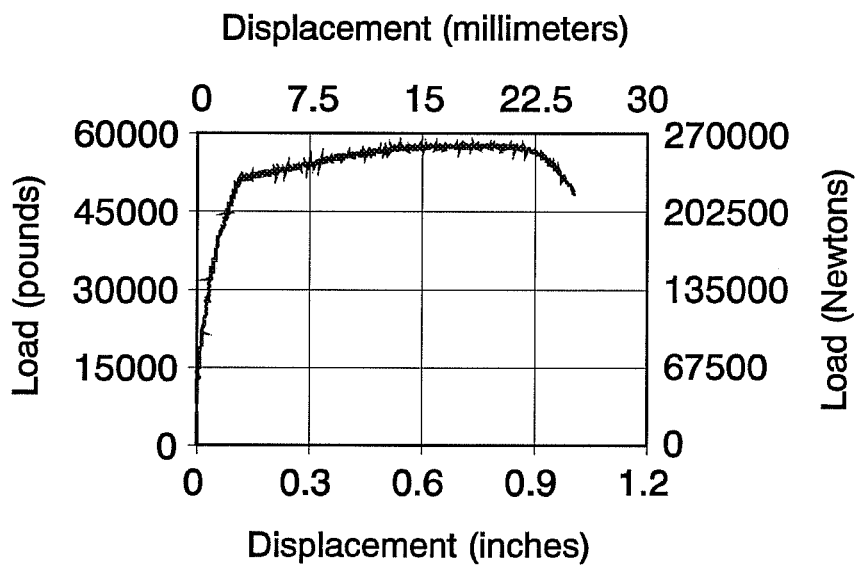
**BTHUC/14**

Ultimate Load = 53900 lbs  
239759 N



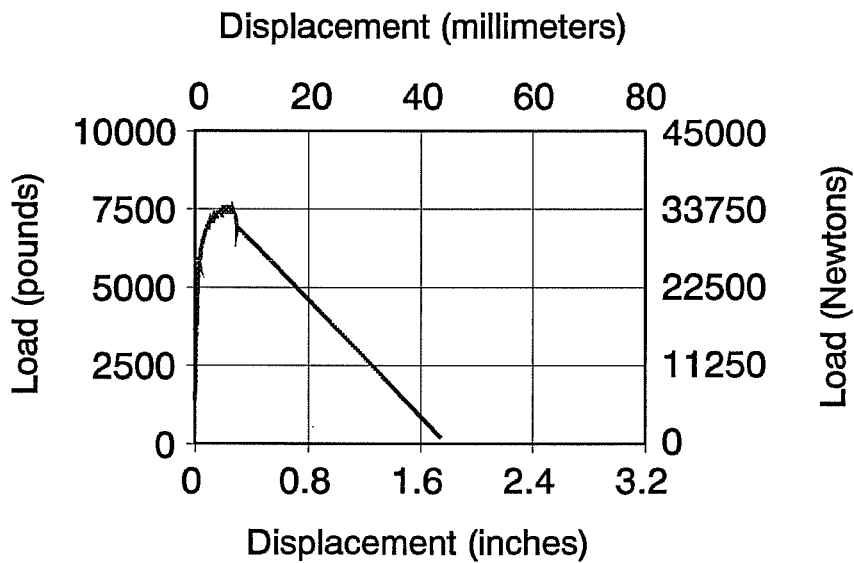
# BTHUC/15

Ultimate Load = 58163 lbs  
258720 N



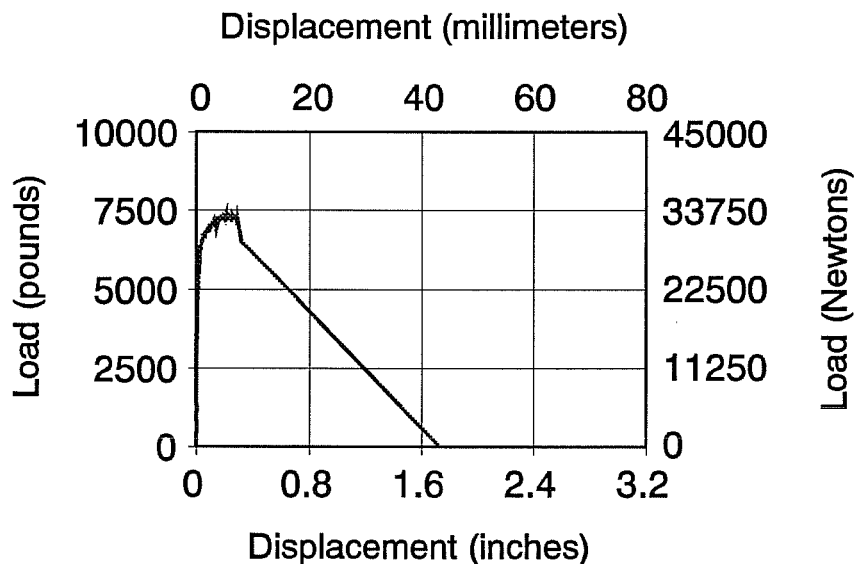
### UFTHSL/01

Ultimate Load = 7599 lbs  
33803 N



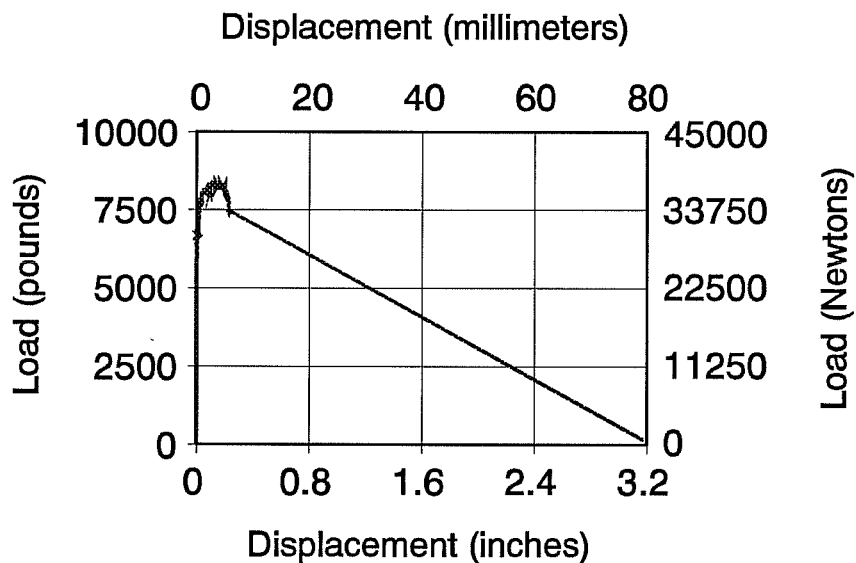
### UFTHSL/02

Ultimate Load = 7363 lbs  
32753 N



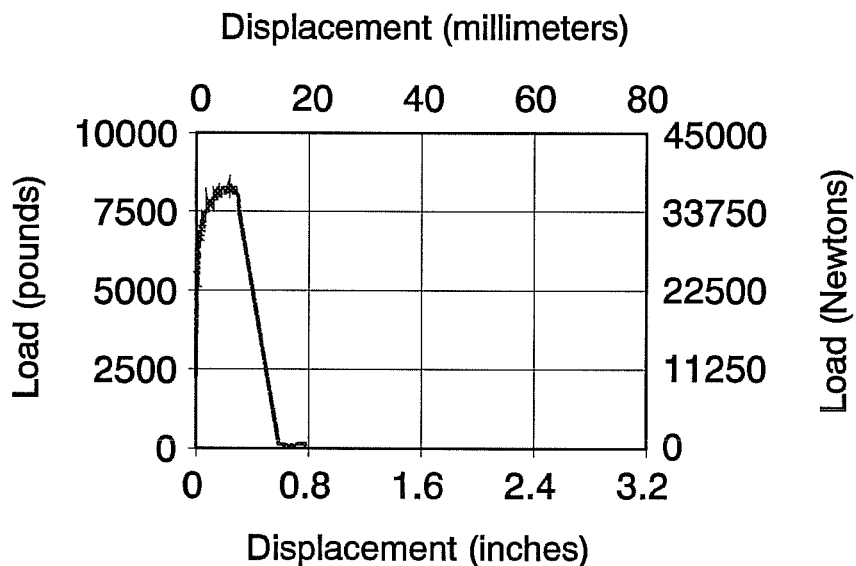
## UFTHSL/04

Ultimate Load = 8402 lbs  
37372 N



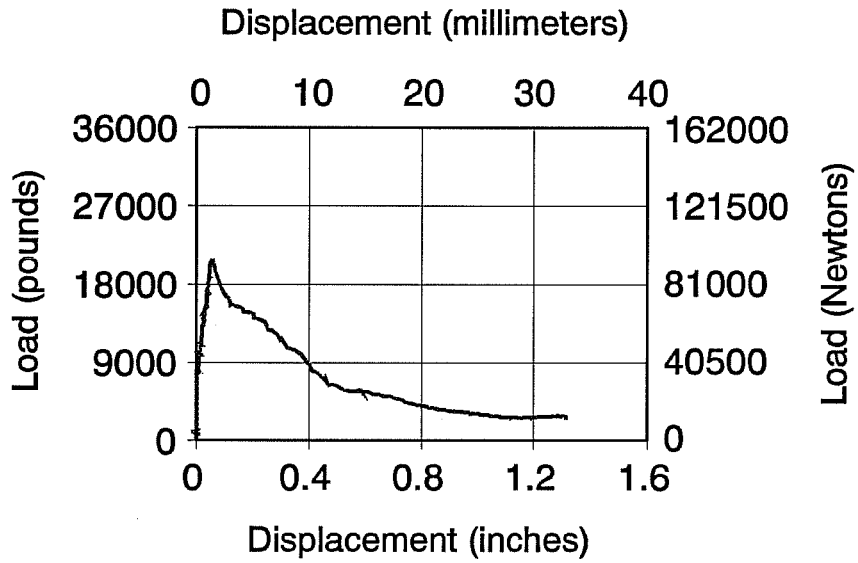
## UFTHSL/05

Ultimate Load = 8307 lbs  
36952 N



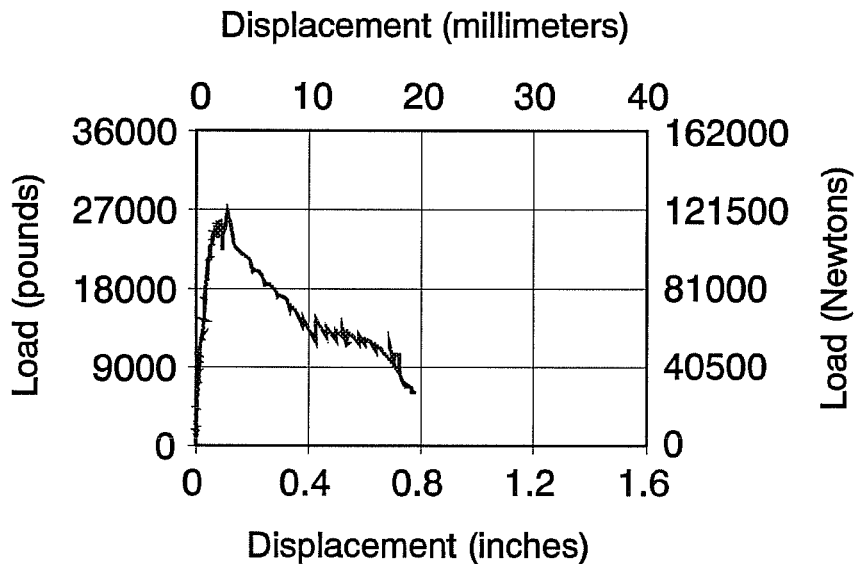
### UFTHSL/21

Ultimate Load = 20674 lbs  
91961 N



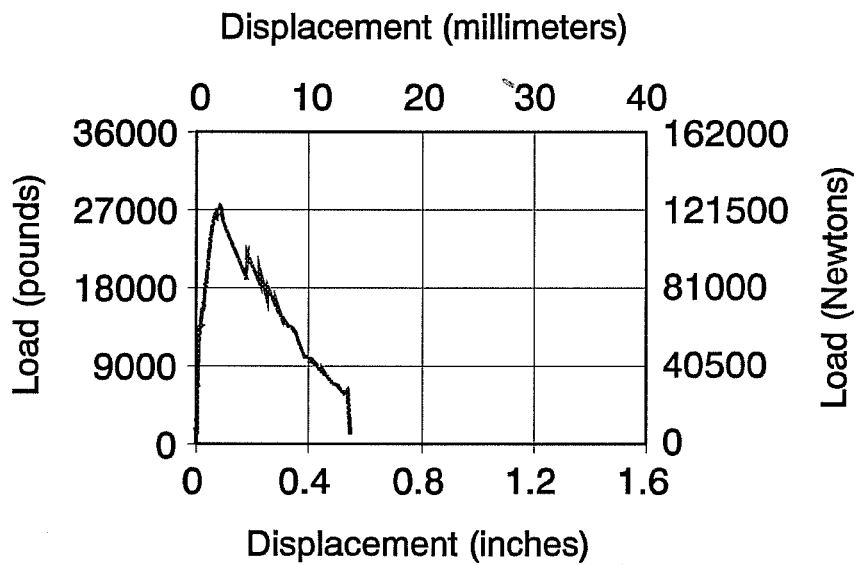
### UFTHSL/22

Ultimate Load = 26762 lbs  
119045 N



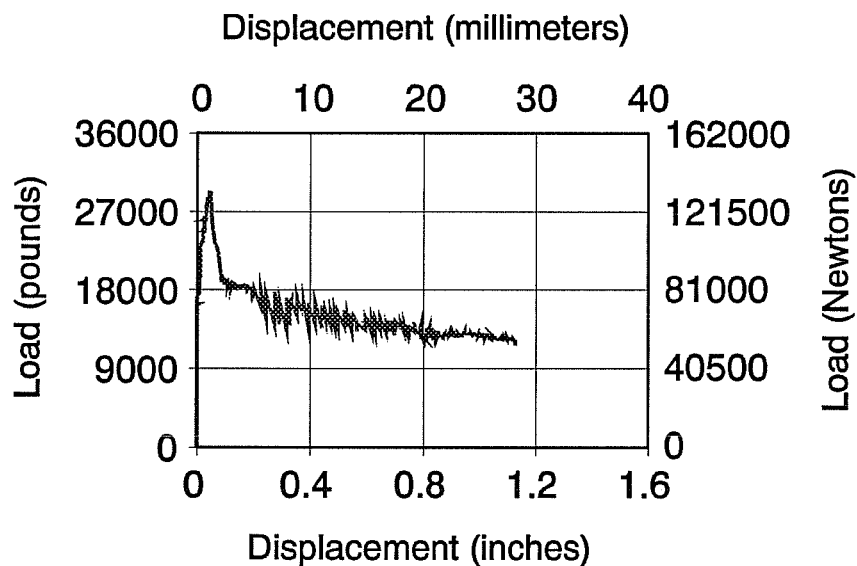
### UFTHSL/23

Ultimate Load = 27423 lbs  
121984 N



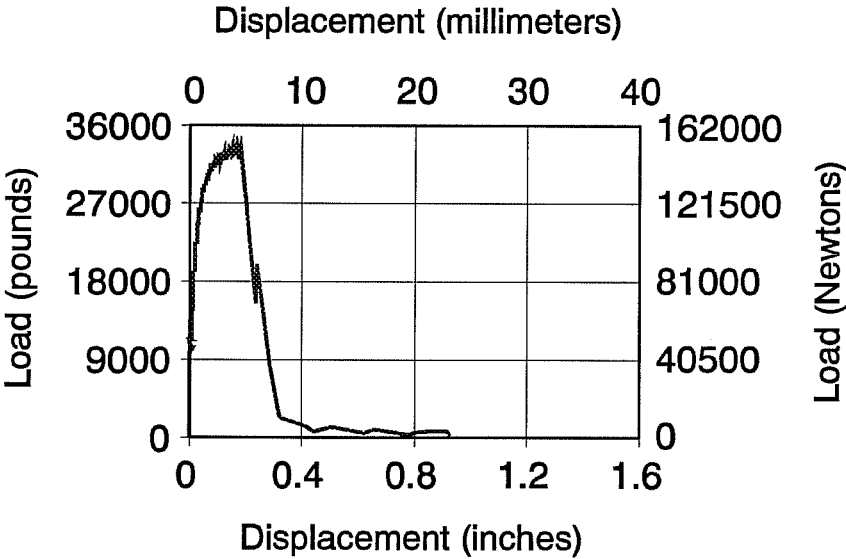
### UFTHSL/24

Ultimate Load = 29150 lbs  
129666 N



# UFTHSL/25

Ultimate Load = 33963 lbs  
151073 N





## REFERENCES

1. ACI Committee 349, Code Requirements for Nuclear Safety Related Structures (ACI 349-85), American Concrete Institute, Detroit, MI, 1985.
2. ICBO Evaluation Service, Inc., "Acceptance Criteria for Expansion Anchors in Concrete and Masonry Elements," International Conference of Building Officials, Whittier, CA, July 1991.
3. Klingner, R. E., "The Role of Plastic Design Approaches in Connections to Concrete for Seismic Loads," Proceedings, Anchorage to Concrete Seminar, Structural Engineers Association of Southern California (SEAOSC), Los Angeles, CA, April 3, 1993.
4. Fastenings to Reinforced Concrete and Masonry Structures: State-of-Art Report, CEB Bulletin D'Information No. 206 and 207, Comite Euro-International du Beton, 1991.
5. Klingner, R.E., Mendonca, J.A., and Malik, J.B., "Effect of Reinforcing Details on the Shear Resistance of Anchor Bolts Under Reversed Cyclic Loading," Journal of the American Concrete Institute, Proceedings Vol. 79, No. 1, January-February 1982, pp. 3-12.
6. Collins, D. M., "Load-Deflection Behavior of Cast-in-Place and Retrofit Concrete Anchors Subjected to Static, Fatigue, and Impact Tensile Loads," M.S. Thesis, The University of Texas at Austin, May 1988.
7. ASTM Designation C31-90a, Standard Practice for Making and Curing Concrete Test Specimens in the Field, American Society for Testing and Materials, Philadelphia, PA, 1990.
8. ASTM Designation C617-87, Standard Practice for Capping Cylindrical Concrete Specimens, American Society for Testing and Materials, Philadelphia, PA, 1988.

9. ASTM Designation C39-86, Standard Test Method for Compressive Strength of Cylindrical Concrete Specimens, American Society for Testing and Materials, Philadelphia, PA, 1986.
10. ASTM Designation E488-90, Standard Test Methods for Strength of Anchors in Concrete and Masonry Elements, American Society for Testing and Materials, Philadelphia, PA, 1990.
11. Personal Communication with Jeff Warmolts. April 1993.
12. Farrow, C. B., "Tensile Capacity of Anchors with Partial or Overlapping Failure Surfaces: Evaluation of Existing Formulas on an LRFD Basis," M.S. Thesis, The University of Texas at Austin, August 1992.

## VITA

Thomas H. Pechillo, Jr. was born in Bridgeport, Connecticut on April 19, 1968. He is the son of Thomas H. and Patricia R. Pechillo of Stratford, Connecticut.

The author was raised in Stratford and graduated Magna Cum Laude from Frank Scott Bunnell High School in June 1986. He then went on to attend The Pennsylvania State University, where he received his Bachelor of Science degree in Civil Engineering in December 1990. During the time he was enrolled at Penn State, he received his Engineer-In-Training certification in the state of Pennsylvania. The author's summer months of 1989 and 1990 were spent working for the structural engineering firm of Spiegel Zamecnik and Shah in New Haven, Connecticut.

From December 1990 until August 1991, the author again worked for Spiegel Zamecnik and Shah. In August 1991, he enrolled in the Graduate School of the University of Texas at Austin. He received a Graduate Assistantship from the University of Texas. He was a teaching assistant for a structural analysis class in the fall semester of 1991 before starting his research on anchors in January 1992.

Permanent Address:  
155 Burbank Avenue  
Stratford, Connecticut 06497

This thesis was typed by the author.